ISOMERIC CROSS SECTION RATIOS FOR
THE Sc-46, Cs-134 AND Re-188 ISOMERS

by

GALE GENE SIMONS

B. S. Kansas State University, 1962

A MASTER'S THESIS

submitted in partial fulfillment of the

requirements for the degree

MASTER OF SCIENCE

Department of Nuclear Engineering

KANSAS STATE UNIVERSITY
Manhattan, Kansas

1965

Approved by:

S. Z. Mikhail
Major Professor

TABLE OF CONTENTS

LIST OF TABLES

LIST OF FIGURES

NOMENCLATURE

A	Nuclide mass
<u>a</u>	Parameter equal to A/8 Mev^{-1}
B	Binding energy
E_o	Excitation energy of compound nucleus
$\overline{E}_{\gamma n}$	Average energy of n^{th} gamma ray emitted from compound nucleus
E_{T1}	Total efficiency for detection of metastable gamma ray
I	Angular momentum of target nucleus
J	Angular momentum of compound nucleus
ℓ	Orbital angular momentum
m	Neutron mass
N_J	Number of levels in compound nucleus with angular momentum J
N_γ	Number of gamma rays emitted from excited nucleus
$P_{J\rightarrow J+1}$	Probability that angular momentum changes from J to J+1 following compound nucleus de-excitation
P_1^0	Photopeak area for metastable state for zero decay time
s	Spin angular momentum
R	Nuclear radius
t	Irradiation time
T	Nuclear temperature
t_{w1}	Decay time of metastable state
t_{w2}	Decay time of stable state
Epi-cadmium	Neutron energy range available in the rotary specimen rack (for cadmium covered samples)

RSR	Neutron energy range available in the rotary specimen rack (for bare samples)
Thermal	Neutron energy range in the thermal column
α	Internal conversion coefficient
Λ_{RIGID}	Rigid moment of inertia
δ_1	Cross section for formation of metastable state
δ_2	Cross section for formation of stable state
λ_1	Decay constant of metastable state
λ_2	Decay constant of stable state
σ	Level density factor or spin cut off factor
$\underline{\sigma}$	Standard deviation of Gaussian curve
$\rho(J)$	Level density with momentum J

1.0 INTRODUCTION

Compound nucleus formation may occur when a nucleus is bombarded by a neutron. The excited states formed can lose their excitation energy by:

1. particle and/or gamma ray emission directly to a stable state energy level,

or

2. particle and/or gamma ray emission to metastable and stable state energy levels.

Nuclides which form metastable and stable states are called nuclear isomers. Besides the difference in energy of the isomeric states, there is a large difference in their angular momentum which tends to slow down the transition from metastable to stable state allowing the metastable state to have a measurable half life. The metastable state is thus characterized by having a measurable half life, otherwise, it is identical to an excited state.

The isomeric cross section ratio gives the proportion of each isomer formed due to a nuclear reaction, and will be defined in this work as the cross section for formation of the metastable state divided by the sum of the cross sections for metastable and stable state formation.

Various authors have used the statistical model for compound nucleus formation to calculate isomeric cross section ratios (30). This model is valid if the nucleus is excited considerably (several Mev). The distribution of the many angular momentum levels acquired by the nucleus under such conditions is called the density of levels and is given by (21)

$$\rho(J) = \rho(0)(2J + 1)\exp(-(J + 1/2)^2/2\sigma^2)$$

where

J = angular momentum of the level

$\rho(0)$ = density of the level with an angular momentum equal to zero

σ = level density parameter

The angular momentum of a metastable state contrary to an excited state, can be determined (5) due to its measurable half life compared to the very short time (less than 10^{-13} seconds) the excited state takes to decay.

Using angular momenta and the level density equation the isomeric cross section ratio can be theoretically calculated. Nuclear parameters needed to calculate the ratio are:

1. spin of original nucleus
2. spin of isomeric states
3. spin of compound state formed
4. method of compound nucleus de-excitation
5. angular momentum change following each step of compound nucleus de-excitation
6. probability of forming states of a given angular momentum following each step in the de-excitation process.

The purpose of the present work was to experimentally determine the isomeric cross section ratios for Re-188,188m, Cs-134,134m, and Sc-46,46m using (n,γ) reactions and to compare them with the ratios calculated theoretically using the statistical model. This comparison also allows the level density parameter, σ, to be determined for various steps in the de-excitation process

2.0 THEORETICAL DEVELOPMENT

2.1 Compound Nucleus Formation and De-excitation

In 1936 Bohr proposed his theory of the compound nucleus. The basic ideas of this theory are (13):

1. The incident particle is absorbed by the initial, or target nucleus to form a compound nucleus.
2. The compound nucleus disintegrates by ejecting a particle (proton, neutron, alpha particle, etc.) or a gamma ray, leaving the final, or product nucleus.

It is assumed that the mode of disintegration of the compound nucleus is independent of the way in which the latter is formed, and depends only on the properties of the compound nucleus itself, such as its energy and angular momentum. The two steps of the compound nucleus formation and de-excitation can then be considered separate processes:

1. incident particle + initial nucleus → compound nucleus
2. compound nucleus → product nucleus + outgoing particle

The nucleus is generally considered a system of particles held together by very strong short-range forces. When the incident particle enters the nucleus, its energy is quickly shared among the nuclear particles before re-emission can occur, and the state of the compound nucleus is then independent of the way it was formed. That this conclusion is reasonable can be shown by the following arguments: On being captured, the incident particle makes available a certain amount of excitation energy, which is nearly equal to the kinetic energy of the captured particle plus its binding energy in the compound nucleus. The magnitude of the excitation energy can be calculated from the masses of the incident particle, target nucleus, and compound nucleus, and the kinetic energy of the incident particle. Consider, for example, the capture of a neutron by Sc-45 to form the excited compound nucleus $({}_{21}Sc^{46})^*$

$$ {}_{21}Sc^{45} + {}_{0}n^{1} \rightarrow ({}_{21}Sc^{46})^* \qquad (1) $$

The masses of the interacting neutron and nucleus are 1.00898 and 44.97008 amu, or a total of 45.97906 amu; that of the compound nucleus is 45.96949 amu, (28). The mass excess is 0.00961 amu, corresponding to 8.95 Mev, to which must be added the kinetic energy of the incident neutron. In the case of a slow neutron, the kinetic energy may be neglected. If the incident neutron has a kinetic energy of 1 Mev, the excitation energy is nearly 9.95 Mev and the energy of the compound nucleus is greater than the energy of the ground state of Sc-46 by this amount. The 8.95 Mev is called the binding energy B. If E_i is the energy of the incident particle then the excitation energy E_o is

$$ E_o = B + E_i \qquad (2) $$

Immediately after the formation of the compound nucleus, the excitation energy may be considered to be concentrated on the captured particle, but after a very short time interactions among the nuclear particles take place leading to a rapid distribution of this excitation energy among the other particles. The distribution presumably takes place in a random way. At a given instant, the excitation energy may be shared among a group of nucleons; at a later time it may be shared by other nucleon groups, or it may eventually again become concentrated on one nucleon or combination of nucleons. In the latter case, if the excitation energy is large enough, one nucleon, or a combination of nucleons, may escape, and the compound nucleus disintegrates into the product nucleus and outgoing particle. The energy that must be concentrated on a single nuclear particle or group of particles in order to separate it from the compound nucleus is called the separation or dissociation energy, and for nuclei with mass number above 25 it is about 8 Mev.

As a result of the random way in which the excitation energy is distributed in the compound nucleus, the latter has a lifetime which is relatively long compared with the time that would be required for a particle to travel across the nucleus. The latter time interval, sometimes called the "natural nuclear time," is of the order of magnitude of the diameter of the nucleus divided by the speed of the incident particle. If the incident particle is a 1-Mev neutron, its speed is about 10^{9} cm per sec. Since the diameter of the nucleus is of the order of 10^{-12} cm, the time required for a 1-Mev neutron to cross the nucleus is of the order of 10^{-21} sec. Even a slow neutron with a velocity of 10^{5} cm per sec would need only about 10^{-17} sec to cross the nucleus. During its relatively long lifetime, the compound nucleus "forgets" how it was formed, and the disintegration is independent of the mode of formation. The compound nucleus may be said to exist in a "quasi-stationary" state, which means that although it exists for a time interval which is very long compared with the natural nuclear time, it can still disintegrate by ejecting one or more nucleons. These quasi-stationary states are usually called virtual states or virtual levels in contrast to bound states or bound levels, which can decay only be emitting gamma radiation.

There are many ways in which the excitation energy of the compound nucleus can be divided among the nuclear particles and, since each distribution is assumed to correspond to a virtual level, there are many possible virtual levels of the compound nucleus. It is reasonable to assume that if the energy of the incident particle is such that the total energy of the system, incident particle plus target nucleus, is equal to the energy of a level, the probability that the compound nucleus will be formed is much greater than if the energy falls in the region between two levels.

Each excited state of the compound nucleus, whether bound or virtual, has a certain mean lifetime which is the average period of time during which the nucleus remains in a given excited state before decaying by emission of either a particle or a gamma ray. The reciprocal of the mean lifetime is the disintegration constant, which gives the probability per unit time of the emission of a particle or gamma ray. The mean lifetime is generally very short, approximately 10^{-13} seconds. An exception to this is the metastable state of an isomer which, in most cases, has a measurable half life.

The mode of de-excitation is dependent, as explained above, upon the energy of the incident particle. De-excitation of the compound nucleus formed by slow neutron capture occurs principally by emission of gamma radiation. A number of gamma rays are emitted until finally de-excitation to the ground state or the metastable state occurs. On the other hand, when a compound nucleus is formed by capturing a 14 Mev neutron, the nucleus has sufficient energy to de-excite by particle emission. For the same available energy of the emitted particle, neutron emission is much more probable than proton emission, which in turn is more probable than alpha emission. The reason for this is the emergent coulomb barrier in the case of charged particle emission.

2.2 Derivation of Equations

The quantum numbers for the individual nucleons in a nucleus arise in the solution of the Schrodinger wave equation. The orbital quantum number ℓ is restricted to zero or positive integers. The spin quantum number s has the value 1/2 for neutrons, protons and electrons, i.e., all elementary particles. The total angular momentum of a neutron or proton will be equal to the vector sum of the angular momenta due to the orbital motion and the spin ($\ell \pm s$). The nucleus as a whole will possess angular momentum I which is the vector sum of the orbital and spin angular momenta of all the neutrons and protons of which it is composed.

When a nucleus with total angular momentum I is bombarded by incident particles the compound nucleus formed will have total angular momentum J given by

$$J = I \pm (\ell \pm s) \tag{3}$$

where ℓ and s are the quantum numbers of the incident particle. For thermal neutrons it is assumed that only s wave neutrons (12), $\ell = 0$, are captured, i.e., no orbital angular momentum is imparted to the target nucleus. The total angular momentum of the compound nucleus will be

$$J = I \pm s \tag{4}$$

If the nucleus is excited several Mev and therefore the statistical model can be applied (5) it is possible to determine the level density, i.e., the number of levels per Mev. Instead of speaking of the angular momentum of each individual level, at high excitation energies, one therefore speaks of the distribution in angular momentum of levels within a small energy interval.

The number of levels in the excited nucleus N_J with total angular momentum J is

$$N_J = N(J) - N(J + 1) \tag{5}$$

where N(J) is the total number of levels with angular momentum less than or equal to J. Bloch (6) has found that N(J) is given in the first approximation by a Gaussian law, therefore

$$N(J) \propto \exp(-J^2/2\sigma^2) \tag{6}$$

where σ is a constant called the spin density parameter. Substitution of expression (6) into (5) gives

$$N_J \propto \exp(-J^2/2\sigma^2) - \exp[-(J + 1)^2/2\sigma^2] \; . \tag{7}$$

Factoring $\exp[-(J^2 + J + 1/4)/2\sigma^2]$ out of each term in expression (7) gives the form

$$N_J \propto \exp[-(J^2 + J + 1/4)/2\sigma^2]\{\exp[(J + 1/4)/2\sigma^2] - \exp[-(J + 3/4)/2\sigma^2]\} \; . \tag{8}$$

For small exponents $e^x \doteq 1 + x$ hence expression (8) becomes

$$N_J \propto \exp[-(J + 1/2)^2/2\sigma^2][1 + (J + 1/4)/2\sigma^2 - 1 + (J + 3/4)/2\sigma^2] \tag{9}$$

which gives

$$N_J = B[(2J + 1)/2\sigma^2]\exp[-(J + 1/2)^2/2\sigma^2] \tag{10}$$

where B is a proportionality constant. If J = 0, N_J is

$$N_o = (B/2\sigma^2)\exp[-(1/2)^2/2\sigma^2] \tag{11}$$

or

$$N_o = (B/2\sigma^2)(1 - 1/8\sigma^2) \tag{12}$$

since $1/(8\sigma^2) << 1$

$$B = 2\sigma^2 N_o \; . \tag{13}$$

Equation (10) becomes

$$N_J = N_o(2J + 1)\exp[-(J + 1/2)^2/2\sigma^2] \tag{14}$$

The density of levels with angular momentum J is therefore given by the level density (6)

$$\rho(J) = \rho(0)(2J + 1)\exp[-(J + 1/2)^2/2\sigma^2] \quad (15)$$

where $\rho(0)$ is the density of levels with zero total angular momentum.

Huizenga (21) has found, by comparing experimental and theoretical isomeric cross section ratios, that the spin density parameter σ is in the range $\sigma = 3$ to $\sigma = 5$ for various isomers. In this case, it was assumed that σ does not vary during compound nucleus de-excitation. It is possible to calculate a value for σ following each step in the de-excitation process,i.e., following the emission of each gamma ray, by using the nuclear temperature and the rigid moment of inertia.

Ericson (12) has shown that σ^2 can be expressed as

$$\sigma^2 = (2\pi)^2\ \Lambda T/h^2 \quad (16)$$

where Λ is the moment of inertia of the nucleus, T is the nuclear temperature and h is Planck's constant.

The excited nucleus can be thought of as a rotator with moment of inertia Λ. At high excitation energies of the nucleus Λ is believed to be given by the rigid moment of inertia (12)

$$\Lambda_{RIGID} = (2/5)mAR^2 \quad (17)$$

where m is the nucleon mass, A is the number of nucleons within the nucleus and R is the nuclear radius ($1.2 \times 10^{-13}\ A^{1/3}$).

The nuclear temperature T is defined by

$$\frac{1}{T} = \frac{d\ell n\rho(A,E)}{dE} \quad (18)$$

where $\rho(A,E)$, the level density, is a function of the number of nucleons within the nucleus and the excitation energy of the nucleus (5). Weisskopf

(5) has shown that the level density can be estimated by*

$$\rho(A,E) = C \exp[2(\underline{a}E)^{1/2}] \tag{19}$$

where C and $\underline{a}$ are parameters which are adjusted empirically. Substitution of the level density given in Eq. (19) into the definition of the nuclear temperature, Eq. (18), gives

$$\frac{1}{T} = \frac{d\ell n\{C \exp[2(\underline{a}E)^{1/2}]\}}{dE} \quad . \tag{20}$$

Following differentiation of Eq. (20) the nuclear temperature is

$$T = (E/\underline{a})^{1/2} \quad . \tag{21}$$

A few values of $\underline{a}$ have been determined experimentally for odd A nuclides (5) but not for even A nuclides. For high excitation energies where the statistical model is valid Wing (33) has stated that the nuclear temperature can be expressed as a function of excitation energy as follows

$$E = \underline{a}T^2 - T \tag{22}$$

where

$$\underline{a} = A/8 \ . \tag{23}$$

To determine E used in Eq. (22) it is necessary to calculate the average energy of the gamma ray emitted. The average energy of a gamma ray emitted from an excited nucleus is (33)

$$\overline{E}_{\gamma 1} = E_o - E_1 = 4(E_o/\underline{a} - 5/\underline{a}^2)^{1/2} \tag{24}$$

where E_o and E_1 are the excitation energies before and after gamma ray emission respectively. The average energy of the n^{th} gamma ray emitted is

$$\overline{E}_{\gamma n} = E_{n-1} - E_n = 4(E_{n-1}/\underline{a} - 5/\underline{a}^2)^{1/2} \tag{25}$$

---

* This is the same level density as given in Eq. (15) expressed in terms of A and E instead of J. Their derivations are completely independent.

Using Eqs. (16), (17), (22), and (25) it is therefore possible to calculate σ following the emission of each gamma ray.

After an excited nucleus emits a gamma ray there will be a change in the distribution of the angular momentum within the nucleus. For a relatively large excitation energy (>2 Mev) the nucleus will contain many nuclear levels each having numerous values of J before and after gamma ray emission. The de-excitation will be primarily by dipole gamma emission ($\ell = 1$) since the probability of gamma ray emission decreases rapidly as ℓ increases, e.g., the probability of $\ell = 1$ is 10^5 times greater than for $\ell = 2$ for a 1 Mev gamma ray.

The level density factor σ can be used to calculate the probability of going from a state of J to a state of J + 1 following gamma emission from the relationship

$$P_{J \to J+1} = \frac{\rho(J+1)}{\rho(J) + \rho(J+1) + \rho(J-1)} \; . \tag{26}$$

Likewise the probabilities of going from J to J and from J to J - 1 are

$$P_{J \to J} = \frac{\rho(J)}{\rho(J) + \rho(J+1) + \rho(J-1)} \tag{27}$$

$$P_{J \to J-1} = \frac{\rho(J-1)}{\rho(J) + \rho(J+1) + \rho(J-1)} \tag{28}$$

After the emission of a single gamma ray, the total angular momentum will be redistributed between the three angular momentum states. Gamma rays will be emitted from an excited nucleus until the excitation energy becomes so low that it is no longer energetically possible for a gamma ray to be emitted. The number of gamma rays emitted will be a function of the original excitation energy. To determine the isomeric cross section ratio, probability values must be calculated following each gamma ray emitted. After the emission of the last gamma ray there will be two different angular momentum states available for population, the metastable and stable states of the isomers. The distribution of the population will depend on the angular momenta of the metastable and stable states. The nuclear states following gamma ray emission will populate the isomeric state having the closest angular momentum to their own, for example, if the metastable and stable states have angular momenta of I = 5 and I = 2 respectively and four gamma rays are emitted in going from the excited to the isomeric states then following emission of gamma ray number three the states with angular momenta of 0, 1, 2, 3 will populate the stable state while those with angular momenta of 4, 5, 6, 7,...., will populate the metastable state. Defining P_{J_f} as the absolute probability that the nucleus will have an angular momentum of J_f before the emission of the fourth gamma ray then the cross section ratio is

$$\frac{\delta_1}{\delta_1 + \delta_2} = \sum_{J_f=4}^{\infty} P_{J_f} \tag{29}$$

where δ_1 and δ_2 are the cross sections for the formation of the metastable and stable states respectively. Eq. (29) may be used to calculate the isomeric cross section ratios using either constant or calculated values of the level density parameter σ as indicated above.

3.0 EXPERIMENTAL DEVELOPMENT

3.1 Theory

It is possible to calculate the isomeric cross section ratios by determining the disintegration rates. A knowledge of the mode of decay, half life, irradiation time and decay time is necessary.

The rate equation for the formation of the metastable state is that of an independently decaying isomer, i.e.,

$$dN_1/dt = R_{s1} - \lambda_1 N_1 \tag{30}$$

where

$$R_{s1} = N\phi\delta_1 \tag{31}$$

and N is the number of target atoms, ϕ is the number of neutrons per second per cm^2, and δ_1 is the cross section in cm^2. Assuming ϕ to be constant, R_{s1} would be a constant for each sample. Solving Eq. (30) by separation of variables gives

$$\lambda_1 N_1 = R_{s1}(1 - e^{-\lambda_1 t}) \tag{32}$$

where $\lambda_1 N_1$ is the disintegration rate of the product formed and t is the irradiation time.

In the cases under consideration, the metastable state decays completely to the ground state, hence a parent-daughter relation exists. The rate equation for the formation of the ground state is

$$dN_2/dt = R_{s2} - \lambda_2 N_2 + \lambda_1 N_1 \tag{33}$$

The subscript 2 refers to the ground state. From Eqs. (32) and (33)

$$dN_2/dt + \lambda_2 N_2 = R_{s2} + R_{s1} - R_{s1}e^{-\lambda_1 t} \tag{34}$$

The solution to Eq. (34) is obtained by solving the homogeneous equation

$$dN_2/dt + \lambda_2 N_2 = 0 \tag{35}$$

and adding the particular solution. The solution to the homogeneous equation is

$$N_2 = Ce^{-\lambda_2 t} \tag{36}$$

The particular solution is obtained by using the method of undetermined coefficients as follows: a solution of the form

$$N_2 = ae^{-\lambda_1 t} + b \tag{37}$$

is assumed, where a and b are the coefficients to be determined. If the derivative of Eq. (37) is taken, then

$$dN_2/dt = -a\lambda_1 e^{-\lambda_1 t} \quad . \tag{38}$$

Substituting Eqs. (37) and (38) into Eq. (34) gives

$$-a\lambda_1 e^{-\lambda_1 t} + \lambda_2 ae^{-\lambda_1 t} + \lambda_2 b = R_{s2} + R_{s1} - R_{s1} e^{-\lambda_1 t} \quad . \tag{39}$$

Equating coefficients of Eq. (39) gives

$$-a\lambda_1 + a\lambda_2 = -R_{s1} \tag{40}$$

$$\lambda_2 b = R_{s2} + R_{s1} \tag{41}$$

thus

$$a = R_{s1}/(\lambda_1 - \lambda_2) \tag{42}$$

and

$$b = (R_{s1} + R_{s2})/\lambda_2 \quad . \tag{43}$$

Equation (37) becomes

$$N_2 = (R_{s1}/(\lambda_1 - \lambda_2))e^{-\lambda_1 t} + (R_{s1} + R_{s2})/\lambda_2 \tag{44}$$

Therefore from Eqs. (36) and (44) Eq. (34) has a solution of the form

$$N_2 = Ce^{-\lambda_2 t} + (R_{s1}/(\lambda_1 - \lambda_2))e^{-\lambda_1 t} + (R_{s1} + R_{s2})/\lambda_2 \quad . \tag{45}$$

Applying the boundary condition that the number of ground state atoms at zero time is zero to Eq. (45)

$$0 = Ce^{o} + (R_{s1}/(\lambda_1 - \lambda_2))e^{o} + (R_{s1} + R_{s2})/\lambda_2 \tag{46}$$

solving for C

$$C = -R_{s1}/(\lambda_1 - \lambda_2) - (R_{s1} + R_{s2})/\lambda_2 \ . \tag{47}$$

From Eq. (45)

$$\lambda_2 N_2 = (R_{s1} + R_{s2})(1 - e^{-\lambda_2 t}) + (\lambda_2 R_{s1}/(\lambda_1 - \lambda_2))(e^{-\lambda_1 t} - e^{-\lambda_2 t}) . \tag{48}$$

In this work the isomeric cross section ratios were determined by counting the same sample for both the metastable and stable state isomers. Therefore

$$R_{s1} = N\phi\delta_1 \tag{49}$$

$$R_{s2} = N\phi\delta_2 \quad . \tag{50}$$

Dividing both sides of Eq. (48) by R_{s1} and applying Eqs. (32), (49), and (50) gives

$$\frac{\lambda_2 N_2}{\lambda_1 N_1}(1 - e^{-\lambda_1 t}) = \frac{1}{\delta_1}\Big[(\delta_1 + \delta_2)(1 - e^{-\lambda_2 t}) + \frac{\lambda_2\delta_1}{\lambda_1 - \lambda_2}(e^{-\lambda_1 t} - e^{-\lambda_2 t})\Big] \ . \tag{51}$$

By rearranging Eq. (51) the ratio of the cross sections is given by

$$\frac{\delta_2}{\delta_1} = \frac{1}{(1 - e^{-\lambda_2 t})}\Big[\frac{\lambda_2 N_2}{\lambda_1 N_1}(1 - e^{-\lambda_1 t}) - \frac{\lambda_2}{\lambda_1 - \lambda_2}(e^{-\lambda_1 t} - e^{-\lambda_2 t})\Big] - 1 \ . \tag{52}$$

Up to this point, no correction has been made for radioactive decay following sample irradiation. This correction is made by multiplying $(\lambda_1 N_1)_{w1}$ by $e^{\lambda_1 t_{w1}}$ and $(\lambda_2 N_2)_{w2}$ by $e^{\lambda_2 t_{w2}}$ where t_{w1} and t_{w2} are the decay times for the metastable and stable states respectively.

For nuclides with a half life much greater than the counting time, so that significant decay does not occur during counting, the ratio of cross sections becomes

$$\frac{\delta_2}{\delta_1} = \frac{1}{(1 - e^{-\lambda_2 t})} \left\{ \frac{(\lambda_2 N_2)_{w2} \, e^{\lambda_2 t_{w2}}}{(\lambda_1 N_1)_{w1} \, e^{\lambda_1 t_{w1}}} (1 - e^{-\lambda_1 t}) - \frac{\lambda_2}{\lambda_1 - \lambda_2} (e^{-\lambda_1 t} - e^{-\lambda_2 t}) \right\} - 1 \tag{53}$$

where $(\lambda_1 N_1)_{w1}$ and $(\lambda_2 N_2)_{w2}$ are the disintegration rates of the sample after waiting times t_{w1} and t_{w2} respectively out of the reactor.

The disintegration rates can be expressed as

$$(\lambda_1 N_1)_{w1} = A_1 / E_{T1} \tag{54}$$

and

$$(\lambda_2 N_2)_{w2} = A_2 / E_{T2} \tag{55}$$

where A_1 and A_2 are the count rates at time t_{w1} and t_{w2} and E_{T1} and E_{T2} are the total efficiencies for detecting the metastable and stable state gamma rays.

When the half life of the metastable state is very short, such that there is appreciable decay during counting, and also the irradiation time, t, is much greater than the half life, the disintegration rate of the metastable state can be expressed as

$$\lambda_1 N_1 = \underset{\sim}{k}_{s1} \tag{56}$$

or

$$\lambda_1 N_1 = \lambda_1 \underset{\sim}{N}_{s1} \tag{57}$$

where R_{s1} is the saturation activity and N_{s1} is the number of radioactive atoms after saturation. Hence,

$$R_{s1} = N\phi\delta_1 \quad . \tag{58}$$

The number of radioactive atoms present after a decay time of t_{w1} seconds is

$$N_{w1} = N_{s1}e^{-\lambda_1 t_{w1}} \quad . \tag{59}$$

The number of disintegrations in counting time t_c seconds is given by

$$N_{t1} = N_{w1} - N_{c1} \tag{60}$$

where N_{c1} is the number of radioactive atoms present after counting. Eq. (60) becomes

$$N_{t1} = N_{w1} - N_{w1}\, \epsilon^{-\lambda_1 t_c} \tag{61}$$

$$N_{t1} = N_{w1}\, (1 - e^{-\lambda_1 t_c}) \tag{62}$$

therefore

$$N_{t1} = N_{s1}e^{-\lambda_1 t_{w1}}\, (1 - e^{-\lambda_1 t_c}) \quad . \tag{63}$$

Multiplying both sides of Eq. (63) by λ_1 gives

$$\lambda_1 N_{t1} = \lambda_1 N_{s1} e^{-\lambda_1 t_{w1}}\, (1 - e^{-\lambda_1 t_c}) \tag{64}$$

also

$$\lambda_1 N_{t1} = R_{s1} e^{-\lambda_1 t_{w1}}\, (1 - e^{-\lambda_1 t_c}) \tag{65}$$

hence

$$R_{s1} = \frac{\lambda_1 N_{t1}}{e^{-\lambda_1 t_{w1}}\, (1 - e^{-\lambda_1 t_c})} \quad . \tag{66}$$

The rate of formation of the ground state, Eq. (33), becomes

$$dN_2/dt = R_{s2} - \lambda_2 N_2 + R_{s1} \tag{67}$$

here R_{s1} is not a function of the irradiation time t. The solution to the homogeneous equation will be the same as that of Eq. (36). The coefficients in the particular solution are

$$a = 1/(\lambda_2 - \lambda_1) \tag{68}$$

and

$$b = R_{s2} + R_{s1} \ . \tag{69}$$

Therefore, the particular solution is

$$N_2 = \frac{1}{\lambda_2 - \lambda_1} e^{-\lambda_1 t} + \frac{R_{s2} + R_{s1}}{\lambda_2} \ .$$

Adding the homogeneous and particular solution, Eq. (67) has a solution of the form

$$N_2 = Ce^{-\lambda_2 t} + \frac{1}{\lambda_2 - \lambda_1} e^{-\lambda_1 t} + \frac{R_{s2} + R_{s1}}{\lambda_2} \ . \tag{70}$$

Applying the boundary condition that the number of stable state atoms at zero time is zero gives

$$C = - \frac{1}{\lambda_2 - \lambda_1} - \frac{R_{s2} + R_{s1}}{\lambda_2} \tag{71}$$

Finally,

$$N_2 = \frac{-e^{-\lambda_2 t}}{\lambda_2 - \lambda_1} - \frac{(R_{s2} + R_{s1})}{\lambda_2} e^{-\lambda_2 t} + \frac{1}{\lambda_2 - \lambda_1} e^{-\lambda_1 t} + \frac{R_{s2} + R_{s1}}{\lambda_2} \tag{72}$$

and

$$\lambda_2 N_2 = (R_{s2} + R_{s1})(1 - e^{-\lambda_2 t}) + \frac{\lambda_2}{\lambda_2 - \lambda_1} (e^{-\lambda_1 t} - e^{-\lambda_2 t}) \ . \tag{73}$$

Dividing Eq. (73) by $\lambda_1 N_{t1}$ and applying Eqs. (58) and (66) gives

$$\frac{\lambda_2 N_2}{\lambda_1 N_{t1}} = \frac{(\delta_2 + \delta_1)(1 - e^{-\lambda_2 t})}{\delta_1 e^{-\lambda_1 t_{w1}}(1 - e^{-\lambda_1 t_c})} + \frac{\lambda_2}{\lambda_2 - \lambda_1} \left(\frac{e^{-\lambda_1 t} - e^{-\lambda_2 t}}{\lambda_1 N_{t1}}\right) . \tag{74}$$

Rearranging gives the equation for the isomeric cross section ratio

$$\frac{\delta_1}{\delta_1 + \delta_2} = \frac{\lambda_1 N_{t1}(1 - e^{-\lambda_2 t})e^{\lambda_1 t_{w1}}}{\left\{(\lambda_2 N_2) - \left(\frac{\lambda_2}{\lambda_2 - \lambda_1}\right)[e^{-\lambda_1 t} - e^{-\lambda_2 t}]\right\}(1 - e^{-\lambda_1 t_c})} \tag{75}$$

where

$$N_{t1} = A_{t1}/E_{T1} \tag{76}$$

also

$$\lambda_2 N_2 = A_2 \, e^{\lambda_2 t_{w2}}/E_{T2} \tag{77}$$

and A_{t1} = number of counts in t_c seconds for metastable state

A_2 = count rate of stable state after waiting time t_{w2}.

It is to be noted that in all results recorded in this study the isomeric cross section ratio is defined as

$$\frac{\delta_1}{\delta_1 + \delta_2} = \frac{1}{1 + \frac{\delta_2}{\delta_1}} \tag{78}$$

3.2 Materials Used and Reactions Studied

Isomeric pairs produced by neutron-gamma reactions on Sc-45, Cs-133, and Re-188 were studied. The materials irradiated were: Semi-Elements Inc. powdered scandium oxide 99.99%, Semi-Elements Inc. crystaline cesium oxide 99.95%, and powdered Fairmont Chemical Co. rhenium metal 99.99%. Table I shows the half lives and gamma rays of the isomeric pairs produced: Sc-46, 46m, Cs-134,134m, and Re-188,188m. The decay schemes of these isomers are shown in Figures 1 through 3, and their gamma ray spectra are shown in Figures 4 through 9.

Since Sc-45 and Cs-133 are 100% isotopically abundant, irradiation of the scandium oxide and cesium oxide produces Sc-46,46m and Cs-134,134m only. Rhenium metal contains 37.07% Re-185 and 62.93% Re-187. Nuclides produced by irradiating natural rhenium metal are Re-186 (90 hr), Re-188 (17 hr) and Re-188m (20 min). It is obvious that a short irradiation time (less than 0.5 min) makes it possible to avoid the undesired excessive Re-186 activity. To determine the significance of the gamma ray interference of Re-186, samples of the rhenium metal were irradiated for 0.5 minutes and counted both after decay of the 20 minute Re-188m and the decay of the 17 hour Re-188. The count rate left due to the Re-186 was found to be negligible compared to the count rate of the Re-188 isomers.

Table I. Gamma ray energies and half lives of nuclides studied.

Parent nuclide	Isomer produced	Gamma rays (Mev)	Half life
Sc-45	Sc-46m	$0.142^{\dagger}$	19s
	Sc-46	$0.885^{\dagger}$, $1.12^{\dagger}$	85d
Cs-133	Cs-134m	$0.127^{\dagger}$, 0.138	3.2h
	Cs-134	0.563, 0.569, $0.605^{\dagger}$, $0.796^{\dagger}$, 1.04, 1.17, 1.37, 1.97	2.07y
Re-187	Re-188m	$0.064^{\dagger}$, 0.169	18.7m
	Re-188	$0.155^{\dagger}$, 0.478, 0.633, 0.828, 0.931, 1.13, 1.31,---	16.7h

† Specific gamma rays used in this study

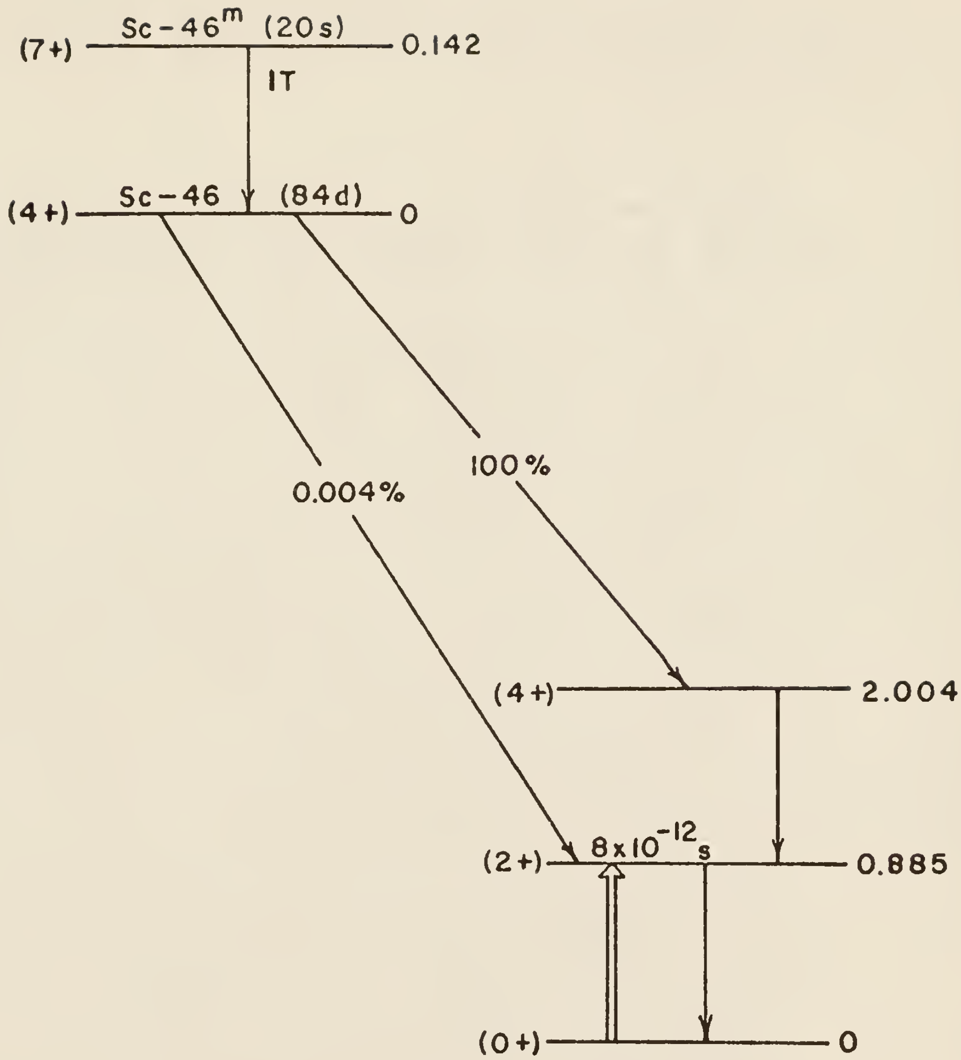

Figure 1 Decay Scheme of Sc $-$ 46^m, Sc $-$ 46.

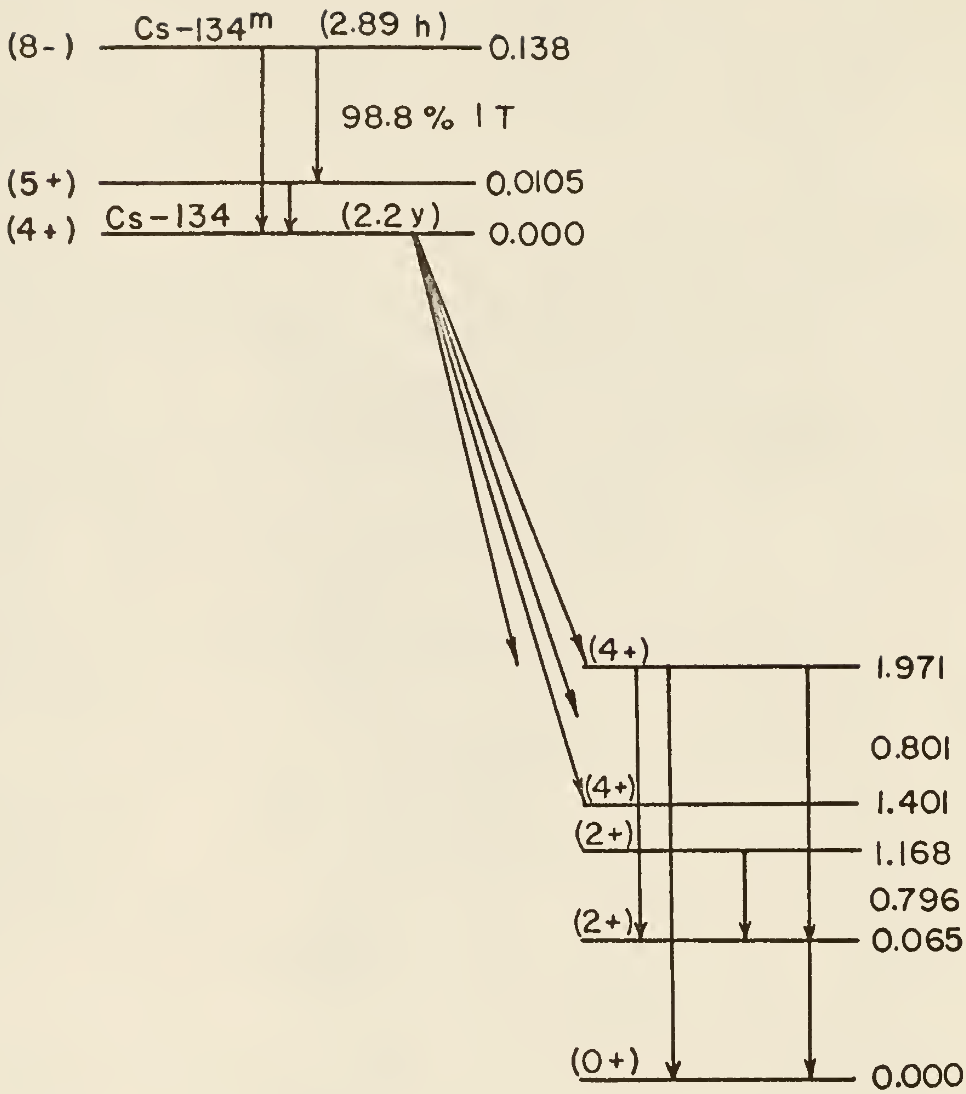

Figure. 2 Decay Scheme of $Cs-134^m$, $Cs-134$.

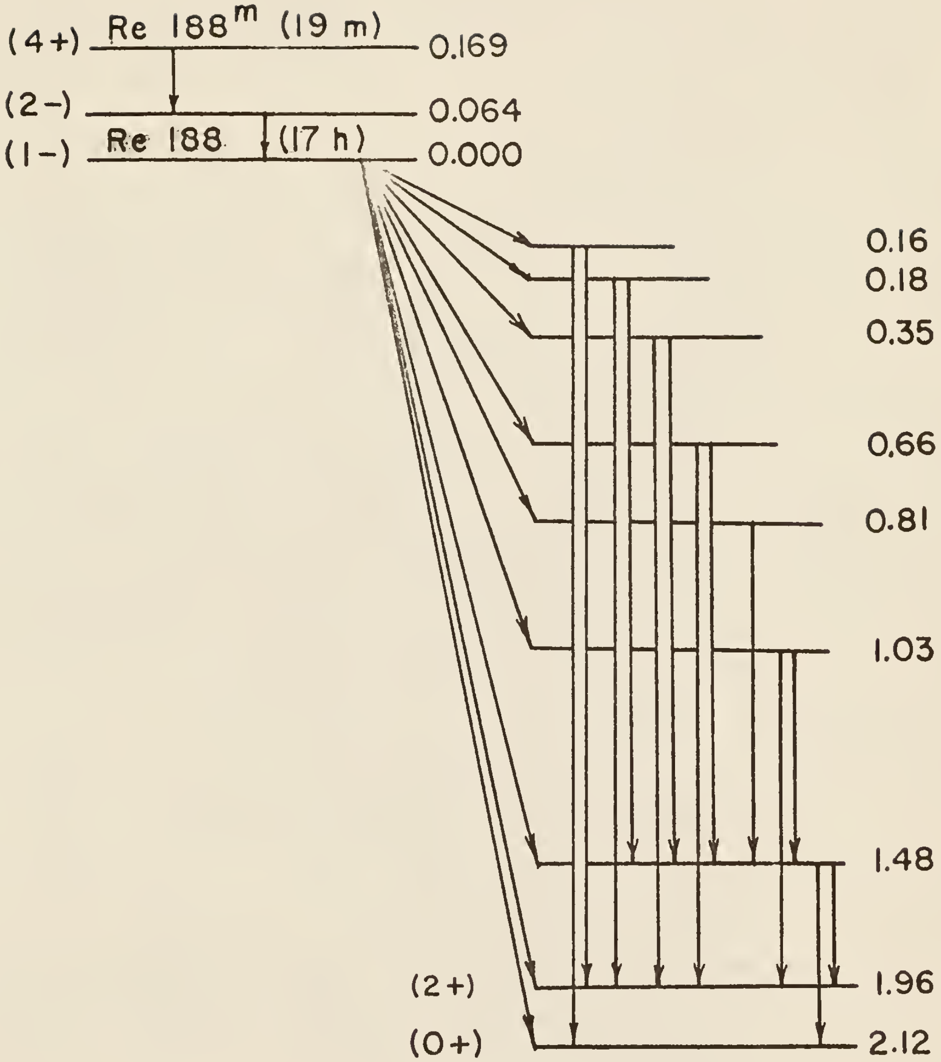

Figure. 3 Decay Scheme of Re —188^m, Re — 188 .

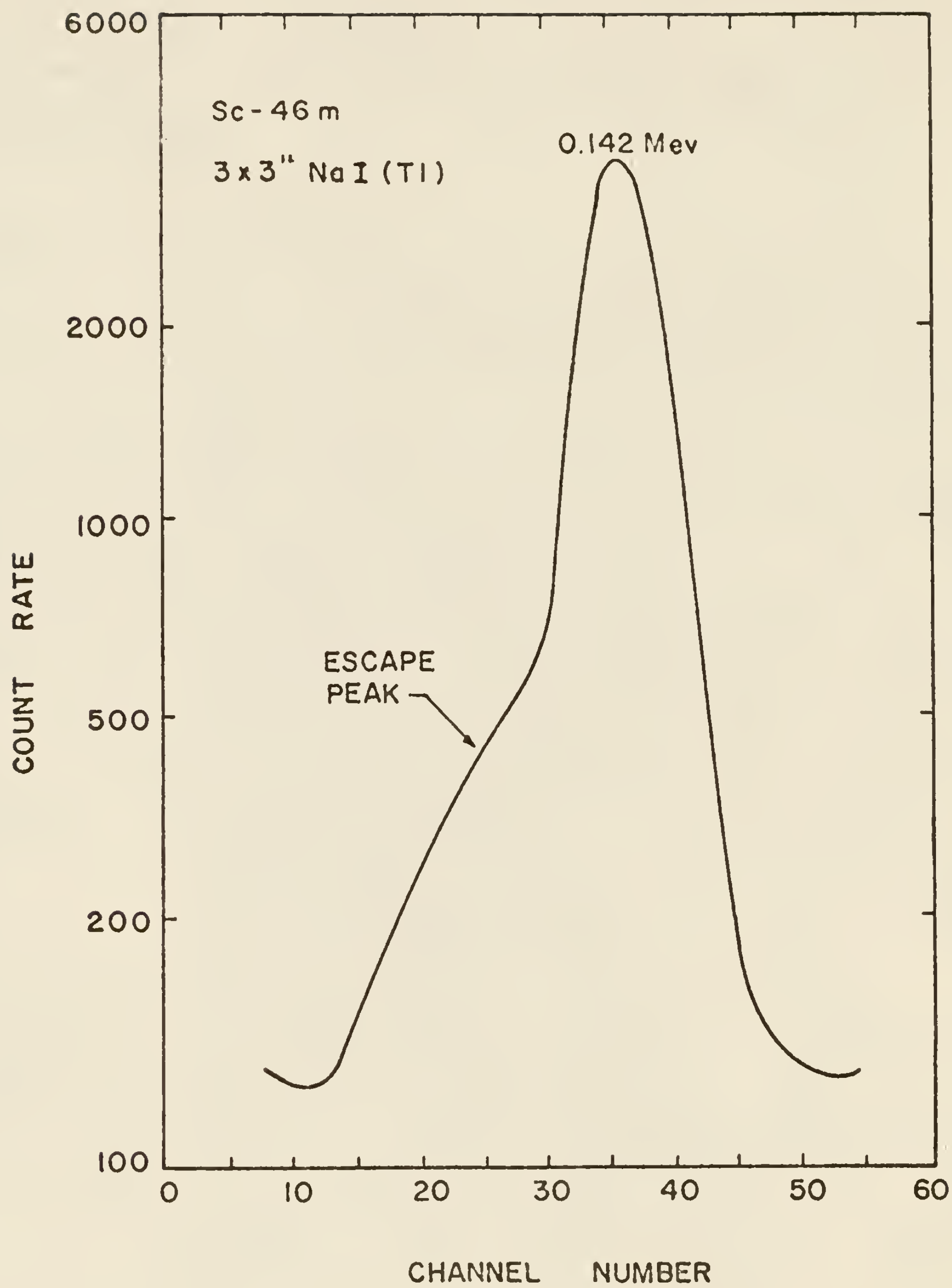

Figure 4 SCANDIUM 46 m SPECTRUM

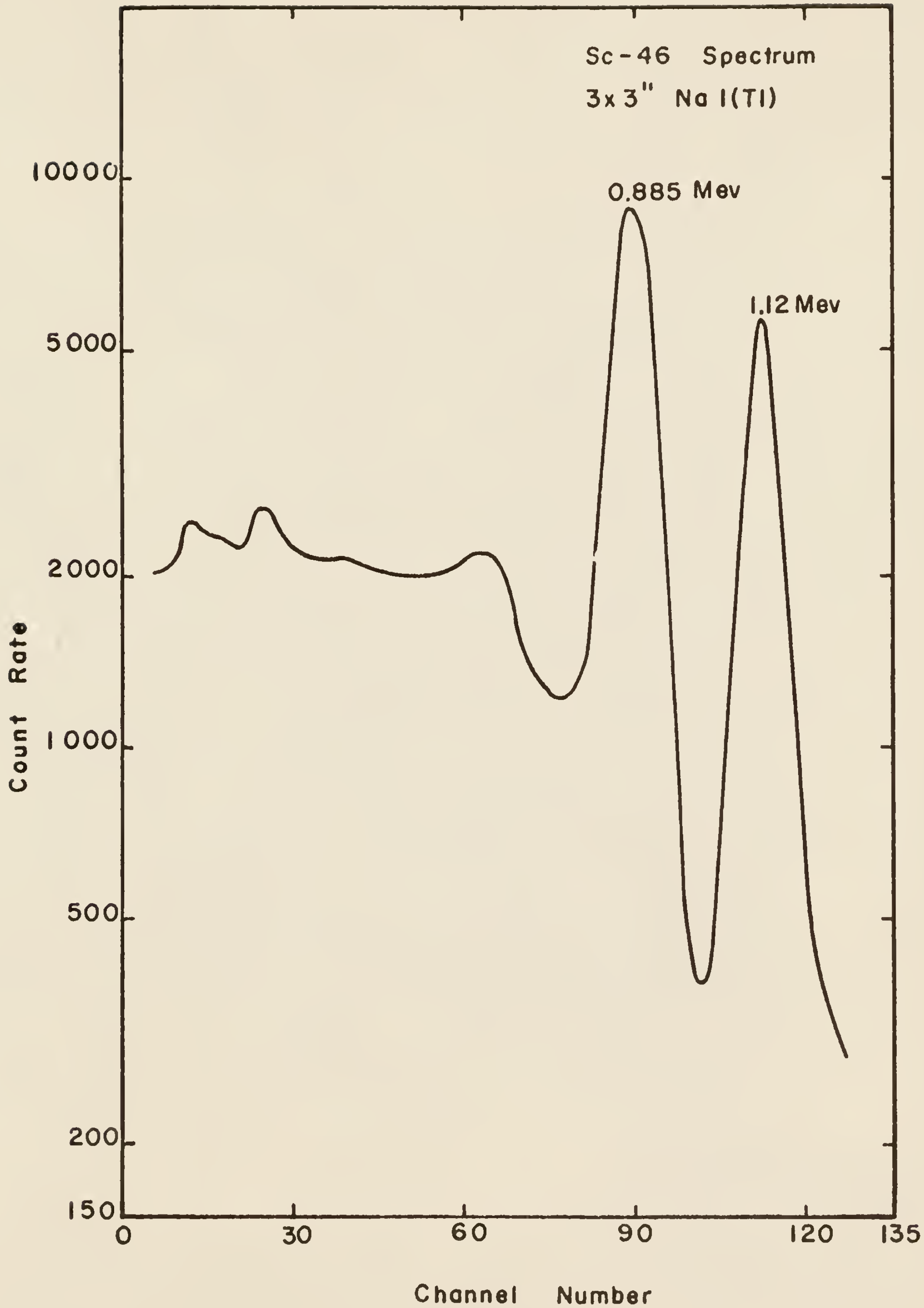

Figure 5 Scandium - 46 Spectrum

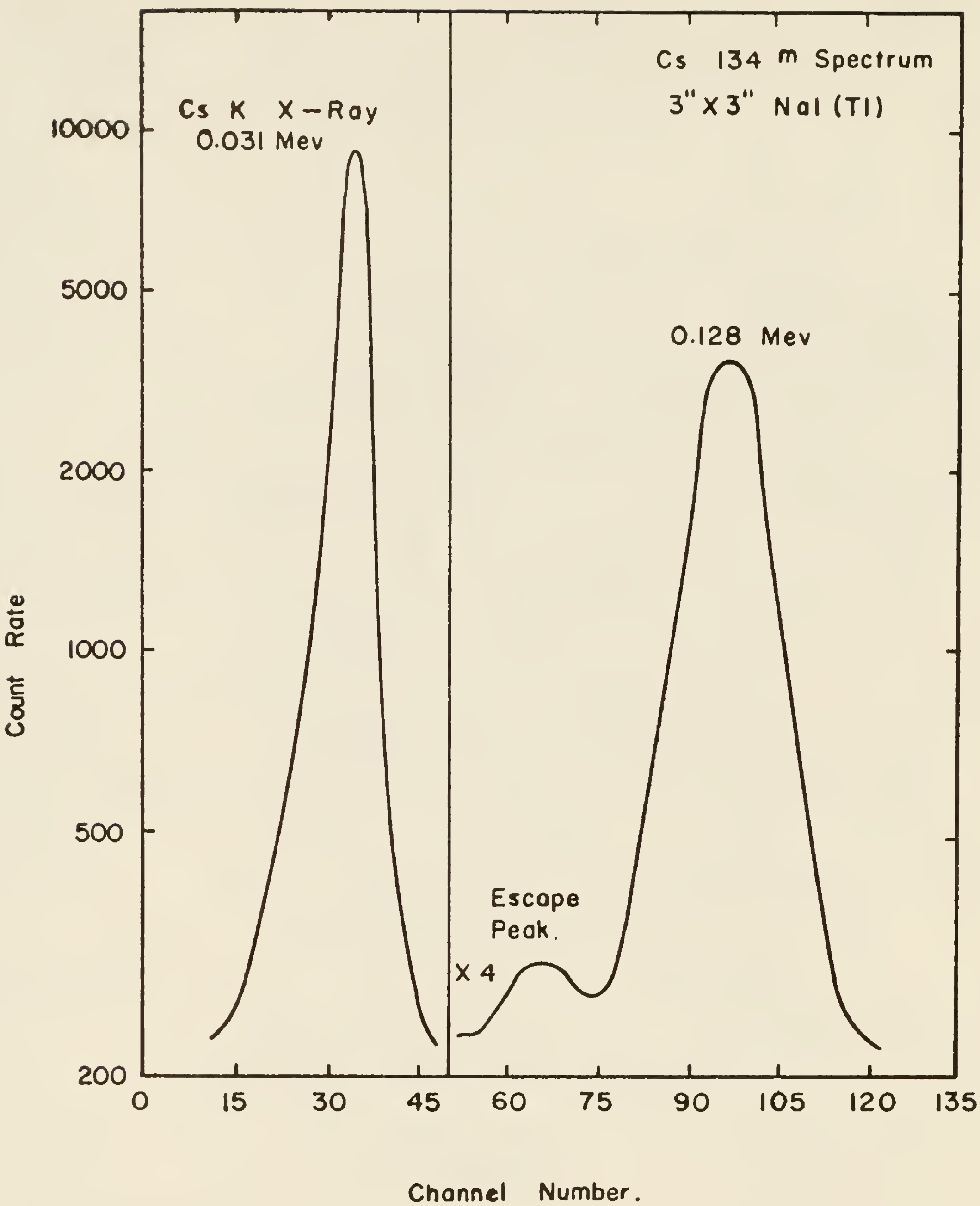

Figure. 6 Cesium 134 m Spectrum .

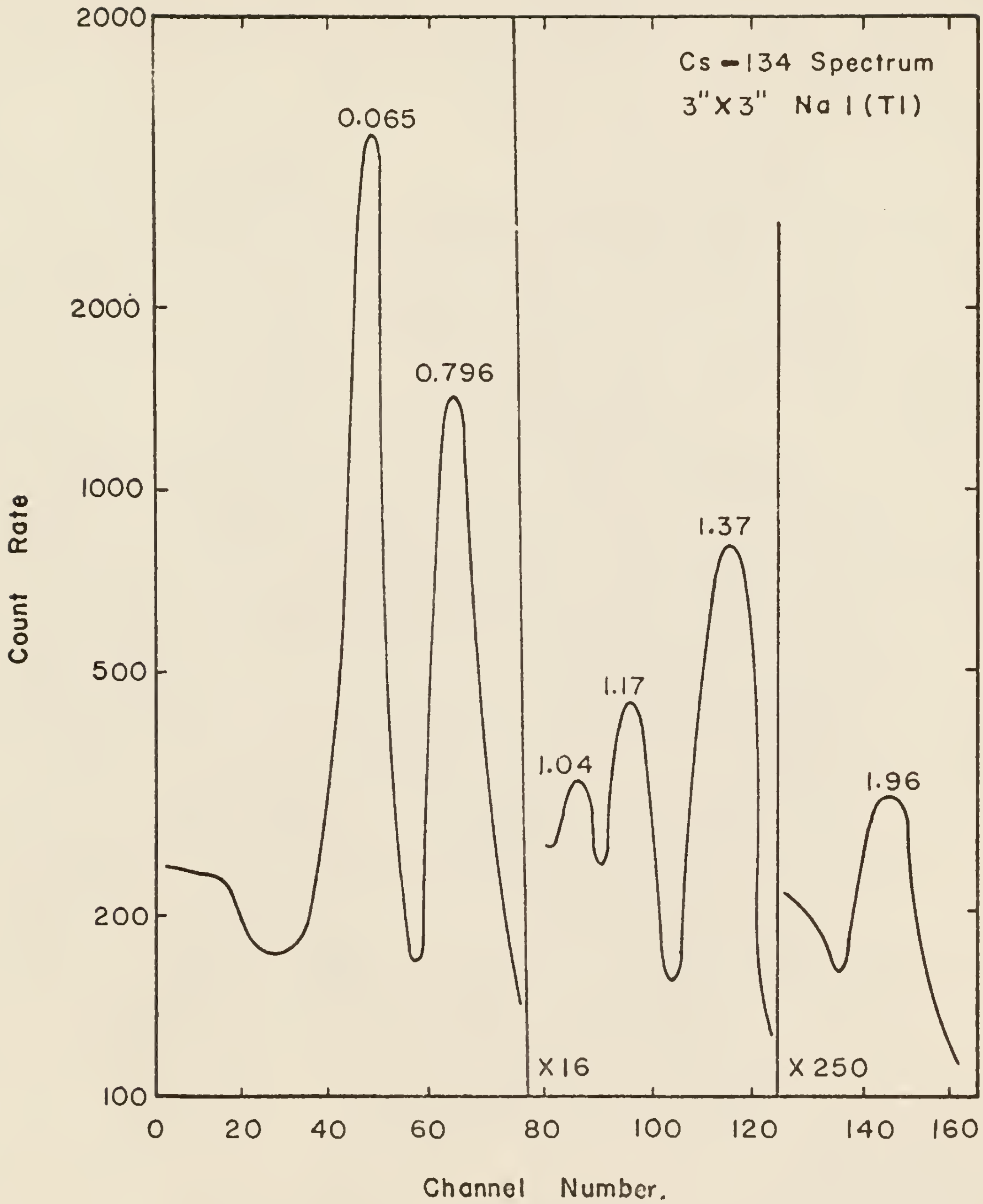

Figure. 7 Cesium — 134 Spectrum. Peak energies are in Mev.

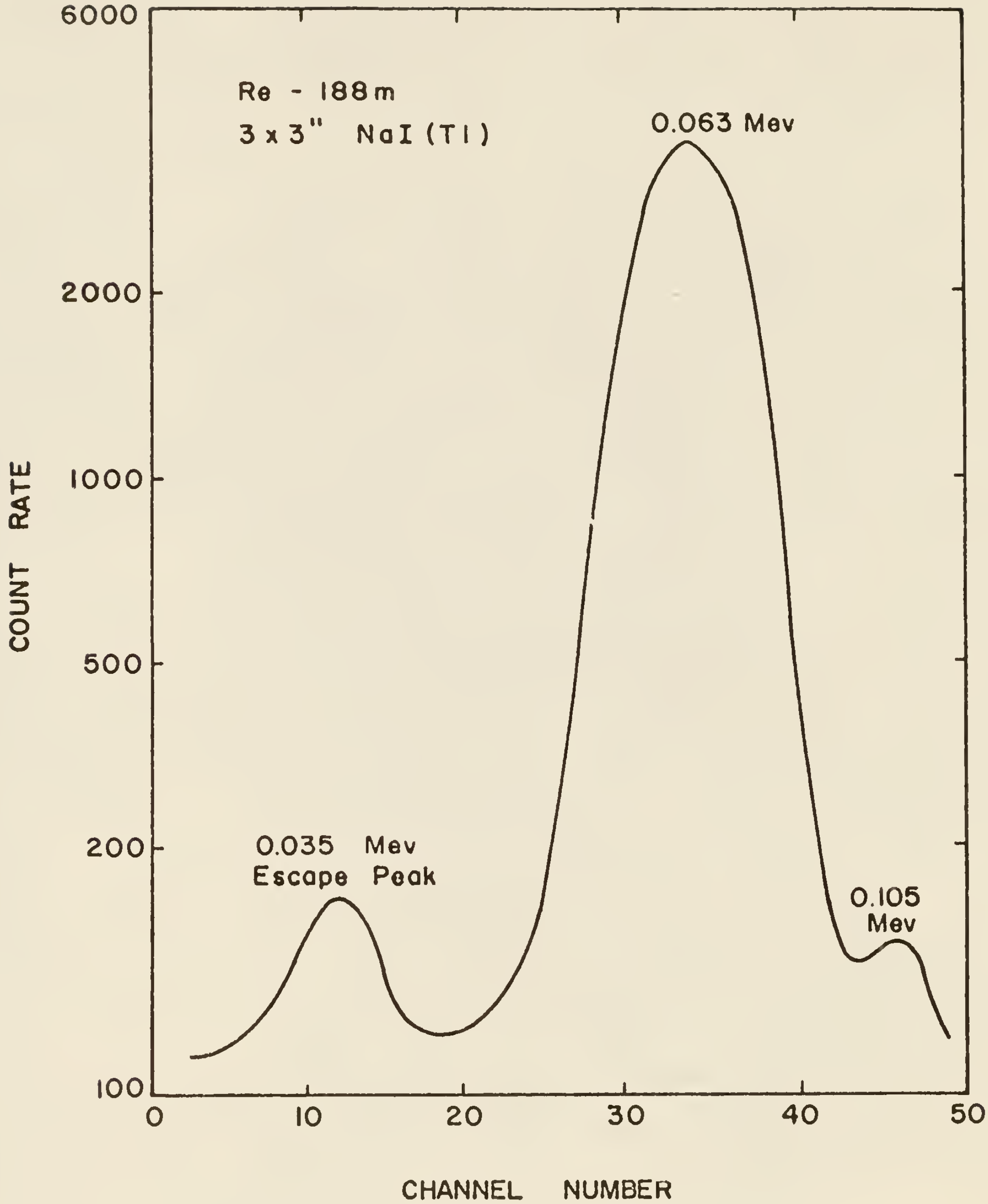

Figure 8 Rhenium 188m Spectrum

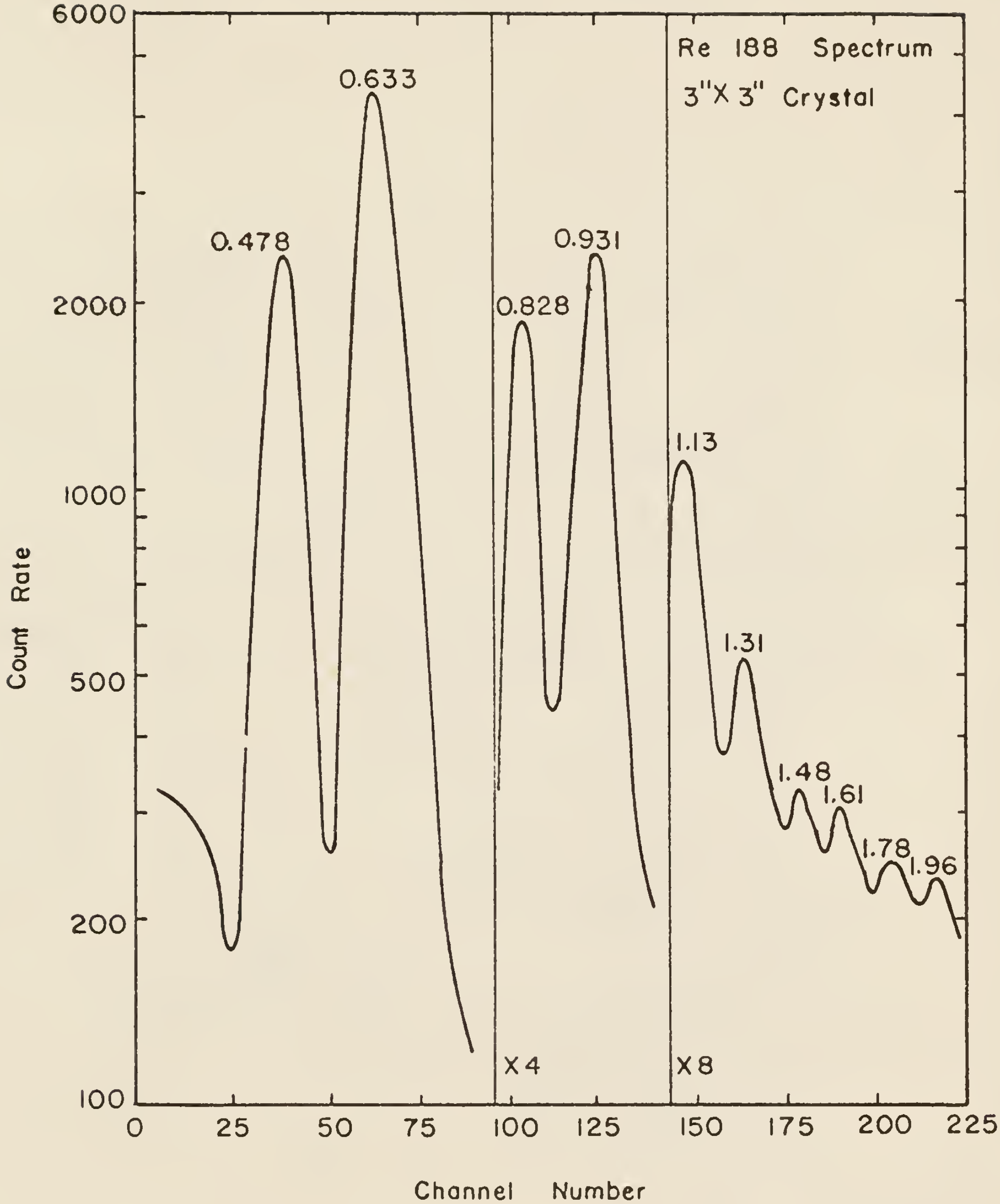

Figure. 9 Rhenium — 188 Spectrum. Peak energies are in Mev.

3.3 Sample Irradiation

Cross section ratios were determined for three ranges of neutron energies; RSR, epi-cadmium and thermal. The RSR and epi-cadmium neutrons were obtained in the rotary specimen rack of the Kansas State University TRIGA Mark II reactor. The average cadmium ratio in the rotary specimen rack, defined as the ratio of the saturation activity of a bare indium foil to the saturation activity of the same foil completely covered with 40 mil cadmium, is approximately 4. At a reactor power level of 100 kilowatts, the total flux, as determined by bare gold foils, was approximately 1.57×10^{12} n/cm^2-sec, and the average epi-cadmium flux, as determined by gold foils wrapped in 40 mil cadmium, was approximately 2.59×10^{11} n/cm^2-sec. Thermal neutrons were obtained in the reactor thermal column where the flux was approximately 10^9 n/cm^2-sec†. To avoid shutting the reactor down after each thermal neutron irradiation a Flex-O-Rabbit pneumatic transfer system with nitrogen supply was used.

One mg of each sample to be irradiated was placed in a small polyethylene vial inside a standard polystyrene irradiation container, Figure 10. To keep the geometry constant during counting, each sample, except scandium samples, was removed from the reactor following irradiation and mounted on scotch tape. It was then placed in a clean polyethylene vial along with a polyethylene insert which held the sample in a fixed position. Samples to be irradiated in the epi-cadmium energy range were placed in 40 mil cadmium cups, irradiated in standard polystyrene vials, then taken out of the cadmium cups and fixed for counting as described above. Due to the short half life of the Sc-46m isomer all scandium samples were mounted on scotch tape and inserted in poly-

† General Atomic special report number GACP-874.

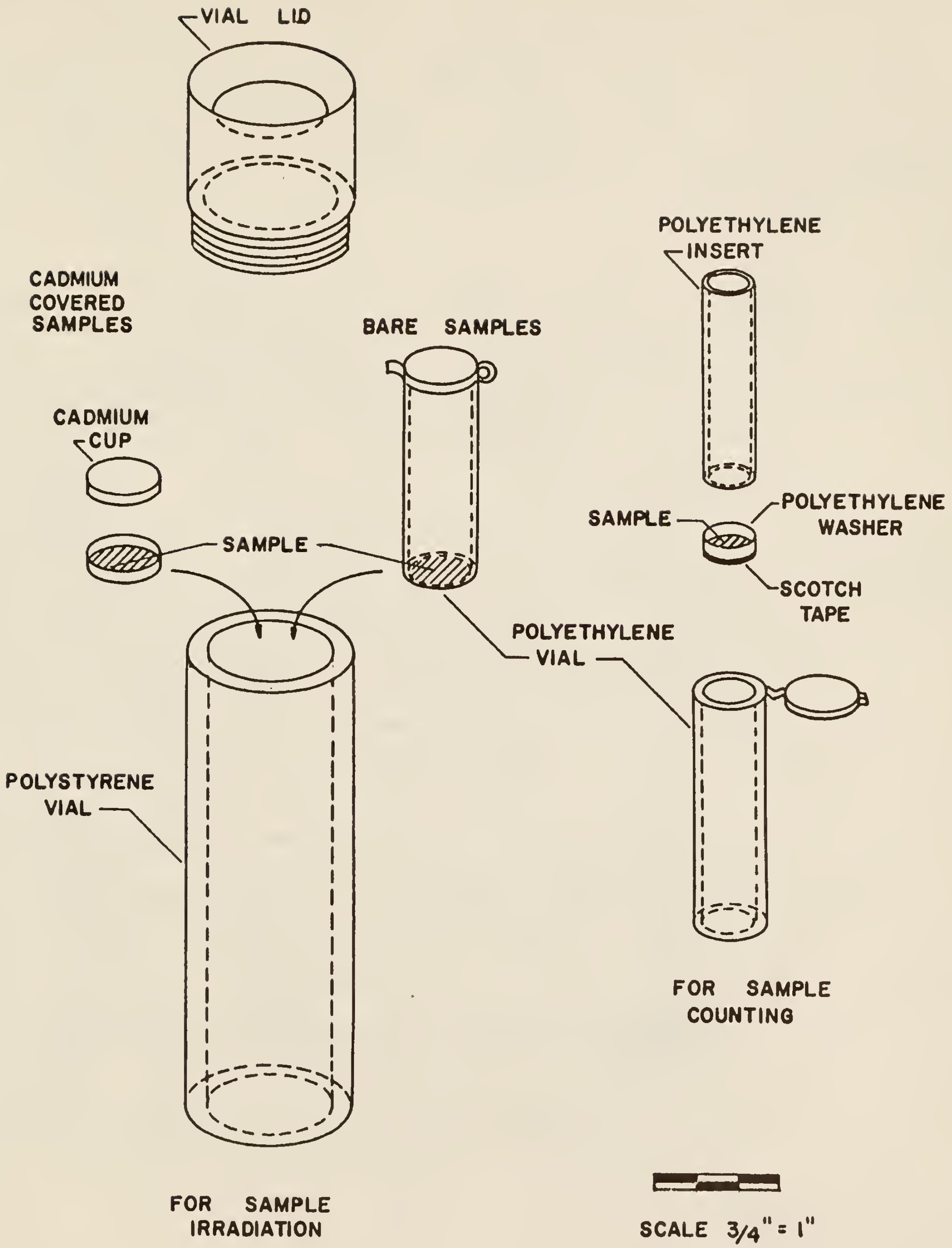

Figure 10 SAMPLE IRRADIATION CONTAINERS

ethylene vials prior to irradiation. Blank samples containing scotch tape, washer, insert and vial were irradiated and counted under the same conditions as the scandium oxide samples, and the count rate was negligible.

Irradiation and decay times were chosen such that the detector was never exposed to count rates in excess of 1,000 cps. This precaution was taken in order to reduce phototube fatigue and hence minimize detector drift. A scintillation detector containing a 2 x 2 inch NaI(Tl) crystal was always used to measure the activity of the sample before counting it by the standardized system to make sure that its count rate was equal to or less than 1,000 cps.

3.4 Counting

3.4.1 General Considerations

Isomeric cross section ratios can be determined by:

Method 1. Following the buildup in gamma ray activity of the stable state due to the direct decay of the metastable state into the stable state.

Method 2. Employing absolute counting and measuring the disintegration rates of the metastable and stable states separately.

Under one or more of the following conditions it is very difficult to use Method 1.

(A) A large difference exists between the metastable and stable state half lives.

(B) Half life of the stable state is very long.

(C) Stable state decays primarily by beta decay.

Each of the isomeric pairs investigated in this work, as indicated below, satisfies at least one of the above conditions. Absolute counting, Method 2, had therefore to be used in every case.

Bishop (4) used the first method to measure the cross section ratio of Cs-134,134m. He stated that his results could be in error since the stable state activity increased only 5% in eight hours due to the large difference in the half lives of the metastable and stable states (3.2 hours and 2.07 years).

The Sc-46,46m isomeric pair (19 sec, 85 day) is an example of condition (A). The buildup in Sc-46 due to the decay of Sc-46m could not easily be followed. During irradiation of Sc-45 the activity of the 19 second Sc-46m became very intense compared to the activity of the 85 day Sc-46, which made it difficult to measure the Sc-46 activity in presence of the Sc-46m. To measure an increase in the activity of the Sc-46 due to direct decay of the Sc-46m the Sc-46 has to be counted immediately upon removal from the neutron flux before appreciable decay of the Sc-46m occurs. In actual experimental trials, a factor of 100 decrease in the activity of the sample in the first two minutes was observed. This change in sample activity caused the Sc-46 photopeak to drift several channels due to short term drift of the photomultiplier tube and hence made it impossible to obtain accurate buildup of the Sc-46 state. An attempt to remove the Sc-46m gamma ray (0.142 Mev) using a lead absorber was made but production of lead X-rays was excessive and caused problems similar to those described above. Assuming the 0.142 Mev Sc-46m gamma ray and the lead X-ray could be completely eliminated, only a very small buildup of the Sc-46 could have been measured. Method 2 had therefore to be used.

Re-188 decays to the ground state primarily by emitting betas. Only about 1% of the decay occurs by beta emission followed by gamma ray emission. The gamma ray buildup in Re-188 activity due to the decay of the Re-188m state is extremely small. Interference of the Re-188m internal conversion electron and gamma rays prohibited integral beta counting.

3.4.2 Absolute Counting

The count rate A of a gamma radioactive sample in the photopeak energy range is related to the number of its radioactive atoms N, and its decay constant λ by

$$A = E_T \lambda N \tag{79}$$

where E_T is the efficiency of counting. For a NaI(Tl) crystal E_T can be expressed as follows

$$E_T = E_E E_P E_I E_X E_G E_A E_B E_C E_R \tag{80}$$

where

E_E = Intrinsic efficiency

E_P = Peak-to-total ratio

E_I = Internal conversion (electron conversion) factor

E_X = Iodine X-ray escape peak factor

E_G = Geometry factor

E_A = Absorption factor

E_B = Backscatter factor

E_C = Coincidence summing factor

E_R = Branching ratio factor

The relative importance of any one of the above factors is dependent, among other things, upon the particular type of decay scheme, gamma ray energy, counting system, source location and type of crystal.

Intrinsic Efficiency

A gamma ray entering a crystal may lose its energy in one of three ways, photo-electric interaction, Compton scattering, or pair production. The probability that the interaction in the crystal will produce a photon with energy large enough to cause an interaction with the photo-cathode and be detected by the counting system is called the intrinsic efficiency. This intrinsic efficiency is a function of the incident gamma ray energy, and the size, type, and shape of the crystal. Extensive work has been done on calculating the theoretical intrinsic efficiency of right circular cylindrical NaI crystals using point and disk sources (19). Hence, the theoretical intrinsic efficiency can be used to determine the disintegration rate of a source from experimental count rate data.

Peak-To-Total Ratio

The pulse-height distribution obtained by a scintillation detector for a monoenergetic gamma ray is unique. If all pulses due to radiation scattered off the radiation shield, beta absorber or other material in the vicinity of the detector are accounted for and subtracted from the total spectrum, the area under the resulting pulse-height distribution curve yields the total number of photons detected by the crystal due to the source in a given time. If a multi-channel pulse-height analyzer is used, the integration can be accomplished by the simple addition of the channel counting rates, since all pulses are accounted for, in one channel or another.

Since it is normally difficult to obtain measurements under ideal conditions, use is usually made of a very convenient quantity: the photo-efficiency or peak-to-total ratio. This quantity, E_p, is the ratio of the number of counts falling under the photopeak to the total number of counts. The peak area is normally defined as that of a symmetrical Gaussian shape, fit to the peak of the experimental photopeak.

By applying the peak-to-total ratio to the experimentally determined photopeak area, the total area under the gamma ray spectrum curve can be obtained.

Internal Conversion

A nucleus in an excited state can pass spontaneously to a state of the same nucleus, but of lower energy, either by emitting a gamma ray with an energy $h\nu$ equal to the difference between the energies of the two nuclear states, or by giving the energy to an electron in the K, L, ..., shell of the same atom. When the energy is given to the electron, it is called internal or electron conversion. The electron is ejected with kinetic energy $h\nu - E_K$, $h\nu - E_L$, ..., where E_K, E_L, ..., are the binding energies of the electrons in the K, L, ..., shells, respectively (29).

The internal conversion coefficient, α, is defined as

$$\alpha = \frac{\lambda_e}{\lambda_g} = \frac{N_e}{N_g} \tag{81}$$

where

N_e = Number of electrons per disintegration

N_g = Number of gamma rays per disintegration

λ_e = Probability of an electron interaction per unit time

λ_g = Probability of a gamma ray interaction per unit time

The total probability λ, is therefore

$$\lambda = \lambda_e + \lambda_g = \lambda_g(1 + \alpha) \tag{82}$$

where α is the total internal conversion coefficient defined as

$$\alpha = \alpha_K + \alpha_L + ---- \tag{83}$$

The α_K, α_L, ..., refer to the internal conversion coefficients for the K, L, ..., shells respectively. In the L shell there are levels L_I, L_{II} and L_{III} giving α_{L_I}, $\alpha_{L_{II}}$, and $\alpha_{L_{III}}$.

The fraction of de-excitations giving a gamma ray is

$$e_g = \frac{1}{1+\alpha} \quad . \tag{84}$$

In addition to the properties of the initial state, the conversion coefficients are strongly dependent on the following parameters: k, where kmc^2 is the transition energy; Z, the atomic number, L the angular momentum change and finally, on the change in parity.

If the nuclear angular momenta for initial and final states are J and J_f, the field radiated can have any angular momentum L for which

$$\Delta J = |J - J_f| \leq L \leq J + J_f \quad . \tag{85}$$

The internal conversion coefficient is therefore

$$\alpha = \sum_L A_L \alpha_L \ , \quad \sum_L A_L = 1 \tag{86}$$

where A_L represents the relative intensities of the gamma rays, of angular momentum L, which are in competition with the conversion electrons. To determine the values of A_L, it has been found that for a magnetic or electric multipole

$$\frac{A_{L+2}}{A_L} \approx \frac{R}{\lambda}^4 << 1.0 \tag{87}$$

where R is the radius of the nucleus and λ is the wavelength.

Also, for magnetic, Mi, and electric, En, multipoles, where i and n correspond to values of L for each multipole,

$$\frac{1 - An}{An} = \frac{Ai}{An} = \frac{(K/L)\alpha(L;En) - \alpha(K;En)}{\alpha(K;Mi) - (K/L)\alpha(L;Mi)} \tag{88}$$

where K/L is the ratio $\alpha(K)/\alpha(L)$, and $\alpha(L;En)$ is the internal conversion coefficient for the L shell corresponding to electric poles of order 2^L. In most cases

$$\frac{A_1}{A_2} \gg 1.0 \quad . \tag{89}$$

Internal conversion coefficients have been measured experimentally for several of the radioactive nuclides, these are tabulated in the Nuclear Data Sheets (26). Rose (29) has theoretically calculated internal conversion coefficients for nuclides with Z numbers from 25 to 95.

Iodine X-Ray Escape Peak

A gamma ray may excite an iodine ion in a NaI(Tl) crystal causing it to emit a 28.4 Kev gamma ray. When this occurs, a peak is formed with energy 28.4 Kev less than the energy of the photopeak, called the "escape peak." At high incident gamma ray energies, e.g., the 0.885 Mev of Sc-46, NaI(Tl) scintillation spectrometer resolution would not separate the escape peak from the photopeak. However, at energies below 150 Kev, e.g., the 142 Kev of Sc-46m, the two peaks do appear separately and a correction must therefore be applied to the photopeak. Since the photopeak has the higher intensity and the higher energy of the two, it is more convenient to use the photopeak alone for making intensity measurements.

Axel (1) has calculated the fraction of iodine x-rays escaping as a function of source geometry and incident gamma ray energy, Figure 11. He used the following geometry identification:

(A) Very "poor" geometry, which is the case of a source in contact with the crystal; it corresponds to a cone with a half angle of 90°.

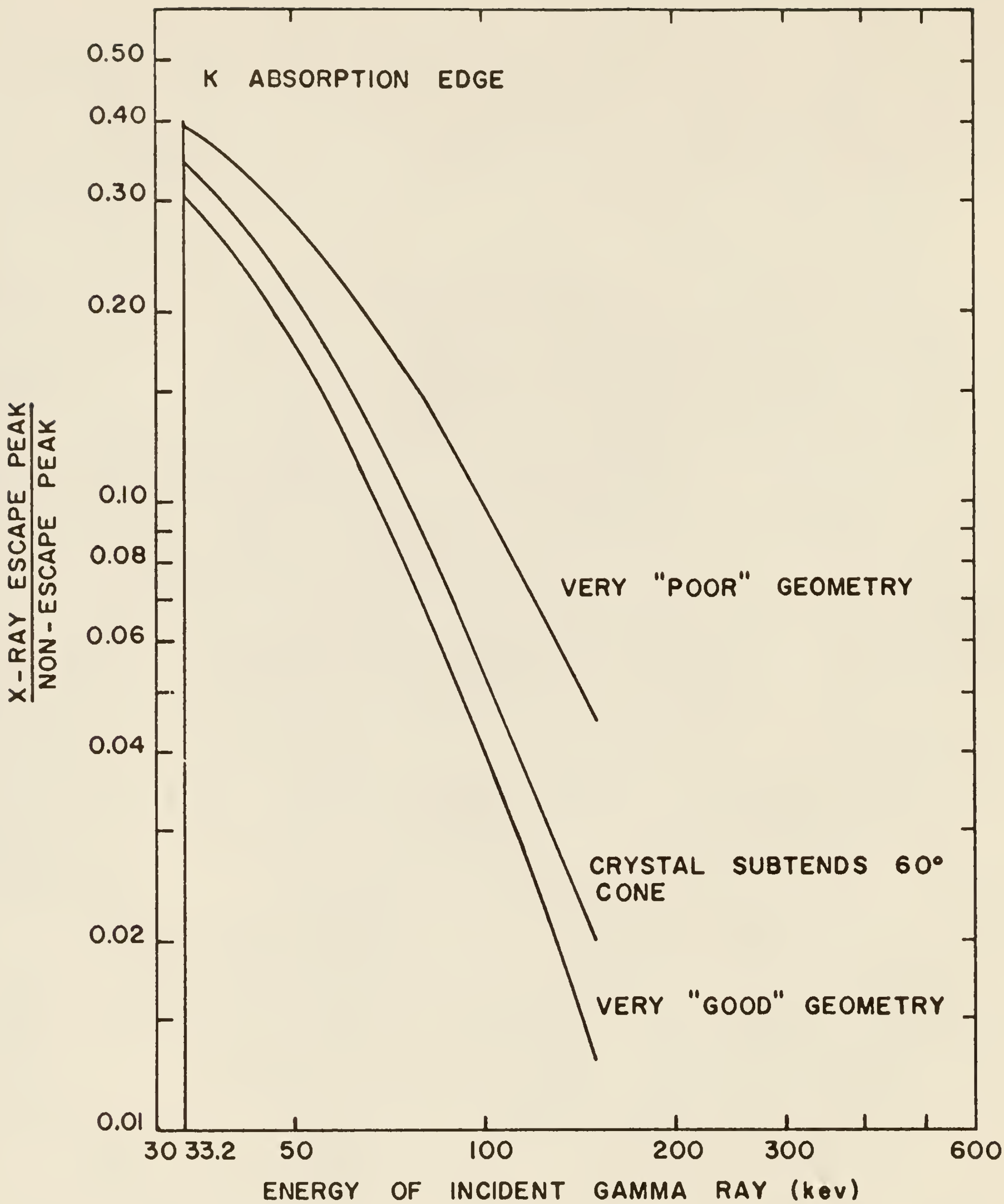

Figure 11 X-RAY ESCAPE PROBABILITY FOR INFINITELY THICK INFINITELY WIDE CRYSTAL.

(B) Intermediate geometry is the case of crystal subtending with the source a cone whose half angle is 60°.

(C) Very good geometry is the case of a well collimated beam incident normally, i.e., when the source is at a great distance from the crystal.

The true photopeak area for gamma rays with energy less than 150 Kev can therefore be determined by applying the iodine x-ray escape peak correction factor to the experimentally measured photopeak area.

Geometry

The geometry factor E_G is the fraction of the total source radiation which is emitted in a direction such that it will strike the sensitive volume of the detector. In most cases, isotropic sources are used, hence, initially all directions are equally probable. The configuration of the source and detector determines the fraction of the source radiation reaching the detector.

Kohl (24) gives methods for calculating E_G for different source and detector arrangements. Methods of calculating geometry factors are also given in Price (27) and Crouthamel (10).

It is evident that in actual experimental work, the geometry factor must be calculated for the particular source and detector configuration used.

Absorption

Gamma ray absorption may occur in the air, sample backing, and/or container, crystal shield, and external absorber. The number of gamma rays entering a crystal is given by

$$N = N_o e^{-\mu_T(E_o)x_T} \tag{90}$$

where N_o is the number of gamma rays emitted by the sample, $\mu_T(E_o)$ is the total absorption coefficient for a gamma ray of energy E_o(16), and x_T is the total thickness of absorber. For multiple absorbers

$$\mu_T(E_o)x_T = \mu_A(E_o)x_A + \mu_B(E_o)x_B \tag{91}$$

where subscripts A and B refer to materials A and B.

Applying the absorption factor to the experimentally measured number of gamma rays incident upon the crystal corrects for the number of source gamma rays absorbed before reaching the crystal.

Backscatter

One of the most important considerations in obtaining good data in scintillation spectrometry is the design of the radiation shield. For convenience it is desirable to reduce the background radiation level to a point where corrections to the data will be small for the moderate strength sources usually prepared in the laboratory.

In any type of analysis of data obtained on the scintillation spectrometer a differentiation must be made between the response of the detector to direct radiation from the source and spurious scattered radiation arising from interaction with the surrounding material; i.e., source holder, beta absorber and radiation shield.

This scattered radiation results from two types of interaction, the photoelectric process and Compton scattering.

The photoeffect is of particular importance in shield design since the cross section for this process is high for low energy photons, particularly in materials such as Pb. This process results in the production of x-rays characteristic of the absorbing material.

The major source of spurious radiation from the shield is due to Compton scattering. The energy distribution observed by a detector from Compton scattering off the walls of the radiation shield depends upon the particular geometrical arrangement of source, shield and detector.

In actual experimental work the backscatter effect can be made negligible by using a large graded shield, see Section 3.4.4.

Coincidence Summing

If two gamma rays are in cascade a third peak of area N_b appears in the spectrum (coincident sum peak) when both gammas are completely absorbed in the crystal. There is also a statistical probability that two independent gamma ray transitions, taking place within the resolving time of the linear amplifier, be completely absorbed in the crystal. If additional area in the sum peak due to these accidental sum events is N_{ab}, the total sum peak will be

$$N_T = N_b + N_{ab}. \tag{92}$$

This area can be measured experimentally and added to the photopeak area N_1 to correct for summing. The sum correction factor is

$$S = (N_1 + N_T)/N_1 \tag{93}$$

Branching Ratio

In a complex de-excitation process the number of gamma rays per disintegration may be equal to or less than unity (22). The branching ratio is defined as the number of gamma rays per disintegration. In absolute counting it is essential to include this ratio. Such ratios can be obtained from references (10 and 26).

Other Factors

Temperature variations and instability of the counting system will also affect the obtainment of accurate data. Ball (2) has determined the temperature coefficient for NaI(Tl) to be -0.1% per degree C. The phototube dynodes are also temperature sensitive, having a temperature coefficient of approximately -0.2% per degree F (23). Phototube fatigue can cause errors due to spectrum shift (7, 9). High voltage stability also is important because a 1% change in high voltage on a ten stage phototube will result in a 7% change in output signal.

It is therefore necessary to maintain the NaI(Tl) scintillation detector at a fairly constant temperature. The choice of photomultiplier tubes is important, tubes with CuBe dynodes have more stability than CsSb dynodes with respect to spectrum shift.

3.4.3 Modified Absolute Counting Equations

For an isomeric pair the ratio of the disintegration rates at the end of the irradiation period is given by

$$\frac{\lambda_2 N_2}{\lambda_1 N_1} = \frac{E_{T1}\ A_2^{\circ}}{E_{T2}\ A_1^{\circ}} \tag{94}$$

where subscript 1 refers to the metastable state, subscript 2 to the ground state and superscript 0 to the activity at the end of irradiation.

Each of the efficiency terms E_{T1} and E_{T2} is composed of the nine factors indicated in Section 3.4.2. These terms have, however, been simplified as follows:

a) The peak to total ratio and intrinsic efficiency were combined to form a peak intrinsic efficiency term E_{PE}.

b) All samples were counted in the same position, the geometry factor was therefore canceled in the ratio.

c) The radiation shield surrounding the counting system was designed to minimize backscattering. Actual data showed that backscattering was negligible.

d) Spectra obtained showed extremely small areas under the summation peaks, the coincidence summing factor was therefore dropped.

As extra precautions, the temperature of the counting system was kept constant within ± 2°F and a very stable high voltage supply was used.

Under the conditions indicated above Eq. (94) takes the form

$$\frac{\lambda_2 N_2}{\lambda_1 N_1} = \frac{E_1 P_2^0}{E_2 P_1^0}$$

where

$$P^0 = \text{photopeak area}$$

$$E = E_{PE} E_I E_X E_A E_R \ . \tag{96}$$

The intrinsic peak efficiency of a 3 x 3 inch crystal with a 1/2 x 1-1/2 inch well was determined by Ross (30) for gamma ray energies between 0.32 and 1.2 Mev. By comparing the intrinsic peak efficiency for a 3 x 3 inch solid crystal to the 3 x 3 inch well crystal and using the accurately known intrinsic peak efficiency for solid 3 x 3 inch crystals in the energy range 0.01 to 0.32 Mev the intrinsic peak efficiency for the 3 x 3 inch well crystal was determined for gamma ray energies of 0.01 to 1.2 Mev, see Figure 12.

Internal conversion coefficients have been determined experimentally for most materials (26). Where possible these experimental values were used; if different values were determined by different authors the values were averaged as shown in Table II. For scandium, theoretical values were taken from Rose (29) and averaged with an approximate value determined experimentally (26).

In this work, Axel's (1) (very poor geometry) values were used for the iodine escape peak correction factor since the source was inside the 3 x 3 inch well crystal.

Table III gives the numerical values for the efficiency factors used, indicating references from which the values were obtained, and energies of the gamma rays investigated.

Table II. Internal conversion coefficients.

Isomer	Reference	Energy (Mev)	K/L	α_K	α_L	α	E_I
Cs-134m	(26)	0.127	---	2.2 2.6 2.8 2.6 Avg. 2.55	---	2.55	0.125
Cs-134	(26)	0.605	6.4 7.0 6.3 7.7 7.2 Avg. 6.9	0.0047 0.0057 0.0058 Avg. 0.0054	0.00078	0.00618	0.994
	(26)	0.796	7.3 8.0 7.0 7.3 Avg. 7.4	0.00251 0.00261 Avg. 0.00254	0.000344	0.00288	0.997
Sc-46m	(26)	0.142	10	---	---	1	0.349
	(29)	0.142	10.9	---	---	2.73 Avg. 1.86	
Sc-46	(26)	0.885	---	---	---	0.0008	0.999
Re-188m	(26)	0.0635	---	---	---	2	0.333
Re-188	(26)	0.155	0.70 0.79 Avg. 0.75	0.40 0.29 0.37 0.353	0.474	0.828	0.547

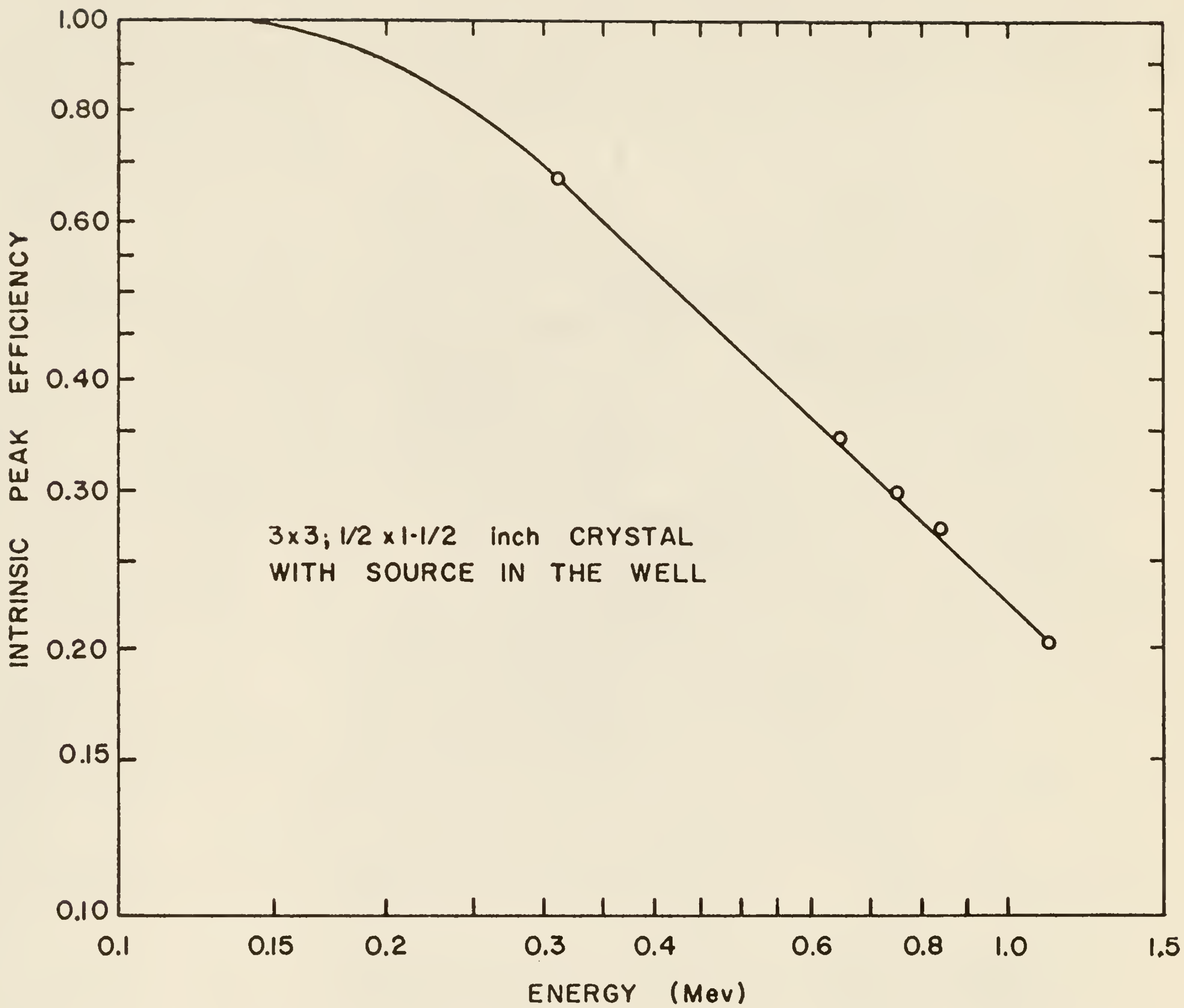

Figure 12 MEASURED INTRINSIC PEAK EFFICIENCY OF VARIOUS NaI(Tl) CRYSTALS.

Table III. Efficiency values for scandium cesium and rhenium

Isomer	Energy (Mev)	E_{PE}	E_I	E_X	E_A	E_R	E
		a	b	c	d	e	
Cs-134m	0.127	1.00	0.125	0.942	0.964	1.00	0.114
Cs-134	0.605	0.352	0.994	1.000	0.981	0.981	0.343
Cs-134	0.796	0.283	0.9972	1.000	0.993	0.725	0.199
Re-188m	0.0635	1.000	0.333	0.826	0.944	1.000	0.269
Re-188	0.155	0.980	0.547	0.959	0.969	1.000	0.508
Sc-46m	0.142	1.000	0.349	0.952	0.966	1.000	0.321
Sc-46	0.885	0.250	0.999	1.000	0.984	1.000	0.249
Sc-46	1.112	0.205	0.999	1.000	0.985	1.000	0.204

Reference number

a 30
b see Table 2
c 1
d 16
e 10, 26

3.4.4 Counting Equipment

A block diagram of the counting equipment used is shown in Figure 13. It consisted of a Technical Measurements Corporation 256 channel pulse height analyzer, a Hewlett Packard Model J44-561-B digital recorder, a Harshaw integral line gamma ray scintillation detector with a Dumont 6363 photo-multiplier tube, a Technical Measurements Corporation Model DS-13 transistorized pre-amplifier, a John Fluke Model 400-BDA power supply, a Reactor Experiments Incorporated pneumatic transfer system with a nitrogen gas supply, and an external timer.

The scintillation detector was composed of a hermetically sealed 3 x 3 inch NaI(Tl) crystal with a 0.015 inch aluminum entrance window attached to a photo-multiplier tube through an optical coupling medium.

A large graded radiation shield (26 x 26 x 24 inches outside dimensions), Figure 14, was designed to reduce the background radiation level to a negligible value compared to that of the sample activity. It had 2 inch thick lead sides constructed from lead bricks; the bricks were supported by 1/4 inch plywood sides and a 3/4 inch plywood top and bottom. The inside of the shield was lined with 20 mil cadmium and 20 mil copper in that order.

The photoelectric process is very high for high Z materials, therefore low energy (0.072 Mev) characteristic x-rays are produced from the lead. The cadmium lining reduces the effect of these lead x-rays and the copper decreases remaining lead x-rays and any cadmium x-rays produced.

Compton scattering is caused by radiation being scattered from the walls of the shield, this radiation would enter the detector with reduced energy. The large dimensions of the shield reduced the probability of Compton scattering. The scintillation detector was located inside the shield so that the

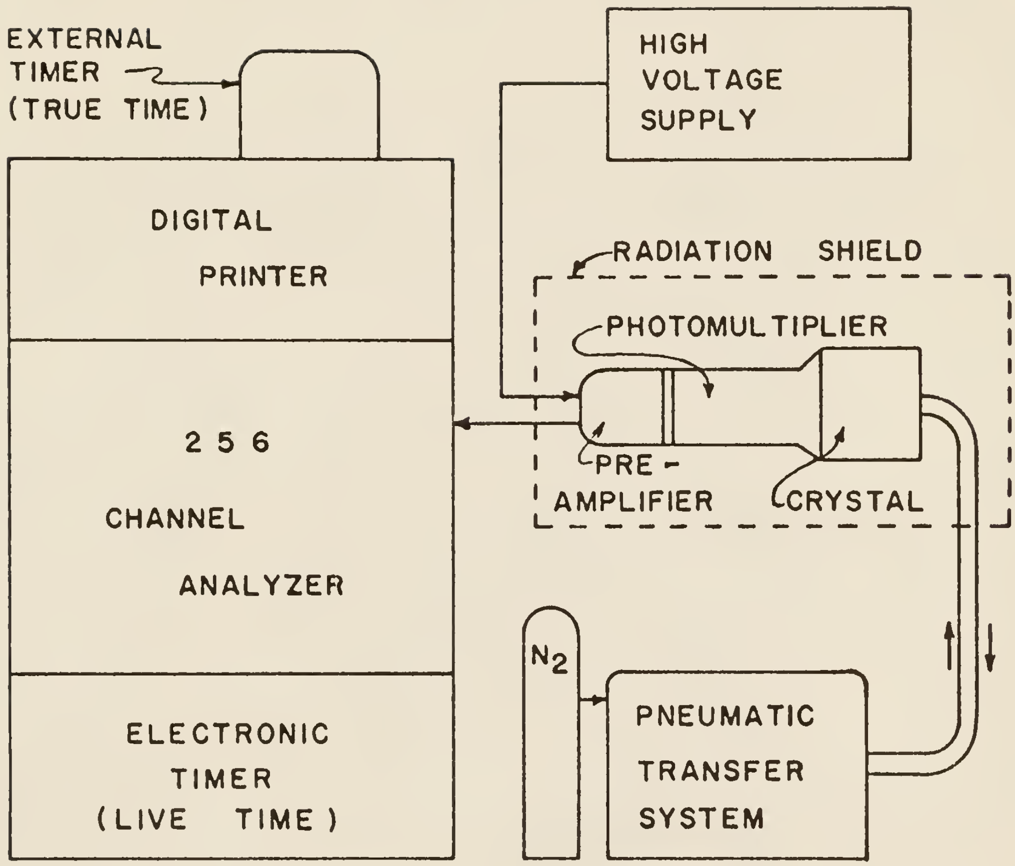

Figure 13 BLOCK DIAGRAM OF COUNTING SYSTEM.

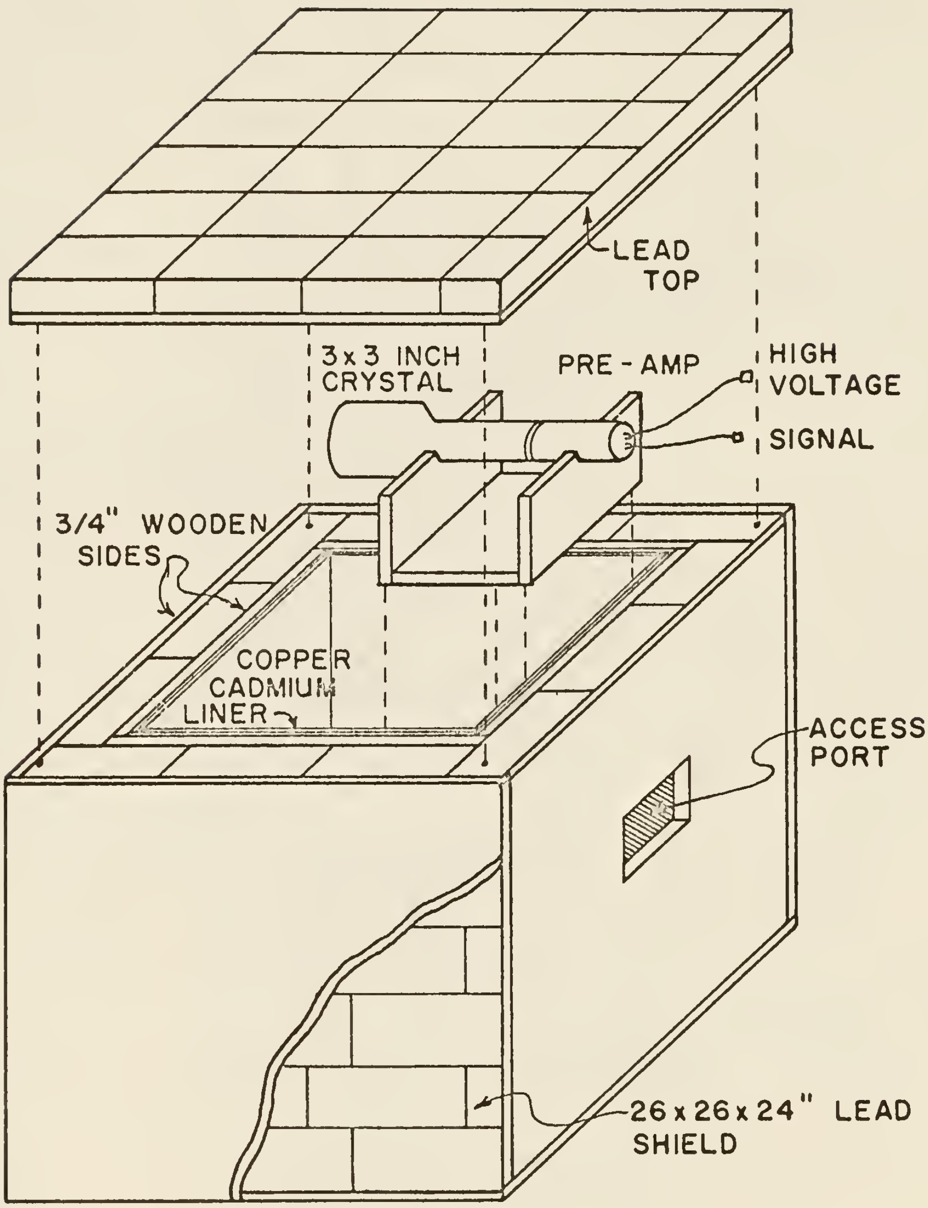

Figure 14 SHIELD AND NaI(Tl) CRYSTAL ASSEMBLY.

NaI(Tl) crystal was centered, i.e., the crystal was positioned at a maximum distance from any scattering surface. Figure 15 shows to what extent the shield reduces the background radiation and also shows the effect the small ungraded shield (4-1/2 x 8 x 8 inches) has compared to the large graded shield on the lead x-rays and Compton scattered radiation.

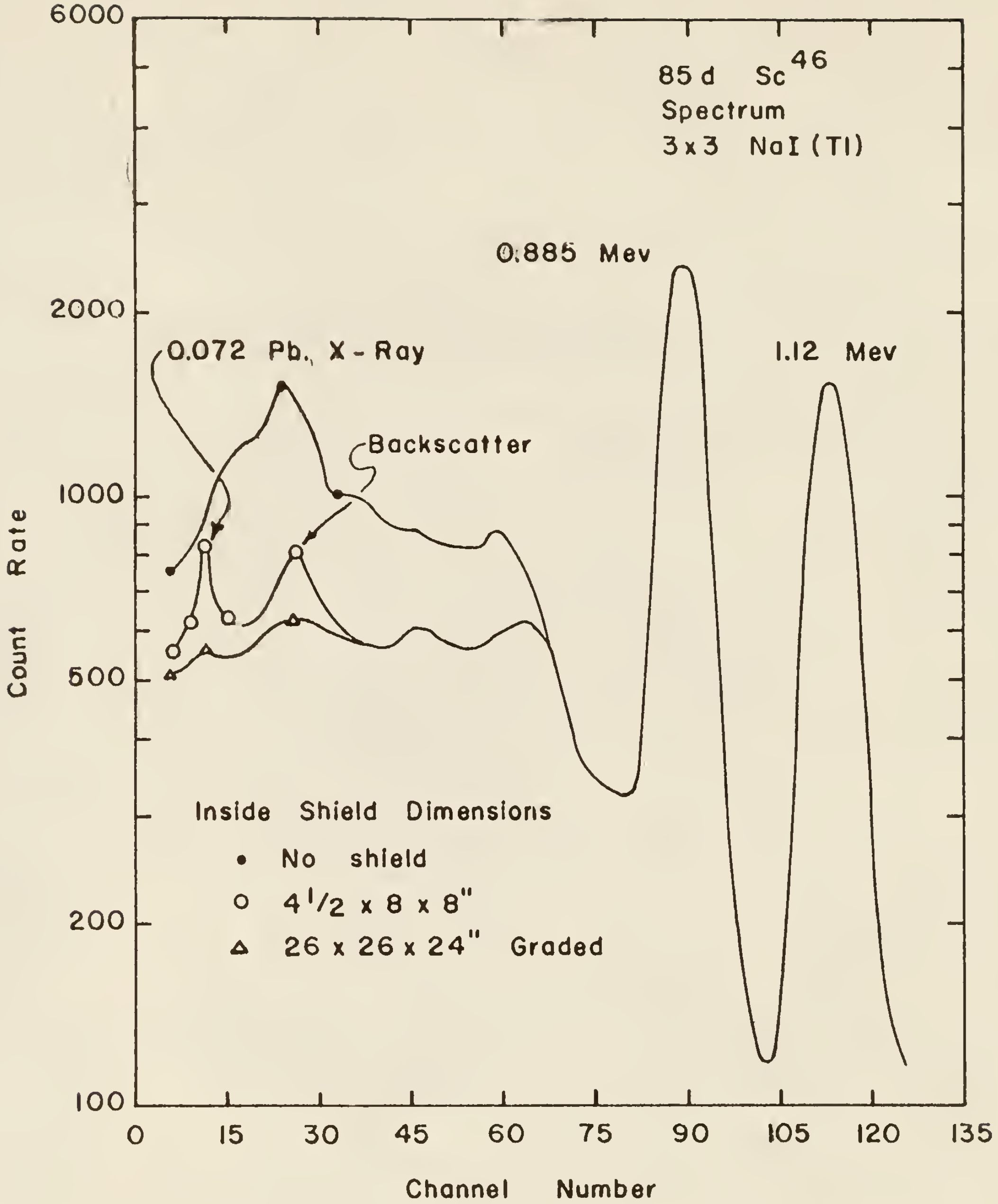

Figure 15 EFFECT OF LEAD SHIELD DESIGN.

3.5 Experimental Procedure

To experimentally determine the isomeric cross section ratios each sample was subjected to the following steps in sequence:

1.) Irradiated in RSR, epi-cadmium and thermal energy neutron fluxes as explained in Section 3.3. Table IV contains the irradiation times and neutron flux values used.

2.) Counted using the counting system described in Section 3.4.4. Table IV shows the decay, irradiation and live-counting times and the number of sets of data taken per isomer, N.

3.) Experimental data were analyzed using the IBM computers as follows: The area under the photopeak was determined by feeding the experimental photopeak data points, corrected for background, into the IBM 1410 computer which fit them to a Gaussian curve (photopeaks are theoretically Gaussian shaped) by the method of least squares combined with Taylor's expansion (see Appendix B). The area under the Gaussian curve which "best fit" the experimental data was then computed. This program is called TOTAL PEAK AREA. This Gaussian area was fed into another computer program, called CROSS SECTION, which corrected it for the Compton distribution and calculated the isomeric cross section ratios (see Appendices C and D).

The goodness of fit of the photopeak to the Gaussian curve was checked by comparing several hand calculated total-peak areas to computer calculated Gaussian areas. The difference did not exceed 0.76%. To check for skewness, the experimental photopeak and Gaussian plots were compared and found to match very closely.

Table V contains the output of the TOTAL PEAK AREA program for a Cs-134 sample. The symbols IMIN and IMAX are the minimum and maximum channel numbers used for the Gaussian fit, X ZERO is the channel number corresponding to the maximum peak count rate SMAX, LAMBDA is the reciprocal of the standard deviation SIGMA, N is the number of iterations and AREA is the total peak area computed.

The output of the CROSS SECTION program for several Cs-134,134m experimental runs is listed in Table VI. The sample number, run number and neutron energy used are listed for each sample where BARE, CD, and TN correspond to RSR, epi-cadmium and thermal neutron energies respectively. The L and H designate the energy of the stable state gamma rays used, for Cs-134 L represents the 0.605 Mev gamma ray and H represents the 0.796 Mev gamma ray.

Table IV. Experimental neutron irradiation and counting data

Isomer Analyzed	N	Neutron Energy	Approximate Flux (n/cm^2-sec)	Time: Irradiation (Min)	Time: Decay (Min)	Time: Counting (Min)
Sc-46m	9	RSR	1.57×10^{12}	5.0	3.0	0.1
	9	Epi-cadmium	2.59×10^{11}	30.0	3.0	0.1
	9	Thermal	1.00×10^{10}	15.0	3.0	0.1
Sc-46	18	RSR	1.57×10^{12}	5.0	990.0	2.0
	18	Epi-cadmium	2.59×10^{11}	30.0	930.0	10.0
	18	Thermal	1.00×10^{10}	15.0	75.0	10.0
Cs-134m	9	RSR	1.57×10^{12}	10.0	30.0	0.5
	9	Epi-cadmium	2.59×10^{11}	21.0	30.0	0.5
	9	Thermal	1.00×10^{10}	126.0	30.0	0.5
Cs-134	18	RSR	1.57×10^{12}	10.0	1570.0	2.5
	18	Epi-cadmium	2.59×10^{11}	21.0	1480.0	5.0
	18	Thermal	1.00×10^{10}	126.0	1000.0	20.0
Re-188m	9	RSR	1.57×10^{12}	0.50	2.0	0.65
	9	Epi-cadmium	2.49×10^{11}	0.50	2.0	0.50
	9	Thermal	1.00×10^{10}	0.75	4.0	0.75
Re-188	9	RSR	1.57×10^{12}	0.50	600.0	3.0
	9	Epi-cadmium	2.59×10^{11}	0.50	580.0	3.0
	9	Thermal	1.00×10^{10}	0.75	565.0	3.0

Table V. Total peak area output for Cs-134.

KANSAS STATE UNIVERSITY IBM 1410 COMPUTING CENTER

CESIUM SAMPLE NUMBER 5 RUN 3 HIGH ENERGY GAMMA

IMIN = 114 IMAX = 135

X ZERO	LAMBDA	SMAX	N
.12100000E 03	.11893620E-00	.84000000E 04	1
.12119428E 03	.13007930E-00	.84026821E 04	2
.12126837E 03	.13976240E-00	.84059102E 04	3
.12128569E 03	.14736640E-00	.84074474E 04	4
.12128188E 03	.15264860E-00	.84077792E 04	5
.12127456E 03	.15584030E-00	.84076918E 04	6
.12126954E 03	.15752880E-00	.84075751E 04	7
.12126702E 03	.15833760E-00	.84075104E 04	8
.12126595E 03	.15870370E-00	.84074852E 04	9
.12126554E 03	.15886560E-00	.84074768E 04	10
.12126539E 03	.15893680E-00	.84074751E 04	11
.12126535E 03	.15896840E-00	.84074760E 04	12
.12126534E 03	.15898250E-00	.84074768E 04	13
.12126534E 03	.15898900E-00	.84074776E 04	14
.12126534E 03	.15899200E-00	.84074776E 04	15
.12126534E 03	.15899330E-00	.84074776E 04	16
.12126534E 03	.15899400E-00	.84074776E 04	17
X ZERO	SIGMA	SMAX	AREA
.12126534E 03	.62895257E 01	.84074776E 04	.13254809E 06

Table VI. Experimental cross section ratios for Cs-134,134m.

CESIUM-134,134M ISOMERIC CROSS SECTION RATIOS USING RSR ENERGY NEUTRONS

Sample	CROSS SECTION RATIO	DEVIATION
CESIUM 1A RUN 4 L	.78790230E-01	0.34341498E-03
CESIUM 1 RUN 5 BARE L	.81422338E-01	0.85228344E-03
CESIUM 1 RUN 6 BARE L	.82004229E-01	0.85908803E-03
CESIUM 3 RUN 1 BARE L	.10977229	0.11188897E-02
CESIUM 5 RUN 1 BARE L	.95990109E-01	0.79232687E-03
CESIUM 5 RUN 2 BARE L	.11290119	0.89429421E-03
CESIUM 5 RUN 3 BARE L	.11261656	0.90195594E-03
CESIUM 1 RUN 4 BARE H	.77190453E-01	0.84137300E-03
CESIUM 3 RUN 1 BARE H	.10251345	0.10289201E-02
CESIUM 3 RUN 2 BARE H	.10631084	0.10582762E-02
CESIUM 3 RUN 3 BARE H	.10642979	0.10634656E-02
CESIUM 5 RUN 1 BARE H	.84005292E-01	0.84554964E-03

Table VI (continued)

CESIUM-134,134M ISOMERIC CROSS SECTION RATIOS USING RSR ENERGY NEUTRONS

CESIUM 5 RUN 2 BARE H	
CROSS SECTION RATIO	DEVIATION
.98994307E-01	0.96357354E-03
CESIUM 5 RUN 3 BARE H	
CROSS SECTION RATIO	DEVIATION
.98740876E-01	0.96980123E-03

CESIUM-134,134M ISOMERIC CROSS SECTION RATIOS USING EPI-CADMIUM ENERGY NEUTRONS

CESIUM 1 RUN 1 CD L	
CROSS SECTION RATIO	DEVIATION
.11481271	0.94057398E-03
CESIUM 1 RUN 2 CD L	
CROSS SECTION RATIO	DEVIATION
.11101626	0.88398753E-03
CESIUM 1 RUN 3 CD L	
CROSS SECTION RATIO	DEVIATION
.10704106	0.88967377E-03
CESIUM 2 RUN 1 CD L	
CROSS SECTION RATIO	DEVIATION
.10002317	0.87615392E-03
CESIUM 2 RUN 3 CD L	
CROSS SECTION RATIO	DEVIATION
.10113262	0.87946661E-03
CESIUM 3 RUN 1 CD L	
CROSS SECTION RATIO	DEVIATION
.98242106E-01	0.96321761E-03
CESIUM 3 RUN 2 CD L	
CROSS SECTION RATIO	DEVIATION
.97946310E-01	0.95993211E-03
CESIUM 3 RUN 3 CD L	
CROSS SECTION RATIO	DEVIATION
.98721384E-01	0.96963127E-03
CESIUM 1 RUN 1 CD H	
CROSS SECTION RATIO	DEVIATION
.98312148E-01	0.96478090E-03

Table VI (continued)

CESIUM-134,134M ISOMERIC CROSS SECTION RATIOS USING EPI-CADMIUM ENERGY NEUTRONS

CESIUM 1 RUN 2 CD H	
CROSS SECTION RATIO	DEVIATION
.93223213E-01	0.87398482E-03
CESIUM 1 RUN 3 CD H	
CROSS SECTION RATIO	DEVIATION
.89528577E-01	0.87008814E-03
CESIUM 2 RUN 1 CD H	
CROSS SECTION RATIO	DEVIATION
.96473118E-01	0.89932143E-03
CESIUM 2 RUN 2 CD H	
CROSS SECTION RATIO	DEVIATION
.95367250E-01	0.89689066E-03
CESIUM 3 RUN 1 CD H	
CROSS SECTION RATIO	DEVIATION
.93169962E-01	0.98790682E-03
CESIUM 3 RUN 2 CD H	
CROSS SECTION RATIO	DEVIATION
.83295691E-01	0.87304863E-03
CESIUM 3 RUN 3 CD H	
CROSS SECTION RATIO	DEVIATION
.89631971E-01	0.94632178E-03

CESIUM-134,134M ISOMERIC CROSS SECTION RATIOS USING THERMAL ENERGY NEUTRONS

CESIUM 1A RUN 3 H TN	
CROSS SECTION RATIO	DEVIATION
.12244014	0.70298035E-03
CESIUM 1A RUN 4 H TN	
CROSS SECTION RATIO	DEVIATION
.11981199	0.69657445E-03
CESIUM 2A RUN 1 H TN	
CROSS SECTION RATIO	DEVIATION
.14511012	0.97218021E-03
CESIUM 2A RUN 2 TN H	
CROSS SECTION RATIO	DEVIATION
.14625925	0.97715834E-03

Table VI (continued)

CESIUM-134,134M ISOMERIC CROSS SECTION RATIOS USING THERMAL ENERGY NEUTRONS

Run	Cross Section Ratio	Deviation
CESIUM 2A RUN 3 TN H	.14810361	0.98280353E-03
CESIUM 2A RUN 4 TN H	.14716425	0.98017585E-03
CESIUM 3A RUN 1 TN H	.14710435	0.10451636E-02
CESIUM 3A RUN 2 TN H	.14577727	0.10402470E-02
CESIUM 3A RUN 3 TN H	.11850617	0.97688604E-03
CESIUM 3A RUN 3 TN L	.14535749	0.10602766E-02
CESIUM 3A RUN 4 TN L	.14991611	0.81956269E-03
CESIUM 3A RUN 4 TN H	.14636307	0.10436764E-02
CESIUM 4A RUN 1 TN H	.14410237	0.96286845E-03
CESIUM 4A RUN 2 TN H	.14475282	0.96580575E-03
CESIUM 4A RUN 6 TN H	.14458023	0.96745119E-03
CESIUM 4A RUN 4 TN H	.14528558	0.97019256E-03

Table VI (continued)

CESIUM-134,134M ISOMERIC CROSS SECTION RATIOS USING THERMAL ENERGY NEUTRONS

CESIUM 1A RUN 1 L TN	
CROSS SECTION RATIO	DEVIATION
.11599509	0.49854665E-03

4.0 RESULTS AND DISCUSSION

4.1 Theoretical Sample Calculation

From Eq. (29), Section 2.2, it is obvious that the isomeric cross section ratio is a function of the probability P_{J_f}. Also Eqs. (26), (27), and (28) show that P_{J_f} is a function of the level density $\rho(J)$ which in turn is a function of the level density factor σ. Therefore, values of σ are needed to calculate isomeric cross section ratios. As indicated in the same section, σ may have a definite value, e.g., 3, 4, ..., or it may be calculated following the emission of each gamma ray. The following is a sample isomeric cross section ratio calculation for the Cs-134,134m isomer using a calculated σ.

To determine the first calculated σ for Cs-134,134m, the excitation energy following thermal neutron bombardment of Cs-133 is calculated from Eq. (2) in Section 2.1:

$$E_o = [(132.9472 + 1.008986) - 133.94896]931$$

$$= 6.731 \text{ Mev}$$

also

$$\underline{a} = A/8 = 134/8 = 16.75 \text{ Mev}^{-1}. \tag{23}$$

The Cs-134 nuclear radius is given by

$$R = 1.2 \times 10^{-13} A^{1/3} \text{ cm} \tag{97}$$

$$= 1.2 \times 10^{-13} (134)^{1/3} = 6.138 \times 10^{-13} \text{ cm} .$$

The rigid moment of inertia is

$$\Lambda_{RIGID} = (2/5)mAR^2 \tag{17}$$

$$= 0.4(1.675 \times 10^{-24}\text{gm})(134)(3.77 \times 10^{-25}\text{cm}^2)$$

$$= 3.39 \times 10^{-47} \text{ gm-cm}^2 .$$

The energy of the first gamma ray emitted from the excited nucleus is

$$\bar{E}_{\gamma 1} = E_0 - E_1 = 4\sqrt{\frac{E_o}{\underline{a}} - \frac{5}{\underline{a}^2}} \tag{24}$$

therefore

$$\bar{E}_{\gamma 1} = 4\sqrt{\frac{6.731}{16.75} - \frac{5}{280.56}} = 2.48 \text{ Mev}$$

and the energy of the excited state following the emission of the first gamma ray is

$$E_1 = E_0 - \bar{E}_{\gamma 1} \tag{98}$$

$$= 6.73 - 2.48 = 4.25 \text{ Mev} .$$

Eq. (22) allows the determination of the nuclear temperature since

$$E_1 = \underline{a}T^2 - T \tag{22}$$

hence

$$T^2 - a^{-1}T - a^{-1}E_1 = 0$$

$$T^2 - 0.0597\ T - 0.2538 = 0$$

$$T = 0.535 \text{ Mev} .$$

Now from Eq. (16)

$$\sigma^2 = \Lambda_{RIGID}\ T\ \hbar^{-2} \tag{16}$$

$$\sigma^2 = \frac{(3.39 \times 10^{-47} \text{ gm-cm}^2)(0.535 \text{ Mev})(1.606 \times 10^{-6} \text{ erg/Mev})}{1.112 \times 10^{-54} \text{ erg}^2 \text{sec}^2}$$

$$\sigma = 5.11$$

therefore $\sigma = 5.11$ following the emission of the first gamma ray. A new σ must be calculated following the emission of each additional gamma ray. This process is repeated until $\bar{E}_{\gamma n}$, Eq. (24), becomes imaginary, hence there is not enough excitation energy for an additional gamma ray to be emitted. Following the steps outlined above, σ was 4.43, 3.6, and 2.57 after the emission of the second, third and fourth gamma rays respectively. After obtaining the four values of σ, the isomeric cross section ratio was calculated for each σ using angular momenta $J = I + 1/2$ and $J = I - 1/2$. The following is a sample isomeric cross section ratio calculation, using a σ of 5.11 as determined above, for Cs-134,134m, when $J = I - 1/2 = 3$.

The level density is

$$\rho(J) = \rho(0)(2J + 1)e^{-(J + 1/2)^2/2\sigma^2} \tag{15}$$

therefore

$$\rho(2) = \rho(0)[(2)(2) + 1]e^{-(2 + 1/2)^2/2(5.11)^2}$$
$$= \rho(0)\ 4.436$$

$$\rho(3) = \rho(0)[(3)(2) + 1]e^{-(3 + 1/2)^2/2(5.11)^2}$$
$$= \rho(0)\ 5.536$$

$$\rho(4) = \rho(0)[(2)(4) + 1]e^{-(4 + 1/2)^2/2(5.11)^2}$$
$$= \rho(0)\ 6.107\ .$$

The probabilities of going from J to J - 1, J, and J + 1 are

$$^1P_2 = {^1P}_{J\rightarrow J-1} = {^1P}_{3\rightarrow 2} = \frac{\rho(2)}{\rho(2) + \rho(3) + \rho(4)} \tag{26}$$
$$= \frac{4.436\ \rho(0)}{(4.44 + 5.54 + 6.11)\rho(0)}$$
$$= 0.276$$

where the subscript 2 corresponds to the angular momentum state of 2 and the superscript 1 corresponds to the probability distribution after the emission of the first gamma ray. Also

$$^1P_3 = {^1P}_{J\rightarrow J} = {^1P}_{3\rightarrow 3} = \frac{\rho(3)}{\rho(2) + \rho(3) + \rho(4)} \tag{27}$$

$$= 0.344$$

and

$$^{1}P_{4} = {}^{1}P_{J\rightarrow J+1} = {}^{1}P_{3\rightarrow 4} = 0.380. \qquad (28)$$

For Cs-134,134m the competing angular momenta levels for the metastable and intermediate level are 8 and 5. Therefore, if one considers the case in which 2 gamma rays are emitted in going to the metastable or stable state of Cs-134, it is assumed that states which, after the first gamma ray de-excitation, have angular momenta 0, 1, 2, 3, 4, 5 or 6 will populate the intermediate level and decay directly to the stable state. On the other hand, states with angular momenta of 7 or above will populate the metastable state.

Hence, for the above example the isomeric cross section ratio following the emission of the second gamma ray will be zero because, as shown above, the maximum angular momentum a state could have is less than 7.

After the emission of the second gamma ray σ acquires a value of 4.43 as indicated above. This σ value was used to calculate the following probabilities

$$^{2}P_{2\rightarrow 1} \qquad {}^{2}P_{2\rightarrow 2} \qquad {}^{2}P_{2\rightarrow 3} \qquad \text{from} \qquad {}^{1}P_{2}$$

$$^{2}P_{3\rightarrow 2} \qquad {}^{2}P_{3\rightarrow 3} \qquad {}^{2}P_{3\rightarrow 4} \qquad \text{from} \qquad {}^{1}P_{3}$$

and

$$^{2}P_{4\rightarrow 3} \qquad {}^{2}P_{4\rightarrow 4} \qquad {}^{2}P_{4\rightarrow 5} \qquad \text{from} \qquad {}^{1}P_{4}.$$

Hence the respective probabilities of having states with angular momenta of $J = 1, 2, 3, 4$ and 5 are

$$^{2}P_{1} = {}^{1}P_{2}\ {}^{2}P_{2\rightarrow 1}$$

$$^{2}P_{2} = {}^{1}P_{2}\ {}^{2}P_{2\rightarrow 2} + {}^{1}P_{3}\ {}^{2}P_{3\rightarrow 2}$$

$$^{2}P_{3} = {}^{1}P_{2}\ {}^{2}P_{2\rightarrow 3} + {}^{1}P_{3}\ {}^{2}P_{3\rightarrow 3} + {}^{1}P_{4}\ {}^{2}P_{4\rightarrow 3}$$

$$^{2}P_{4} = {}^{1}P_{3}\ {}^{2}P_{3\to4} + {}^{1}P_{4}\ {}^{2}P_{4\to4}$$

and
$$^{2}P_{5} = {}^{1}P_{4}\ {}^{2}P_{4\to5}.$$

The above procedure must be repeated for the rest of the gamma rays emitted. See Section 4.3, Table IX for a complete tabulation of σ's and isomeric cross section ratios.

Table VII contains sample IBM 1620 computer output for Cs-134,134m theoretical calculations. Included in it is the output for J = I + 1/2 and J = I - 1/2, for calculated σ's and constant σ's from 3 to 5. Column one gives the angular momentum before gamma emission, JI, column two, JFI, gives the probability of an excited state having the angular momentum in column one, column three gives the angular momentum following gamma ray emission, JF, column four, FJF, gives the probability that an excited state will have angular momentum given in column three, and column five, SUM FJF, is the summation of probabilities given in column four.

It is of interest to note that for σ's of 3, 4, and 5 Table VII is also valid for Sc-46,46m since I = 7/2 for Sc-45 and Cs-133. Similar theoretical calculations were performed for Re-188,188m, Tables VIII, IX, and X contain tabulated results for the above three isomeric pairs.

TABLE VII. THEORETICAL ISOMERIC CROSS SECTION RATIOS FOR CS-134,134M

CS-133+N=CS-134+GAMMA CALC SIGMA J=I+1/2

NOR. SPIN DIST. AFTER EMISSION OF GAMMA RAY NO 1

SPIN CUT OFF FACTOR= 5.103
MULTIPOLARITY OF GAMMA-RAY EMISSION 1
JF(MAX)=JI(MAX)+L= 5.00

JI	JFI	JF	FJF	SUM FJF
.0	0.00000000	0.0	0.00000000	0.00000000
1.0	0.00000000	1.0	0.00000000	0.00000000
2.0	0.00000000	2.0	0.00000000	0.00000000
3.0	0.00000000	3.0	0.31105010	0.31105010
4.0	0.10000000E+01	4.0	0.34298049	0.65403059
		5.0	0.34596945	0.10000000E+01

NOR. SPIN DIST. AFTER EMISSION OF GAMMA RAY NO 2

SPIN CUT OFF FACTOR= 4.426
MULTIPOLARITY OF GAMMA-RAY EMISSION 1
JF(MAX)=JI(MAX)+L= 6.00

JI	JFI	JF	FJF	SUM FJF
.0	0.00000000	0.0	0.00000000	0.00000000
1.0	0.00000000	1.0	0.00000000	0.00000000
2.0	0.00000000	2.0	0.89885724E-01	0.89885724E-01
3.0	0.31105010	3.0	0.22076145	0.31064717
4.0	0.34298049	4.0	0.35628313	0.66693030
5.0	0.34596945	5.0	0.23019569	0.89712599
		6.0	0.10287401	0.10000000E+01

NOR. SPIN DIST. AFTER EMISSION OF GAMMA RAY NO 3

SPIN CUT OFF FACTOR= 3.601
MULTIPOLARITY OF GAMMA-RAY EMISSION 1
JF(MAX)=JI(MAX)+L= 7.00

JI	JFI	JF	FJF	SUM FJF
.0	0.00000000	0.0	0.00000000	0.00000000
1.0	0.00000000	1.0	0.22384959E-01	0.22384959E-01
2.0	0.89885724E-01	2.0	0.10183412	0.12421907
3.0	0.22076145	3.0	0.24365124	0.36787031
4.0	0.35628313	4.0	0.29054546	0.65841577
5.0	0.23019569	5.0	0.22641772	0.88483349
6.0	0.10287401	6.0	0.92227413E-01	0.97706090
		7.0	0.22939070E-01	0.99999997

TABLE VII (CONTINUED)

NOR. SPIN DIST. AFTER EMISSION OF GAMMA RAY NO 4

SPIN CUT OFF FACTOR= 2.507
MULTIPOLARITY OF GAMMA-RAY EMISSION 1
JF(MAX)=JI(MAX)+L= 8.00

JI	JFI	JF	FJF	SUM FJF
.0	0.00000000	0.0	0.33609777E-02	0.33609777E-02
1.0	0.22384959E-01	1.0	0.39787994E-01	0.43148971E-01
2.0	0.10183412	2.0	0.14731053	0.19045950
3.0	0.24365124	3.0	0.26024232	0.45070182
4.0	0.29054546	4.0	0.28031407	0.73101589
5.0	0.22641772	5.0	0.17899504	0.91001093
6.0	0.92227413E-01	6.0	0.72592408E-01	0.98260333
7.0	0.22939070E-01	7.0	0.15558111E-01	0.99816144
		8.0	0.18385390E-02	0.99999997

INPUT DATA FOR
CS-133+N=CS-134+GAMMA CALC SIGMA J=I+1/2

```
 5
+.00000000E+00   JI= 00.0
+.00000000E+00   JI= 01.0
+.00000000E+00   JI= 02.0
+.00000000E+00   JI= 03.0
+.10000000E+01   JI= 04.0
 2
+.13294720E+03 +.13394896E+03 +.10089860E+01 +.13400000E+03
 1
```

TABLE VII (CONTINUED)

CS-133+N=CS-134+GAMMA CONST SIGMA J=I+1/2

NOR. SPIN DIST. AFTER EMISSION OF GAMMA RAY NO 1

SPIN CUT OFF FACTOR= 3.000
MULTIPOLARITY OF GAMMA-RAY EMISSION 1
JF(MAX)=JI(MAX)+L= 5.00

JI	JFI	JF	FJF	SUM FJF
.0	0.00000000	0.0	0.00000000	0.00000000
1.0	0.00000000	1.0	0.00000000	0.00000000
2.0	0.00000000	2.0	0.00000000	0.00000000
3.0	0.00000000	3.0	0.41623791	0.41623791
4.0	0.10000000E+01	4.0	0.34313632	0.75937423
		5.0	0.24062577	0.10000000E+01

NOR. SPIN DIST. AFTER EMISSION OF GAMMA RAY NO 2

SPIN CUT OFF FACTOR= 3.000
MULTIPOLARITY OF GAMMA-RAY EMISSION 1
JF(MAX)=JI(MAX)+L= 6.00

JI	JFI	JF	FJF	SUM FJF
.0	0.00000000	0.0	0.00000000	0.00000000
1.0	0.00000000	1.0	0.00000000	0.00000000
2.0	0.00000000	2.0	0.14707479	0.14707479
3.0	0.41623791	3.0	0.29036347	0.43743826
4.0	0.34313632	4.0	0.35251099	0.78994925
5.0	0.24062577	5.0	0.16190906	0.95185831
		6.0	0.48141696E-01	0.10000000E+01

NOR. SPIN DIST. AFTER EMISSION OF GAMMA RAY NO 3

SPIN CUT OFF FACTOR= 3.000
MULTIPOLARITY OF GAMMA-RAY EMISSION 1
JF(MAX)=JI(MAX)+L= 7.00

JI	JFI	JF	FJF	SUM FJF
.0	0.00000000	0.0	0.00000000	0.00000000
1.0	0.00000000	1.0	0.40038654E-01	0.40038654E-01
2.0	0.14707479	2.0	0.15603201	0.19607066
3.0	0.29036347	3.0	0.30325092	0.49932158
4.0	0.35251099	4.0	0.28193419	0.78125577
5.0	0.16190906	5.0	0.16317393	0.94442970
6.0	0.48141696E-01	6.0	0.47540447E-01	0.99197014
		7.0	0.80298129E-02	0.99999995

TABLE VII (CONTINUED)

NOR. SPIN DIST. AFTER EMISSION OF GAMMA RAY NO 4

SPIN CUT OFF FACTOR= 3.000
MULTIPOLARITY OF GAMMA-RAY EMISSION 1
JF(MAX)=JI(MAX)+L= 8.00

JI	JFI	JF	FJF	SUM FJF
.0	0.00000000	0.0	0.55095211E-02	0.55095211E-02
1.0	0.40038654E-01	1.0	0.57267517E-01	0.62777038E-01
2.0	0.15603201	2.0	0.18357869	0.24635572
3.0	0.30325092	3.0	0.28170671	0.52806243
4.0	0.28193419	4.0	0.26207724	0.79013967
5.0	0.16317393	5.0	0.14629662	0.93643629
6.0	0.47540447E-01	6.0	0.52122822E-01	0.98855911
7.0	0.80298129E-02	7.0	0.10324816E-01	0.99888392
		8.0	0.11160321E-02	0.99999995

NOR. SPIN DIST. AFTER EMISSION OF GAMMA RAY NO 5

SPIN CUT OFF FACTOR= 3.000
MULTIPOLARITY OF GAMMA-RAY EMISSION 1
JF(MAX)=JI(MAX)+L= 9.00

JI	JFI	JF	FJF	SUM FJF
.0	0.55095211E-02	0.0	0.78802997E-02	0.78802997E-02
1.0	0.57267517E-01	1.0	0.76640559E-01	0.84520858E-01
2.0	0.18357869	2.0	0.19446793	0.27898878
3.0	0.28170671	3.0	0.27584457	0.55483335
4.0	0.26207724	4.0	0.24103258	0.79586593
5.0	0.14629662	5.0	0.13832980	0.93419573
6.0	0.52122822E-01	6.0	0.51479447E-01	0.98567517
7.0	0.10324816E-01	7.0	0.12447056E-01	0.99812222
8.0	0.11160321E-02	8.0	0.17487258E-02	0.99987094
		9.0	0.12898839E-03	0.99999992

NOR. SPIN DIST. AFTER EMISSION OF GAMMA RAY NO 6

SPIN CUT OFF FACTOR= 3.000
MULTIPOLARITY OF GAMMA-RAY EMISSION 1
JF(MAX)=JI(MAX)+L= 10.00

JI	JFI	JF	FJF	SUM FJF
.0	0.78802997E-02	0.0	0.10546128E-01	0.10546128E-01
1.0	0.76640559E-01	1.0	0.89132215E-01	0.99678343E-01
2.0	0.19446793	2.0	0.20590352	0.30558186
3.0	0.27584457	3.0	0.26897576	0.57455762
4.0	0.24103258	4.0	0.22835245	0.80291007
5.0	0.13832980	5.0	0.13030538	0.93321545
6.0	0.51479447E-01	6.0	0.50877318E-01	0.98409276
7.0	0.12447056E-01	7.0	0.13354523E-01	0.99744728
8.0	0.17487258E-02	8.0	0.23041847E-02	0.99975146

TABLE VII (CONTINUED)

CS-133+N=CS-134+GAMMA CONST SIGMA J=I+1/2

NOR. SPIN DIST. AFTER EMISSION OF GAMMA RAY NO 1

SPIN CUT OFF FACTOR= 4.000
MULTIPOLARITY OF GAMMA-RAY EMISSION 1
JF(MAX)=JI(MAX)+L= 5.00

JI	JFI	JF	FJF	SUM FJF
.0	.00000000E-99	0.0	.00000000E-99	.00000000E-99
1.0	.00000000E-99	1.0	.00000000E-99	.00000000E-99
2.0	.00000000E-99	2.0	.00000000E-99	.00000000E-99
3.0	.00000000E-99	3.0	.34522179E+00	.34522179E+00
4.0	.10000000E+01	4.0	.34567589E+00	.69089768E+00
		5.0	.30910232E+00	.10000000E+01

NOR. SPIN DIST. AFTER EMISSION OF GAMMA RAY NO 2

SPIN CUT OFF FACTOR= 4.000
MULTIPOLARITY OF GAMMA-RAY EMISSION 1
JF(MAX)=JI(MAX)+L= 6.00

JI	JFI	JF	FJF	SUM FJF
.0	.00000000E-99	0.0	.00000000E-99	.00000000E-99
1.0	.00000000E-99	1.0	.00000000E-99	.00000000E-99
2.0	.00000000E-99	2.0	.10389458E+00	.10389458E+00
3.0	.34522179E+00	3.0	.23991915E+00	.34381373E+00
4.0	.34567589E+00	4.0	.35818978E+00	.70200351E+00
5.0	.30910232E+00	5.0	.21232425E+00	.91432776E+00
		6.0	.85672217E-01	.99999997E+00

NOR. SPIN DIST. AFTER EMISSION OF GAMMA RAY NO 3

SPIN CUT OFF FACTOR= 4.000
MULTIPOLARITY OF GAMMA-RAY EMISSION 1
JF(MAX)=JI(MAX)+L= 7.00

JI	JFI	JF	FJF	SUM FJF
.0	.00000000E-99	0.0	.00000000E-99	.00000000E-99
1.0	.00000000E-99	1.0	.24867469E-01	.24867469E-01
2.0	.10389458E+00	2.0	.10877950E+00	.13364696E+00
3.0	.23991915E+00	3.0	.24990884E+00	.38355580E+00
4.0	.35818978E+00	4.0	.28875442E+00	.67231022E+00
5.0	.21232425E+00	5.0	.21860913E+00	.89091935E+00
6.0	.85672217E-01	6.0	.87635260E-01	.97855461E+00
		7.0	.21445332E-01	.99999994E+00

TABLE VII (CONTINUED)

NOR. SPIN DIST. AFTER EMISSION OF GAMMA RAY NO 4

SPIN CUT OFF FACTOR= 4.000
MULTIPOLARITY OF GAMMA-RAY EMISSION 1
JF(MAX)=JI(MAX)+L= 8.00

JI	JFI	JF	FJF	SUM FJF
.0	.00000000E-99	0.0	.31227259E-02	.31227259E-02
1.0	.24867469E-01	1.0	.34837277E-01	.37960002E-01
2.0	.10877950E+00	2.0	.12644978E+00	.16440978E+00
3.0	.24990884E+00	3.0	.23142357E+00	.39583335E+00
4.0	.28875442E+00	4.0	.27064458E+00	.66647793E+00
5.0	.21860913E+00	5.0	.20010314E+00	.86658107E+00
6.0	.87635260E-01	6.0	.99538169E-01	.96611923E+00
7.0	.21445332E-01	7.0	.29015036E-01	.99513426E+00
		8.0	.48656470E-02	.99999990E+00

NOR. SPIN DIST. AFTER EMISSION OF GAMMA RAY NO 5

SPIN CUT OFF FACTOR= 4.000
MULTIPOLARITY OF GAMMA-RAY EMISSION 1
JF(MAX)=JI(MAX)+L= 9.00

JI	JFI	JF	FJF	SUM FJF
.0	.31227259E-02	0.0	.43746820E-02	.43746820E-02
1.0	.34837277E-01	1.0	.45717747E-01	.50092429E-01
2.0	.12644978E+00	2.0	.13229694E+00	.18238936E+00
3.0	.23142357E+00	3.0	.22593492E+00	.40832428E+00
4.0	.27064458E+00	4.0	.25085716E+00	.65918144E+00
5.0	.20010314E+00	5.0	.19311447E+00	.85229591E+00
6.0	.99538169E-01	6.0	.10176218E+00	.95405809E+00
7.0	.29015036E-01	7.0	.36782588E-01	.99084067E+00
8.0	.48656470E-02	8.0	.81569506E-02	.99899762E+00
		9.0	.10022490E-02	.99999986E+00

NOR. SPIN DIST. AFTER EMISSION OF GAMMA RAY NO 6

SPIN CUT OFF FACTOR= 4.000
MULTIPOLARITY OF GAMMA-RAY EMISSION 1
JF(MAX)=JI(MAX)+L= 10.00

JI	JFI	JF	FJF	SUM FJF
.0	.43746820E-02	0.0	.57409943E-02	.57409943E-02
1.0	.45717747E-01	1.0	.52219832E-01	.57960826E-01
2.0	.13229694E+00	2.0	.13836717E+00	.19632799E+00
3.0	.22593492E+00	3.0	.21957587E+00	.41590386E+00
4.0	.25085716E+00	4.0	.23943053E+00	.65533439E+00
5.0	.19311447E+00	5.0	.18553340E+00	.84086779E+00
6.0	.10176218E+00	6.0	.10401388E+00	.94488167E+00
7.0	.36782588E-01	7.0	.41451823E-01	.98633349E+00
8.0	.81569506E-02	8.0	.11481654E-01	.99781514E+00
9.0	.10022490E-02	9.0	.19971824E-02	.99981232E+00

TABLE VII (CONTINUED)

CS-133+N=CS-134+GAMMA CONST SIGMA J=I+1/2

NOR. SPIN DIST. AFTER EMISSION OF GAMMA RAY NO 1

SPIN CUT OFF FACTOR= 5.000
MULTIPOLARITY OF GAMMA-RAY EMISSION 1
JF(MAX)=JI(MAX)+L= 5.00

JI	JFI	JF	FJF	SUM FJF
.0	0.00000000	0.0	0.00000000	0.00000000
1.0	0.00000000	1.0	0.00000000	0.00000000
2.0	0.00000000	2.0	0.00000000	0.00000000
3.0	0.00000000	3.0	0.31328689	0.31328689
4.0	0.10000000E+01	4.0	0.34324141	0.65652830
		5.0	0.34347171	0.10000000E+01

NOR. SPIN DIST. AFTER EMISSION OF GAMMA RAY NO 2

SPIN CUT OFF FACTOR= 5.000
MULTIPOLARITY OF GAMMA-RAY EMISSION 1
JF(MAX)=JI(MAX)+L= 6.00

JI	JFI	JF	FJF	SUM FJF
.0	0.00000000	0.0	0.00000000	0.00000000
1.0	0.00000000	1.0	0.00000000	0.00000000
2.0	0.00000000	2.0	0.86973414E-01	0.86973414E-01
3.0	0.31328689	3.0	0.21552692	0.30250033
4.0	0.34324141	4.0	0.35332229	0.65582262
5.0	0.34347171	5.0	0.23516038	0.89098300
		6.0	0.10901702	0.10000000E+01

NOR. SPIN DIST. AFTER EMISSION OF GAMMA RAY NO 3

SPIN CUT OFF FACTOR= 5.000
MULTIPOLARITY OF GAMMA-RAY EMISSION 1
JF(MAX)=JI(MAX)+L= 7.00

JI	JFI	JF	FJF	SUM FJF
.0	0.00000000	0.0	0.00000000	0.00000000
1.0	0.00000000	1.0	0.19549424E-01	0.19549424E-01
2.0	0.86973414E-01	2.0	0.89911018E-01	0.10946044
3.0	0.21552692	3.0	0.22233271	0.33179315
4.0	0.35332229	4.0	0.28290689	0.61470004
5.0	0.23516038	5.0	0.24142568	0.85612572
6.0	0.10901702	6.0	0.11162265	0.96774837
		7.0	0.32251667E-01	0.10000000E+01

TABLE VII (CONTINUED)

NOR. SPIN DIST. AFTER EMISSION OF GAMMA RAY NO 4

SPIN CUT OFF FACTOR= 5.000
MULTIPOLARITY OF GAMMA-RAY EMISSION 1
JF(MAX)=JI(MAX)+L= 8.00

JI	JFI	JF	FJF	SUM FJF
.0	0.00000000	0.0	0.23505461E-02	0.23505461E-02
1.0	0.19549424E-01	1.0	0.26984861E-01	0.29335407E-01
2.0	0.89911018E-01	2.0	0.10324004	0.13257544
3.0	0.22233271	3.0	0.20387995	0.33645539
4.0	0.28290689	4.0	0.26344540	0.59990079
5.0	0.24142568	5.0	0.22032989	0.82023068
6.0	0.11162265	6.0	0.12694882	0.94717950
7.0	0.32251667E-01	7.0	0.43882833E-01	0.99106233
		8.0	0.89377066E-02	0.10000000E+01

NOR. SPIN DIST. AFTER EMISSION OF GAMMA RAY NO 5

SPIN CUT OFF FACTOR= 5.000
MULTIPOLARITY OF GAMMA-RAY EMISSION 1
JF(MAX)=JI(MAX)+L= 9.00

JI	JFI	JF	FJF	SUM FJF
.0	0.23505461E-02	0.0	0.32445539E-02	0.32445539E-02
1.0	0.26984861E-01	1.0	0.34908295E-01	0.38152848E-01
2.0	0.10324004	2.0	0.10669130	0.14484414
3.0	0.20387995	3.0	0.19714555	0.34198969
4.0	0.26344540	4.0	0.24259871	0.58458840
5.0	0.22032989	5.0	0.21203574	0.79662414
6.0	0.12694882	6.0	0.12994364	0.92656778
7.0	0.43882833E-01	7.0	0.55959885E-01	0.98252766
8.0	0.89377066E-02	8.0	0.15145322E-01	0.99767298
		9.0	0.23270542E-02	0.10000000E+01

NOR. SPIN DIST. AFTER EMISSION OF GAMMA RAY NO 6

SPIN CUT OFF FACTOR= 5.000
MULTIPOLARITY OF GAMMA-RAY EMISSION 1
JF(MAX)=JI(MAX)+L= 10.00

JI	JFI	JF	FJF	SUM FJF
.0	0.32445539E-02	0.0	0.41972366E-02	0.41972366E-02
1.0	0.34908295E-01	1.0	0.39324040E-01	0.43521276E-01
2.0	0.10669130	2.0	0.11024001	0.15376128
3.0	0.19714555	3.0	0.18977510	0.34353638
4.0	0.24259871	4.0	0.23007002	0.57360640
5.0	0.21203574	5.0	0.20313659	0.77674299
6.0	0.12994364	6.0	0.13299050	0.90973349
7.0	0.55959885E-01	7.0	0.63431286E-01	0.97316477
8.0	0.15145322E-01	8.0	0.21552016E-01	0.99471678
9.0	0.23270542E-02	9.0	0.47129892E-02	0.99942976
		10.0	0.57025478E-03	0.10000000E+01

TABLE VII (CONTINUED)

CS-133+N=CS-134+GAMMA CALC SIGMA J=I-1/2

NOR. SPIN DIST. AFTER EMISSION OF GAMMA RAY NO 1

SPIN CUT OFF FACTOR= 5.103

MULTIPOLARITY OF GAMMA-RAY EMISSION 1

JF(MAX)=JI(MAX)+L= 4.00

JI	JFI	JF	FJF	SUM FJF
.0	0.00000000	0.0	0.00000000	0.00000000
1.0	0.00000000	1.0	0.00000000	0.00000000
2.0	0.00000000	2.0	0.27598292	0.27598292
3.0	0.10000000E+01	3.0	0.34433494	0.62031786
		4.0	0.37968214	0.10000000E+01

NOR. SPIN DIST. AFTER EMISSION OF GAMMA RAY NO 2

SPIN CUT OFF FACTOR= 4.426

MULTIPOLARITY OF GAMMA-RAY EMISSION 1

JF(MAX)=JI(MAX)+L= 5.00

JI	JFI	JF	FJF	SUM FJF
.0	0.00000000	0.0	0.00000000	0.00000000
1.0	0.00000000	1.0	0.63992546E-01	0.63992546E-01
2.0	0.27598292	2.0	0.19580893	0.25980147
3.0	0.34433494	3.0	0.36007035	0.61987182
4.0	0.37968214	4.0	0.25618715	0.87605897
		5.0	0.12394102	0.99999999

NOR. SPIN DIST. AFTER EMISSION OF GAMMA RAY NO 3

SPIN CUT OFF FACTOR= 3.601

MULTIPOLARITY OF GAMMA-RAY EMISSION 1

JF(MAX)=JI(MAX)+L= 6.00

JI	JFI	JF	FJF	SUM FJF
.0	0.00000000	0.0	0.82625023E-02	0.82625023E-02
1.0	0.63992546E-01	1.0	0.71712124E-01	0.79974626E-01
2.0	0.19580893	2.0	0.21638082	0.29635544
3.0	0.36007035	3.0	0.29781498	0.59417042
4.0	0.25618715	4.0	0.25879253	0.85296295
5.0	0.12394102	5.0	0.11574259	0.96870554
		6.0	0.31294439E-01	0.99999997

NOR. SPIN DIST. AFTER EMISSION OF GAMMA RAY NO 4

SPIN CUT OFF FACTOR= 2.507

MULTIPOLARITY OF GAMMA-RAY EMISSION 1

JF(MAX)=JI(MAX)+L= 7.00

JI	JFI	JF	FJF	SUM FJF
.0	0.82625023E-02	0.0	0.10767178E-01	0.10767178E-01
1.0	0.71712124E-01	1.0	0.10208195	0.11284912
2.0	0.21638082	2.0	0.23483615	0.34768527
3.0	0.29781498	3.0	0.30085656	0.64854183
4.0	0.25879253	4.0	0.22140822	0.86995005
5.0	0.11574259	5.0	0.10188329	0.97183334
6.0	0.31294439E-01	6.0	0.24854081E-01	0.99668742
		7.0	0.33125550E-02	0.99999997

TABLE VII (CONTINUED)

NOR. SPIN DIST. AFTER EMISSION OF GAMMA RAY NO 1

SPIN CUT OFF FACTOR= 3.000
MULTIPOLARITY OF GAMMA-RAY EMISSION 1
JF(MAX)=JI(MAX)+L= 4.00

JI	JFI	JF	FJF	SUM FJF
.0	.00000000E-99	0.0	.00000000E-99	.00000000E-99
1.0	.00000000E-99	1.0	.00000000E-99	.00000000E-99
2.0	.00000000E-99	2.0	.35334308E+00	.35334308E+00
3.0	.10000000E+01	3.0	.35445395E+00	.70779703E+00
		4.0	.29220295E+00	.99999998E+00

NOR. SPIN DIST. AFTER EMISSION OF GAMMA RAY NO 2

SPIN CUT OFF FACTOR= 3.000
MULTIPOLARITY OF GAMMA-RAY EMISSION 1
JF(MAX)=JI(MAX)+L= 5.00

JI	JFI	JF	FJF	SUM FJF
.0	.00000000E-99	0.0	.00000000E-99	.00000000E-99
1.0	.00000000E-99	1.0	.96191736E-01	.96191736E-01
2.0	.35334308E+00	2.0	.25361772E+00	.34980945E+00
3.0	.35445395E+00	3.0	.37604104E+00	.72585049E+00
4.0	.29220295E+00	4.0	.20383790E+00	.92968839E+00
		5.0	.70311546E-01	.99999993E+00

NOR. SPIN DIST. AFTER EMISSION OF GAMMA RAY NO 3

SPIN CUT OFF FACTOR= 3.000
MULTIPOLARITY OF GAMMA-RAY EMISSION 1
JF(MAX)=JI(MAX)+L= 6.00

JI	JFI	JF	FJF	SUM FJF
.0	.00000000E-99	0.0	.13236469E-01	.13236469E-01
1.0	.96191736E-01	1.0	.10457671E+00	.11781317E+00
2.0	.25361772E+00	2.0	.27243565E+00	.39024882E+00
3.0	.37604104E+00	3.0	.31056642E+00	.70081524E+00
4.0	.20383790E+00	4.0	.21288498E+00	.91370022E+00
5.0	.70311546E-01	5.0	.72232484E-01	.98593270E+00
		6.0	.14067161E-01	.99999986E+00

TABLE VII (CONTINUED)

NOR. SPIN DIST. AFTER EMISSION OF GAMMA RAY NO 4
SPIN CUT OFF FACTOR= 3.000
MULTIPOLARITY OF GAMMA-RAY EMISSION 1
JF(MAX)=JI(MAX)+L= 7.00

JI	JFI	JF	FJF	SUM FJF
.0	.13236469E-01	0.0	.14390283E-01	.14390283E-01
1.0	.10457671E+00	1.0	.12603348E+00	.14042376E+00
2.0	.27243565E+00	2.0	.26027115E+00	.40069491E+00
3.0	.31056642E+00	3.0	.29798269E+00	.69867760E+00
4.0	.21288498E+00	4.0	.19776073E+00	.89643833E+00
5.0	.72232484E-01	5.0	.82337506E-01	.97877583E+00
6.0	.14067161E-01	6.0	.18877636E-01	.99765346E+00
		7.0	.23463345E-02	.99999979E+00

NOR. SPIN DIST. AFTER EMISSION OF GAMMA RAY NO 5
SPIN CUT OFF FACTOR= 3.000
MULTIPOLARITY OF GAMMA-RAY EMISSION 1
JF(MAX)=JI(MAX)+L= 8.00

JI	JFI	JF	FJF	SUM FJF
.0	.14390283E-01	0.0	.17342843E-01	.17342843E-01
1.0	.12603348E+00	1.0	.13180192E+00	.14914476E+00
2.0	.26027115E+00	2.0	.26198327E+00	.41112803E+00
3.0	.29798269E+00	3.0	.28279366E+00	.69392169E+00
4.0	.19776073E+00	4.0	.19364544E+00	.88756713E+00
5.0	.82337506E-01	5.0	.84524674E-01	.97209180E+00
6.0	.18877636E-01	6.0	.23733246E-01	.99582504E+00
7.0	.23463345E-02	7.0	.38486076E-02	.99967364E+00
		8.0	.32610697E-03	.99999974E+00

NOR. SPIN DIST. AFTER EMISSION OF GAMMA RAY NO 6
SPIN CUT OFF FACTOR= 3.000
MULTIPOLARITY OF GAMMA-RAY EMISSION 1
JF(MAX)=JI(MAX)+L= 9.00

JI	JFI	JF	FJF	SUM FJF
.0	.17342843E-01	0.0	.18136610E-01	.18136610E-01
1.0	.13180192E+00	1.0	.13735145E+00	.15548806E+00
2.0	.26198327E+00	2.0	.26008216E+00	.41557022E+00
3.0	.28279366E+00	3.0	.27632088E+00	.69189110E+00
4.0	.19364544E+00	4.0	.18882346E+00	.88071456E+00
5.0	.84524674E-01	5.0	.86773532E-01	.96748809E+00
6.0	.23733246E-01	6.0	.26543974E-01	.99403206E+00
7.0	.38486076E-02	7.0	.53033731E-02	.99933543E+00
8.0	.32610697E-03	8.0	.62657107E-03	.99996200E+00
		9.0	.37690839E-04	.99999969E+00

TABLE VII (CONTINUED)

CS-133+N=CS-134+GAMMA CONST SIGMA J=I-1/2

NOR. SPIN DIST. AFTER EMISSION OF GAMMA RAY NO 1

SPIN CUT OFF FACTOR= 4.000
MULTIPOLARITY OF GAMMA-RAY EMISSION 1
JF(MAX)=JI(MAX)+L= 4.00

JI	JFI	JF	FJF	SUM FJF
.0	0.00000000	0.0	0.00000000	0.00000000
1.0	0.00000000	1.0	0.00000000	0.00000000
2.0	0.00000000	2.0	0.30095026	0.30095026
3.0	0.10000000E+01	3.0	0.34929506	0.65024532
		4.0	0.34975465	0.99999997

NOR. SPIN DIST. AFTER EMISSION OF GAMMA RAY NO 2

SPIN CUT OFF FACTOR= 4.000
MULTIPOLARITY OF GAMMA-RAY EMISSION 1
JF(MAX)=JI(MAX)+L= 5.00

JI	JFI	JF	FJF	SUM FJF
.0	0.00000000	0.0	0.00000000	0.00000000
1.0	0.00000000	1.0	0.72033322E-01	0.72033322E-01
2.0	0.30095026	2.0	0.21106909	0.28310241
3.0	0.34929506	3.0	0.36571824	0.64882065
4.0	0.34975465	4.0	0.24306934	0.89188999
		5.0	0.10810998	0.99999997

NOR. SPIN DIST. AFTER EMISSION OF GAMMA RAY NO 3

SPIN CUT OFF FACTOR= 4.000
MULTIPOLARITY OF GAMMA-RAY EMISSION 1
JF(MAX)=JI(MAX)+L= 6.00

JI	JFI	JF	FJF	SUM FJF
.0	0.00000000	0.0	0.90455656E-02	0.90455656E-02
1.0	0.72033322E-01	1.0	0.76012569E-01	0.85058134E-01
2.0	0.21106909	2.0	0.22186444	0.30692257
3.0	0.36571824	3.0	0.29789922	0.60482179
4.0	0.24306934	4.0	0.25319021	0.85801200
5.0	0.10810998	5.0	0.11202371	0.97003571
		6.0	0.29964233E-01	0.99999994

TABLE VII (CONTINUED)

NOR. SPIN DIST. AFTER EMISSION OF GAMMA RAY NO 4

SPIN CUT OFF FACTOR= 4.000
MULTIPOLARITY OF GAMMA-RAY EMISSION 1
JF(MAX)=JI(MAX)+L= 7.00

JI	JFI	JF	FJF	SUM FJF
.0	0.90455656E-02	0.0	0.95452584E-02	0.95452584E-02
1.0	0.76012569E-01	1.0	0.89050287E-01	0.98595545E-01
2.0	0.22186444	2.0	0.20732605	0.30592159
3.0	0.29789922	3.0	0.28211530	0.58803689
4.0	0.25319021	4.0	0.23446223	0.82249912
5.0	0.11202371	5.0	0.12888300	0.95138212
6.0	0.29964233E-01	6.0	0.41117173E-01	0.99249929
		7.0	0.75006044E-02	0.99999989

NOR. SPIN DIST. AFTER EMISSION OF GAMMA RAY NO 5

SPIN CUT OFF FACTOR= 4.000
MULTIPOLARITY OF GAMMA-RAY EMISSION 1
JF(MAX)=JI(MAX)+L= 8.00

JI	JFI	JF	FJF	SUM FJF
.0	0.95452584E-02	0.0	0.11182466E-01	0.11182466E-01
1.0	0.89050287E-01	1.0	0.90684217E-01	0.10186668
2.0	0.20732605	2.0	0.20424415	0.30611083
3.0	0.28211530	3.0	0.26419637	0.57030720
4.0	0.23446223	4.0	0.22890153	0.79920873
5.0	0.12888300	5.0	0.13346073	0.93266946
6.0	0.41117173E-01	6.0	0.52860578E-01	0.98553003
7.0	0.75006044E-02	7.0	0.12768068E-01	0.99829809
		8.0	0.17017847E-02	0.99999987

NOR. SPIN DIST. AFTER EMISSION OF GAMMA RAY NO 6

SPIN CUT OFF FACTOR= 4.000
MULTIPOLARITY OF GAMMA-RAY EMISSION 1
JF(MAX)=JI(MAX)+L= 9.00

JI	JFI	JF	FJF	SUM FJF
.0	0.11182466E-01	0.0	0.11387647E-01	0.11387647E-01
1.0	0.90684217E-01	1.0	0.92162010E-01	0.10354966
2.0	0.20424415	2.0	0.19861697	0.30216663
3.0	0.26419637	3.0	0.25475843	0.55692506
4.0	0.22890153	4.0	0.22245898	0.77938404
5.0	0.13346073	5.0	0.13816190	0.91754594
6.0	0.52860578E-01	6.0	0.60408980E-01	0.97795492
7.0	0.12768068E-01	7.0	0.18247041E-01	0.99620196
8.0	0.17017847E-02	8.0	0.34473605E-02	0.99964932
		9.0	0.35054097E-03	0.99999986

TABLE VII (CONTINUED)

CS-133+N=CS-134+GAMMA CONST SIGMA J=I-1/2

NOR. SPIN DIST. AFTER EMISSION OF GAMMA RAY NO 1

SPIN CUT OFF FACTOR= 5.000
MULTIPOLARITY OF GAMMA-RAY EMISSION 1
JF(MAX)=JI(MAX)+L= 4.00

JI	JFI	JF	FJF	SUM FJF
.0	0.00000000	0.0	0.00000000	0.00000000
1.0	0.00000000	1.0	0.00000000	0.00000000
2.0	0.00000000	2.0	0.27761588	0.27761588
3.0	0.10000000E+01	3.0	0.34471244	0.62232832
		4.0	0.37767167	0.99999999

NOR. SPIN DIST. AFTER EMISSION OF GAMMA RAY NO 2

SPIN CUT OFF FACTOR= 5.000
MULTIPOLARITY OF GAMMA-RAY EMISSION 1
JF(MAX)=JI(MAX)+L= 5.00

JI	JFI	JF	FJF	SUM FJF
.0	0.00000000	0.0	0.00000000	0.00000000
1.0	0.00000000	1.0	0.62401027E-01	0.62401027E-01
2.0	0.27761588	2.0	0.19170333	0.25410435
3.0	0.34471244	3.0	0.35635542	0.61045977
4.0	0.37767167	4.0	0.25982069	0.87028046
		5.0	0.12971953	0.99999999

NOR. SPIN DIST. AFTER EMISSION OF GAMMA RAY NO 3

SPIN CUT OFF FACTOR= 5.000
MULTIPOLARITY OF GAMMA-RAY EMISSION 1
JF(MAX)=JI(MAX)+L= 6.00

JI	JFI	JF	FJF	SUM FJF
.0	0.00000000	0.0	0.75028549E-02	0.75028549E-02
1.0	0.62401027E-01	1.0	0.64716050E-01	0.72218904E-01
2.0	0.19170333	2.0	0.19849734	0.27071624
3.0	0.35635542	3.0	0.28655659	0.55727283
4.0	0.25982069	4.0	0.26802517	0.82529800
5.0	0.12971953	5.0	0.13352935	0.95882735
		6.0	0.41172638E-01	0.99999998

TABLE VII (CONTINUED)

NOR. SPIN DIST. AFTER EMISSION OF GAMMA RAY NO 4

SPIN CUT OFF FACTOR= 5.000
MULTIPOLARITY OF GAMMA-RAY EMISSION 1
JF(MAX)=JI(MAX)+L= 7.00

JI	JFI	JF	FJF	SUM FJF
.0	0.75028549E-02	0.0	0.77812042E-02	0.77812042E-02
1.0	0.64716050E-01	1.0	0.74548332E-01	0.82329536E-01
2.0	0.19849734	2.0	0.18270396	0.26503349
3.0	0.28655659	3.0	0.26798379	0.53301728
4.0	0.26802517	4.0	0.24578010	0.77879738
5.0	0.13352935	5.0	0.15267262	0.93147000
6.0	0.41172638E-01	6.0	0.56349430E-01	0.98781943
		7.0	0.12180540E-01	0.99999997

NOR. SPIN DIST. AFTER EMISSION OF GAMMA RAY NO 5

SPIN CUT OFF FACTOR= 5.000
MULTIPOLARITY OF GAMMA-RAY EMISSION 1
JF(MAX)=JI(MAX)+L= 8.00

JI	JFI	JF	FJF	SUM FJF
.0	0.77812042E-02	0.0	0.89633992E-02	0.89633992E-02
1.0	0.74548332E-01	1.0	0.74684251E-01	0.83647650E-01
2.0	0.18270396	2.0	0.17732872	0.26097637
3.0	0.26798379	3.0	0.24783070	0.50880707
4.0	0.24578010	4.0	0.23766168	0.74646875
5.0	0.15267262	5.0	0.15710613	0.90357488
6.0	0.56349430E-01	6.0	0.72277478E-01	0.97585235
7.0	0.12180540E-01	7.0	0.20772085E-01	0.99662443
		8.0	0.33755184E-02	0.99999994

NOR. SPIN DIST. AFTER EMISSION OF GAMMA RAY NO 6

SPIN CUT OFF FACTOR= 5.000
MULTIPOLARITY OF GAMMA-RAY EMISSION 1
JF(MAX)=JI(MAX)+L= 9.00

JI	JFI	JF	FJF	SUM FJF
.0	0.89633992E-02	0.0	0.89797415E-02	0.89797415E-02
1.0	0.74684251E-01	1.0	0.74705334E-01	0.83685075E-01
2.0	0.17732872	2.0	0.16994750	0.25363257
3.0	0.24783070	3.0	0.23603214	0.48966471
4.0	0.23766168	4.0	0.22877652	0.71844123
5.0	0.15710613	5.0	0.16164375	0.88008498
6.0	0.72277478E-01	6.0	0.82405690E-01	0.96249067
7.0	0.20772085E-01	7.0	0.29746890E-01	0.99223756
8.0	0.33755184E-02	8.0	0.68835421E-02	0.99912110
		9.0	0.87886239E-03	0.99999996

4.2 Scandium-46,46m Isomers

The average experimentally measured isomeric cross section ratios for Sc-46,46m were 0.4955 ± 0.063, 0.5645 ± 0.0365, and 0.5048 ± 0.0500 for RSR, thermal, and epi-cadmium energy neutrons respectively, Table VIII. Either 9 or 18 sets of data were taken per isomer, Table IV. The above isomeric cross section ratios are averages of the total number of sets of data obtained. The deviation listed is one half the difference between the maximum and minimum isomeric cross section ratios.

The angular momentum of the parent nuclide, Sc-45, was I = 7/2; the angular momenta of the Sc-46m and Sc-46 states were 7 and 4 respectively, Table VIII.

In calculating the theoretical isomeric cross section ratio, as explained above, all excited states with angular momentum equal to or greater than 6 were assumed to populate the metastable state following the emission of the last gamma ray. Isomeric cross section ratios were computed using J = I + 1/2 = 4 and J = I - 1/2 = 3 for values of constant σ ranging from 3 to infinity and number of gamma rays emitted, N_γ, ranging from 3 to 6, Table VIII. These theoretically determined ratios were always smaller than the experimental ratios, the ratios obtained for J = 4 being much closer than the ones using J = 3, Table VIII and Figure 16.

The Chart of the Nuclides (8) lists 10 and 13 barns for the formation cross sections of Sc-46 and Sc-46m respectively. This gives a cross section ratio of 0.435 which agrees relatively well with the experimental ratios determined in this work.

Table VIII. Isomeric cross section ratios for Sc-46,46m using (n,γ) reactions

Target Spin (I)	Competing levels	Capturing state	Level density factor (σ)	N_γ	Calculated ratio
7/2	7, 4	J = I + 1/2 = 4	3	3	0.0481
			3	4	0.0556
			3	5	0.0636
			3	6	0.0658
			4	3	0.0857
			4	4	0.1091
			4	5	0.1334
			4	6	0.1477
			5	3	0.1090
			5	4	0.1439
			5	5	0.1798
			5	6	0.2034
			6	3	0.1236
			6	4	0.1657
			6	5	0.2088
			6	6	0.2384
			7	3	0.1327
			7	4	0.1796
			7	5	0.2276
			7	6	0.2610
			8	3	0.1389
			8	4	0.1892
			8	5	0.2402
			8	6	0.2767
			10	3	0.1464
			10	4	0.2007
			10	5	0.2555
			10	6	0.2947
			∞	3	0.1605
			∞	4	0.2222
			∞	5	0.2840
			∞	6	0.3280
			2.108†	2	0.0174
			1.621†	3	0.0379

Table VIII (continued)

Target Spin (I)	Competing levels	Capturing state	Level density factor (σ)	N_γ	Calculated ratio
7/2	7, 4	J = I - 1/2 = 3	3	3	0.0000
			3	4	0.0141
			3	5	0.0212
			4	3	0.0000
			4	4	0.0299
			4	5	0.0486
			5	3	0.0000
			5	4	0.0412
			5	5	0.0686
			∞	3	0.0000
			∞	4	0.0688
			∞	5	0.1182
			2.108†	2	0.0000
			1.621†	3	0.0059

Experimental Ratios

RSR energy	Thermal energy	Epi-cadmium energy
0.4955 ± 0.0630	0.5645 ± 0.0365	0.5084 ± 0.0500

† Calculated σ

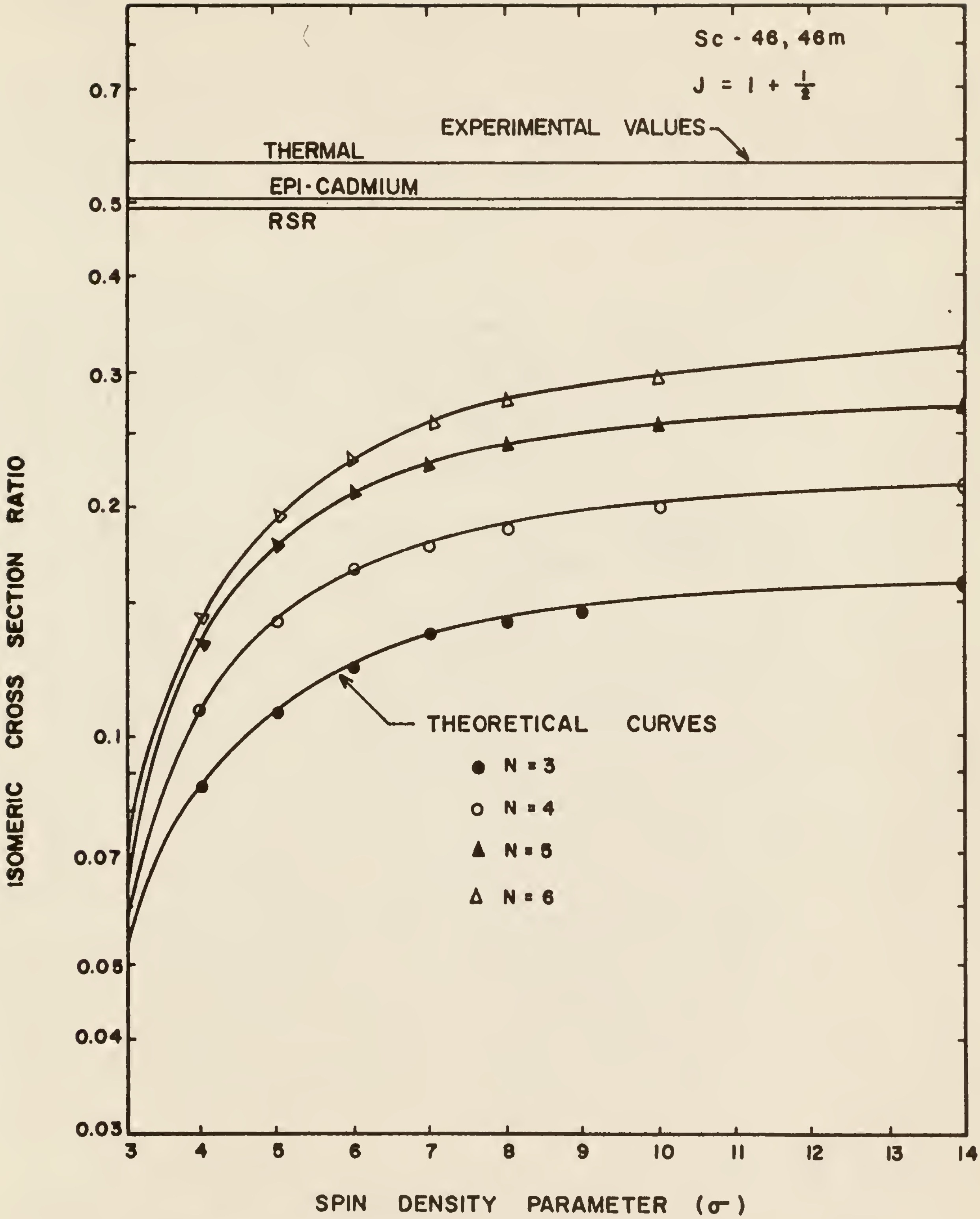

Figure 16 THEORETICAL and EXPERIMENTAL ISOMERIC CROSS SECTION RATIOS for Sc·46, 46 m

4.3 Cesium-134,134m Isomers

For the Cs-134,134m isomers the average experimental isomeric cross section ratios were 0.0952 ± 0.0178, 0.1368 ± 0.0165, and 0.1057 ± 0.0153 for RSR, thermal and epi-cadmium energy neutrons respectively, Table IX.

The angular momentum of Cs-133 before neutron bombardment was I = 7/2. The angular momenta of the Cs-134m and Cs-134 states are 8 and 4 respectively with an intermediate level between the Cs-134m and Cs-134 levels having angular momentum of 5, Table IX. In all calculations, if there was an intermediate energy level between the metastable and stable state it was assumed that the competing angular momenta are those of the intermediate level and the metastable state (21).

Following the emission of the last gamma ray, all excited states with angular momenta equal to or greater than 7 were assumed to populate the metastable state. Ratios were calculated using constant σ ranging from 3 to infinity and calculated σ for $J = I + 1/2 = 4$ and $J = I - 1/2 = 3$.

Using a σ value of 8, with a $J = I + 1/2 = 4$, and N_γ between 5 and 6, the theoretical ratios were between 0.08178 and 0.1157, Table IX, which agreed with the experimental ratios, Figure 17.

It is worth mentioning that Bishop (4) determined experimentally the isomeric cross section ratio of Cs-134,134m by following the buildup of Cs-134 from decay of Cs-134m. His reported value was 0.09; also Hughes (20) gave a value of 0.10 for the same ratio. These two values agree with the experimental ratios found in this work.

Table IX. Isomeric cross section ratios for Cs-134,134m using (n,γ) reactions.

Target Spin (I)	Competing levels	Capturing state	Level density factor (σ)	N_γ	Calculated ratio
7/2	8, (5), 4	J = I + 1/2 = 4	3	3	0.0000
			3	4	0.0080
			3	5	0.0114
			3	6	0.0143
			4	3	0.0000
			4	4	0.0215
			4	5	0.0339
			4	6	0.0458
			5	3	0.0000
			5	4	0.0323
			5	5	0.0528
			5	6	0.0734
			6	3	0.0000
			6	4	0.0397
			6	5	0.0552
			6	6	0.0928
			7	3	0.0000
			7	4	0.0449
			7	5	0.0753
			7	6	0.1063
			8	3	0.0000
			8	4	0.0485
			8	5	0.0818
			8	6	0.1157
			∞	3	0.0000
			∞	4	0.0617
			∞	5	0.1056
			∞	6	0.1450
			4.43†	2	0.0000
			3.60†	3	0.0229
			2.51†	4	0.0174
7/2	8, (5), 4	J = I - 1/2 = 3	3	3	0.0000
			3	4	0.0000
			3	5	0.0024

Table IX (continued)

Target Spin (I)	Competing level	Capturing state	Level density factor (σ)	N_γ	Calculated ratio
7/2	8, (5), 4	J = I - 1/2 = 3	4	3	0.0000
			4	4	0.0000
			4	5	0.0075
			5	3	0.0000
			5	4	0.0000
			5	5	0.0122
			∞	3	0.0000
			∞	4	0.0000
			∞	5	0.0265
			4.43†	2	0.0000
			3.60†	3	0.0000
			2.51†	4	0.0033

Experimental Ratios

RSR energy	Thermal	Epi-cadmium
0.0952 ± 0.0178	0.1368 ± 0.0165	0.1057 ± 0.0153

† Calculated σ

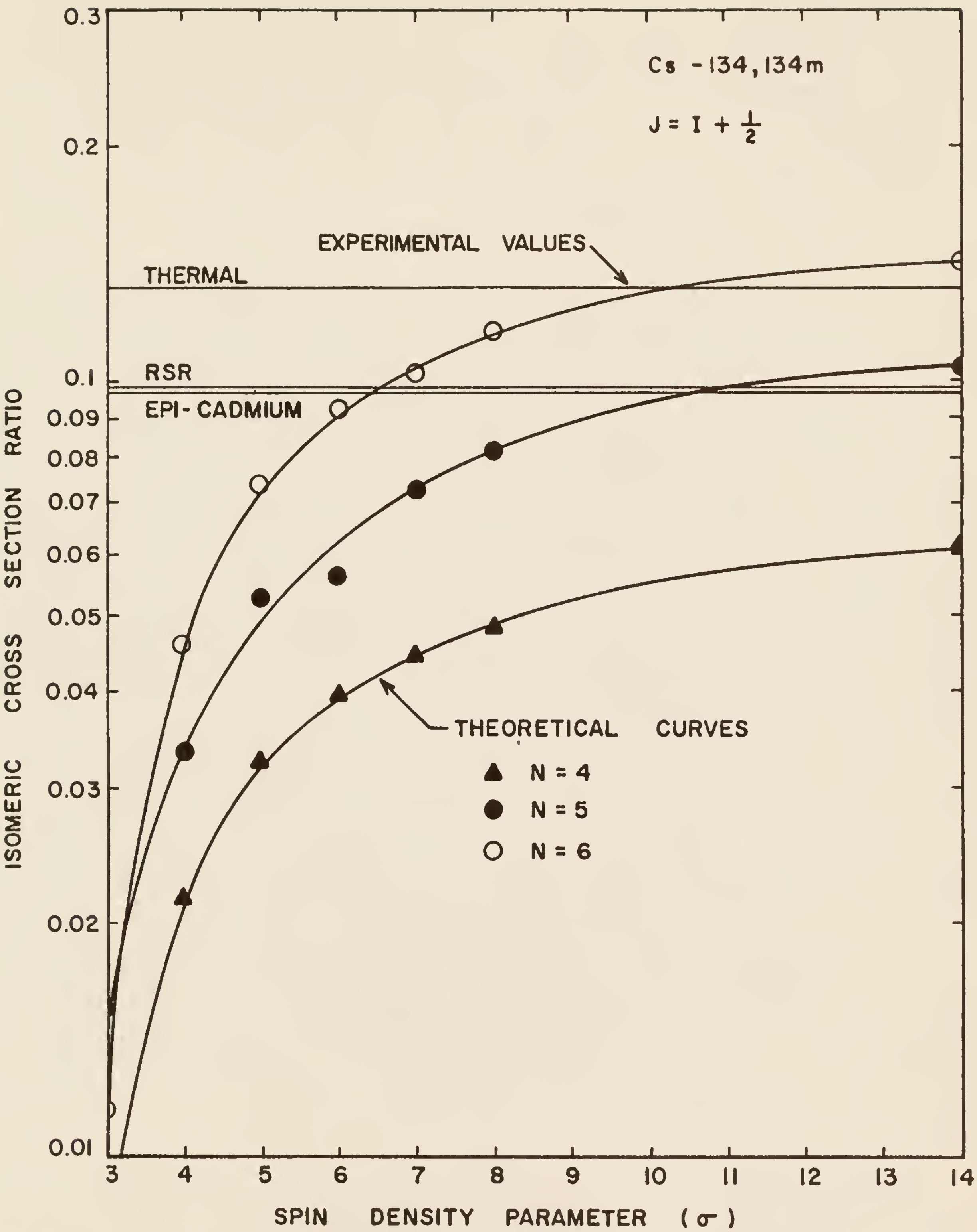

Figure 17 THEORETICAL and EXPERIMENTAL ISOMERIC CROSS SECTION RATIOS for Cs-134, 134m

4.4 Rhenium-188,188m Isomers

The average experimental isomeric cross section ratios for Re-188,188m were 0.1578 ± 0.0145, 0.1618 ± 0.010, and 0.1381 ± 0.0124 for RSR, thermal, and epi-cadmium energy neutrons respectively.

The angular momentum of the parent nuclide Re-187 was I = 5/2. The angular momentum of Re-188m and Re-188 were 4 and 1 respectively, there is also an intermediate level with angular momentum 2.

Theoretical ratios were determined by assuming that all excited states with angular momenta equal to or greater than 4 would populate the metastable state following the emission of the last gamma ray.

Using a $\sigma = 3$, $J = I - 1/2 = 2$, and N_γ between 4 and 5 theoretical ratios were between 0.1386 and 0.1737, Table X, this range includes the experimental values, Figure 18.

Table X. Isomeric cross section ratios for Re-188,188m using (n,γ) reactions.

Target Spin (I)	Competing levels	Capturing state	Level density factor (σ)	N_γ	Calculated ratio
5/2	4, (2), 1	J = I + 1/2 = 3	3	3	0.2741
			3	4	0.2992
			3	5	0.3013
			4	3	0.3512
			4	4	0.3952
			4	5	0.4120
			5	3	0.3896
			5	4	0.4427
			5	5	0.4670
			∞	3	0.4606
			∞	4	0.5291
			∞	5	0.5660
			5.15†	2	0.3805
			3.75†	3	0.3616
			2.99†	4	0.3648
5/2	4, (2), 1	J = I - 1/2 = 2	3	3	0.1065
			3	4	0.1386
			3	5	0.1737
			4	3	0.1429
			4	4	0.1938
			4	5	0.2475
			5	3	0.1621
			5	4	0.2234
			5	5	0.2868
			∞	3	0.2000
			∞	4	0.2815
			∞	5	0.3630
			5.15†	2	0.0000
			3.76†	3	0.1466
			2.99†	4	0.1698

Table X (continued)

Experimental Ratios		
RSR energy	Thermal energy	Epi-cadmium energy
0.1578 ± 0.0145	0.1618 ± 0.0100	0.1381 ± 0.0124

† Calculated σ

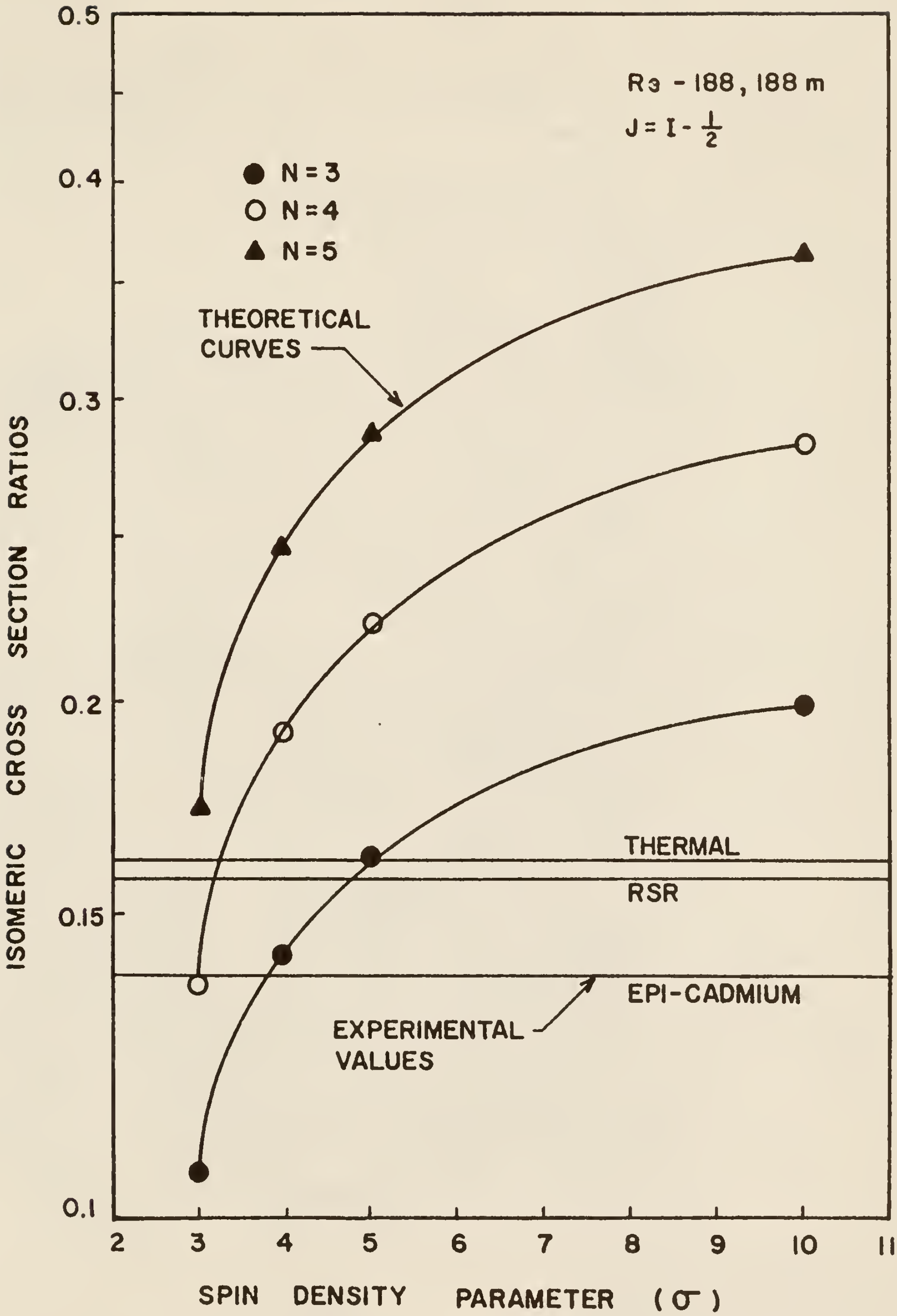

Figure 18 THEORETICAL and EXPERIMENTAL ISOMERIC CROSS SECTION RATIOS for Re - 188, 188m.

4.5 Conclusions

Matching experimentally determined isomeric cross section ratios with the corresponding theoretically calculated ratios for the three isomeric pairs Sc-46,46m, Cs-134,134m, and Re-188,188m led to the following conclusions:

1.) In the case of Re-188,188m, theoretical and experimental values agreed very well for a σ between 3 and 4, $N_\gamma = 4$ and $J = I - 1/2$, Figure 18. Also, very good agreement was found using a calculated σ when $N_\gamma = 4$ and $J = I - 1/2$, Table X. It is to be noted that in both cases agreement was obtained for $J = I - 1/2$ and that values obtained using $J = I + 1/2$ were far from being in agreement with experimental values.

2.) In the case of Cs-134,134m, theoretical and experimental values agreed for a σ between 7 and 8, $N_\gamma = 6$ and $J = I + 1/2$, Figure 17. Using a calculated σ, experimental ratios were greater than the theoretical values. Also, theoretical cross section ratios obtained using $J = I + 1/2$ were in much closer agreement with the experimental values than for $J = I - 1/2$.

3.) For Sc-46,46m the theoretically calculated values were always less than those experimentally determined for all values of σ provided N_γ was less or equal to 6, Figure 16. The average number of gamma rays emitted from an excited nucleus is approximately 4 (15). In this work $N_\gamma = 6$ was chosen as an arbitrary maximum, although agreement could have been obtained between theoretical and experimental ratios by increasing N_γ above 6.

4.) The statistical model seems to be applicable to the Re-188,188m isomeric pair for the same range of σ (3 to 5) and $N_\gamma = 4$ as found to give agreement in several other cases reported in the literature (4), and (31). On the other hand, agreement in the case of Cs-134, 134m was only obtained by using higher values of N_{γ} and σ. For Sc-46, 46m the statistical model does not seem to hold.

5.) For the experimentally determined isomeric cross section ratios no obvious energy dependence was noted with the exception that the ratios were higher for thermal energy neutrons than for either RSR or epi-cadmium energy neutrons, Figure 19. As expected, the ratios determined for RSR and epi-cadmium energy neutrons were in agreement within the limits of experimental error.

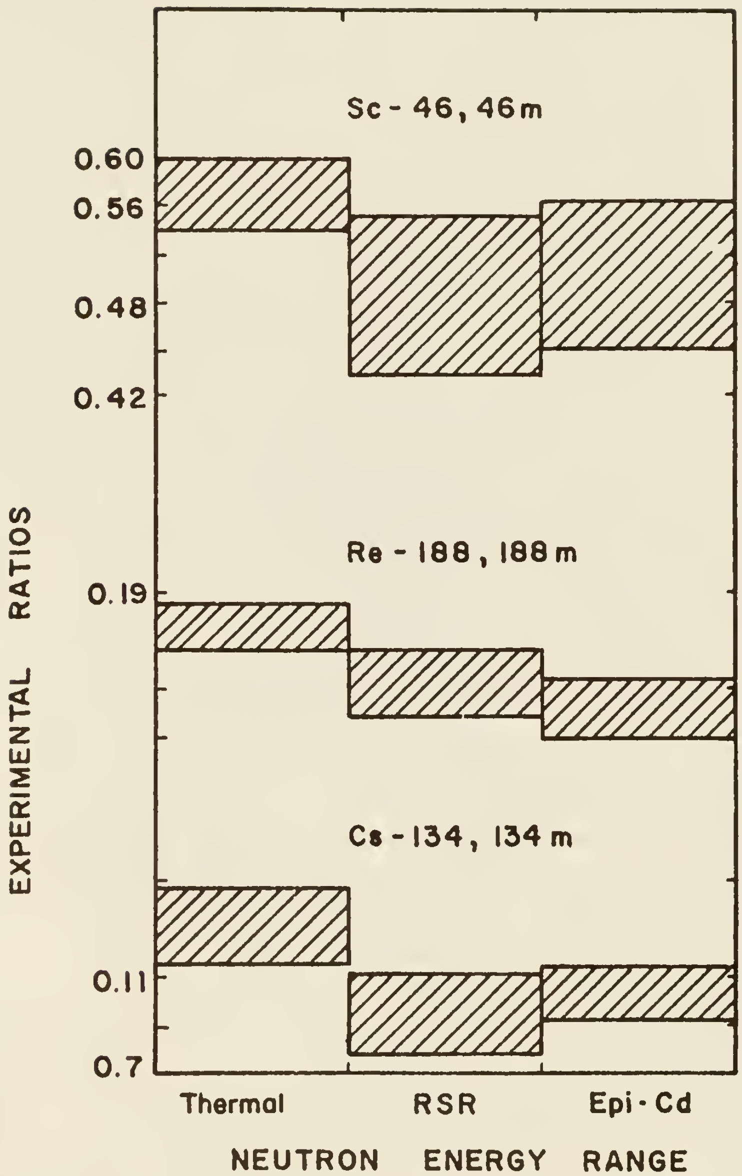

Figure. 19 VARIATION IN THE EXPERIMENTAL ISOMERIC CROSS SECTION RATIOS

5.0 SUGGESTIONS FOR FURTHER STUDY

In this work isomeric cross section ratios were studied using (n,γ) reactions produced by reactor neutron bombardment. Although extensive work has been done using this type of reaction there are still several isomers which have not been investigated, e.g., Y-90,90m, Pd-109,109m, Pd-111,111m, Yb-177,177m, and Pt-199,199m.

Isomeric cross section ratios may also be determined for (n,xp), (n,2n), (p,n), (p,p), and (γ,n) reactions where the p represents some type of charged particle and x is an integer. Relatively little work has been done using any of the above reactions.

Newer models of nuclear structure are being developed and calculations similar to the ones done in this investigation will be needed to check the applicability of these models.

6.0 ACKNOWLEDGEMENT

The author wishes to express his sincerest gratitude to Dr. S. Z. Mikhail under whose direction this work has been done. Thanks are extended to Mr. R. W. Clack for his advice concerning the experimental phase of this work and for his many hours spent in the operation of the TRIGA Mark II Reactor. Appreciation is also extended to Dr. W. R. Kimel and Dr. J. O. Mingle for their contribution to this work. Gratitude is extended to the Department of Nuclear Engineering of the Kansas Engineering Experiment Station for financial support of this research.

7.0 LITERATURE CITED

1. Axel, Peter
   Escape Peak Correction to Gamma Ray Intensity Measurements Made with Sodium Iodide Crystals, BNL-271, 1953.

2. Ball, W. P. and Booth, R.
   Scintillation Temperature Coefficients, Bull. Am. Phys. Soc. 31, 183, 1956.

3. Bethe, H. A.
   Nuclear Processes as Many-Body Problems, Nuclear Physics, Bul. 9, No. 2, pp. 69-82, April 1937.

4. Bishop, C. T.
   Isomeric Cross Section Ratios for Some (n,γ) and (α,xn) Reactions, ANL-6405, 1961.

5. Blatt, J. M. and Weisskopf, V. F.
   Theoretical Nuclear Physics, John Wiley and Sons, New York, 1960.

6. Bloch, C.
   Theory of Nuclear Level Density, Phys. Rev., Vol. 93, No. 5, pp. 1094-1106, 1953.

7. Cathey, L.
   Fatigue in Photomultipliers, IRE Transactions Nucl. Sci. NS5:3, p. 109, 1958.

8. Chart of the Nuclides, Knolls Atomic Power Laboratory Naval Reactors, U.S.A.E.C., Sixth Edition, Dec. 1961.

9. Covell, D. F. and Euler, B. A.
   Gain Shift Versus Counting Rate in Certain Multiplier Phototubes, U. S. Naval Radiological Defense Laboratory, San Francisco, California, 1961.

10. Crouthanel, C. E.
    Applied Gamma Ray Spectrometry, The MacMillian Co., New York, 1960.

11. Ericson, Torleif
    On Angular Distributions in Compound Nucleus Processes, Nuclear Physics, Vol. 11, pp. 284-293, 1958.

12. Ericson, Torleif
    A Statistical Analysis of Excited Nuclear States, Nuclear Physics, Vol. 11, pp. 481-491, 1959.

13. Evans, R. D.
    The Atomic Nucleus, McGraw-Hill Book Co., 1955.

14. Fowler, R. H.
    Statistical Mechanics, Cambridge, 1936.

15. Groshev, L. V. and Demidov, A. M.
Proceedings of the Second United Nations International Conference on the Peaceful Uses of Atomic Energy, Geneva, 1958, Vol. 15, p. 138, paper P/2029, 1958.

16. Grotenhuis, M.
Lecture Notes on Reactor Shielding, ANL-6000, 1959.

17. Hafner, W. L., Huizenga, J. R., and Vandenbosch, R.
Computer Program for Calculating the Relative Yields of Isomers Produced in Nuclear Reactions, ANL-6662, 1962.

18. Harshaw Scintillation Phosphors, The Harshaw Chemical Company, Cleveland, Ohio, 1962.

19. Heath, R. L.
Scintillation Spectrometry Gamma Ray Spectrum Catalogue, IDO-16408, 1957.

20. Hughes, D. J. and Schwartz, R. B.
Neutron Cross Sections, BNL-327, 2nd Ed. and Suppl. No. 1, 1958.

21. Huizenga, J. R. and Vandenbosch, R.
Interpretation of Isomeric Cross Section Ratios for (n,γ) and (γ,n) Reactions, Physical Review, Vol. 120, No. 4, pp. 1305-1312, Nov. 1960.

22. Kaplan, Irving
Nuclear Physics, Addison-Wesley, 1955.

23. Kinard, F. E.
Temperature Dependence of Photomultiplier Gain, Nucleonics 15, April 1957.

24. Kohl, J., Zentner, R. D. and Lukens, H. R.
Radioisotope Applications Engineering, Van Nostrand Co., N. J., 1961.

25. Lier, C. Van
On the Statistical Calculation of the Density of the Energy Levels of the Nuclei, Phsica, Vol. IV, No. 2, pp. 531-542, July 1937.

26. Nuclear Data Sheets, Nuclear Data Division, Oak Ridge National Laboratory, Oak Ridge, Tennessee.

27. Price, W. J.
Nuclear Radiation Detection, McGraw-Hill Book Co., New York, 1958.

28. Radiological Health Handbook, U. S. Department of Health, Education and Welfare, Washington 25, D. C., 1960.

29. Rose, M. E.
Internal Conversion Coefficients, Interscience Publishing Co., N. Y., 1958.

30. Ross, D. A.
Medical Gamma Ray Spectrometry, ORNL-2808 /ORINS-30, 1959.

31. Vandenbosch, R. and Huizenga, J. R.
Isomeric Cross Section Ratios for Reactions Producing the Isomeric Pair Hg-197,197m, Physical Review, Vol. 120, No. 4, pp. 1313-1318, Nov. 1960.

32. Wing, James
Isomeric Yield Ratios in Nuclear Reactions, ANL-6598, Sept. 1962.

33. Wing, James
Personal Correspondence, Chemistry Division, Argonne National Laboratory, Argonne, Illinois.

APPENDIX A

Description of IBM-1620 Computer Program Used to Calculate Theoretically Isomeric Cross Section Ratios.

The following program computes the isomeric cross section ratio for isomers produced by (n,γ) reactions. The probability of the excited nucleus decaying from a state J_i to state J_f, following gamma ray emission, is assumed to be proportional to the density of final states with spin J_f. The total normalized yield of J_f is given by the following formula:

$$F_{J_f} = \sum_{J_i=|J_f-\ell|}^{J_f+\ell} \frac{P(J_f)\delta_{J_iJ_f}}{\sum_{J_f=|J_i-\ell|}^{J_i+\ell} P(J_f)} \qquad \text{(A-1)}$$

where

$$P(J_f) = (2J_f + 1)\exp[-(J_f + 1/2)^2/2\sigma^2] \qquad \text{(A-2)}$$

and

$$\delta_{J_iJ_f} = 1 \quad \text{if} \quad |J_i - J_f| \leq \ell \leq |J_i + J_f| \qquad \text{(A-3)}$$

$$= 0 \quad \text{otherwise}$$

where ℓ is the multipolarity of gamma emission and σ is the level density factor.

Constant and calculated values of σ were used, σ was calculated using

$$\sigma^2 = \frac{\Lambda T}{\hbar^2} \qquad \text{(A-4)}$$

where the rigid moment of inertia Λ_{RIGID} is

$$\Lambda_{RIGID} = 2/5\ mAR^2 \tag{A-5}$$

and the nuclear temperature T is given by

$$E_{n+1} = aT^2 - T \tag{A-6}$$

also the average energy of the gamma ray emitted is

$$\bar{E}_{\gamma n+1} = E_n - E_{n+1} = 4(E_n/a - 5/a^2)^{1/2} \tag{A-7}$$

where

$\hbar$ = Plancks constant divided by 2π

m = nucleon mass

A = atomic mass

R = radius of nucleus

a = A/8

E_n = energy of excited level before emission of n^{th} gamma ray

E_{n+1} = energy of excited level before emission of $n+1^{st}$ gamma ray

If $E_n - E_{n+1}$ is less than or equal to zero the program will halt since the energy of the $n+1^{st}$ gamma ray would be less than or equal to zero.

LOGIC DIAGRAM FOR APPENDIX A

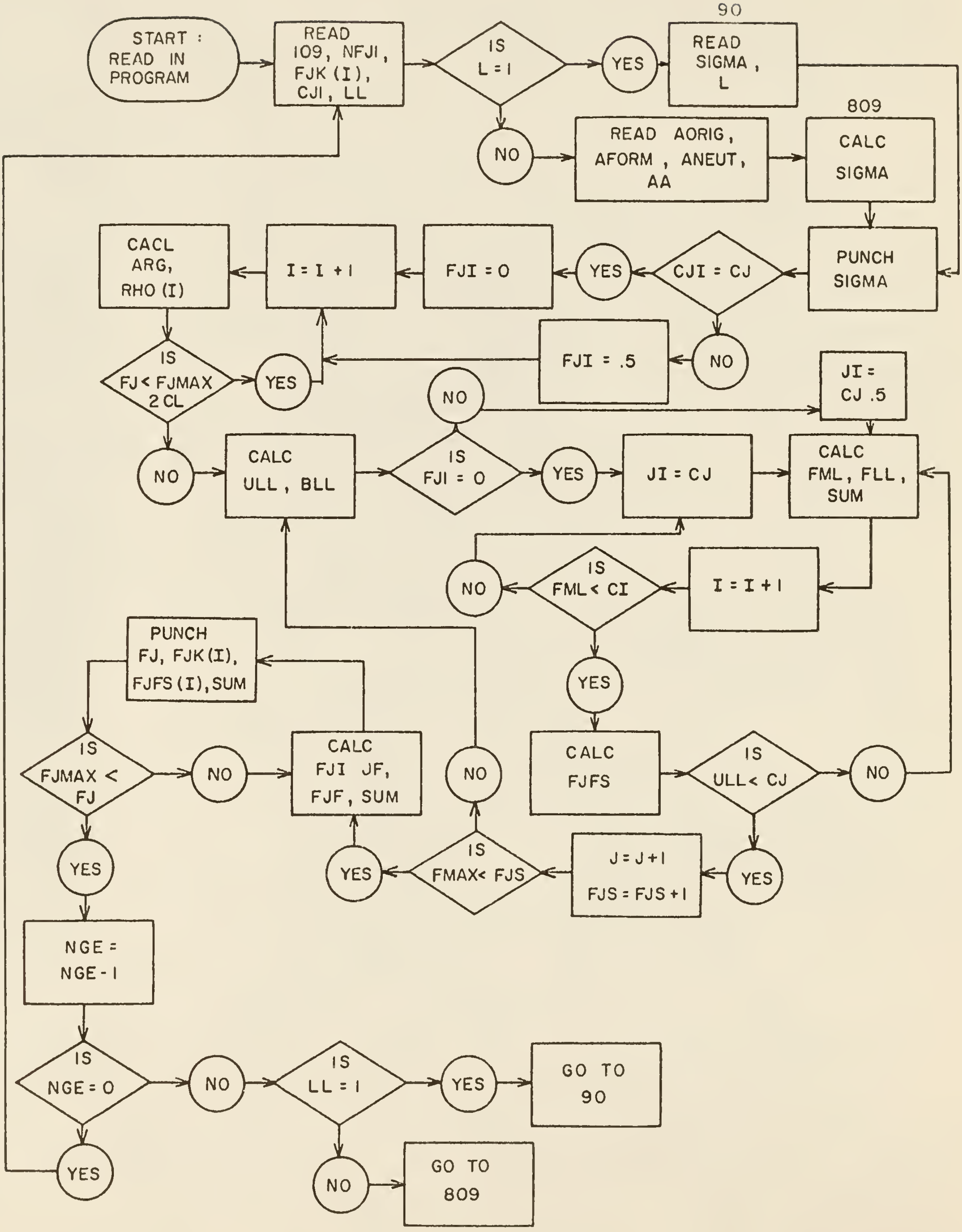

Table A. Symbols used in the theoretical isomeric cross section ratio calculations.

Symbol	Meaning
NFJI	Equals I + 1/2
FJK(I)	Probability that state $J_i = y$ is formed upon neutron bombardment
SIGMA	Level density factor
AORIG	Atomic mass of the original nucleus before neutron bombardment
AFORM	Atomic mass of the excited nucleus
ANEUT	Neutron mass
EO	Excitation energy following neutron bombardment
NGE	Number of gammas emitted
ULL	$J_f + \ell$ upper limit on outer sum
BLL	$\lvert J_f - \ell \rvert$ lower limit on outer sum
FML	$J_i + \ell$ upper limit on inner sum
FLL	$\lvert J_i - \ell \rvert$ lower limit on inner sum
RHO(I)	Level density
I	Spin of the original nucleus
L	Multipolarity of gamma ray emitted
CJI	Angular momentum, 0, 1, 2, ..., I + 1/2
JI	Momentum after neutron bombardment
JFI	Probability that the momentum is JI
JF	Momentum after gamma emission
FJF	Probability that the momentum is JF
FJFS(I)	Same as FJF

```
C      NORMALIZED SPIN DISTRIBUTION IN NUCLEAR REACTIONS
C      FOLLOWING GAMMA RAY EMISSION USING A CALCULATED
C      OR A CONSTANT SIGMA                    11/25/64          G. G. SIMONS
C
C
      DIMENSION RHO(100),FJK(100),FJFS(100),PJF(100)
   10 FORMAT(1X12HENERGY LEVEL,3X12HRIGID MOMENT,8X5HSIGMA,9X4HTEMP)
   11 FORMAT(3X7HI=JC-.5,7X7HI=JC+.5,8X6HFJK(1),8X6HFJK(2))
   12 FORMAT(2XE10.4,6XE10.4,4XE10.4,4XE10.4,//)
   99 FORMAT(I3)
  109 FORMAT(50H                                                  )
  111 FORMAT (F6.3)
  775 FORMAT(24X36HMULTIPOLARITY OF GAMMA-RAY EMISSION I2)
  776 FORMAT(46HNOR. SPIN DIST. AFTER EMISSION OF GAMMA RAY NO I2,//)
  778 FORMAT(24X20HSPIN CUT OFF FACTOR=F6.3)
  780 FORMAT(2X2HJI,8X3HJFI,9X2HJF,8X3HFJF,10X9HSUM    FJF)
  782 FORMAT(F5.1,1XE15.8,1XF5.1,3(1XE15.8))
  783 FORMAT(22XF5.1,2(1XE15.8))
  990 FORMAT (E15.8,5XF5.1)
 6616 FORMAT(4(E10.4))
 6617 FORMAT(4X31HENERGY OF EMITTED GAMMA RAY IS F10.4,//)
 6663 FORMAT(4(E15.8))
 7779 FORMAT(24X18HJF(MAX)=JI(MAX)+L=F6.2,//)
 1001 DO 101 I=1,100
      PJF(I)=0.0
      RHO(I)=0.0
      FJK(I)=0.0
      FJFS(I)=0.0
  101 PJC(I)=0.0
  100 READ 109
      PUNCH 109
 9001 READ 99,NFJI
      DO 142 I = 1,NFJI
  142 READ 990,FJK(I),CJI
      NGE = 10.
 9002 NGC=1
      READ 99,LL
      GO TO (98,908),LL
  908 READ 6663,AORIG,AFORM,ANEUT,AA
      READ 99, L
      EO = ((AORIG+ANEUT)-AFORM)*931.
      A = AA/8.
      RR = (1.2E-13*(AA**(1./3.)))**2
      RIGID = .4*1.6745E-24*AA*RR
  809 YY=((EO/A)-(5./A**2))
      IF(YY) 1001,1001,338
  338 EGAM = 4.*SQRT(YY)
      EN = EO-EGAM
      TEMP = ((1./A)+SQRT((1./A)**2+4.*EN/A))/2.
      SIGMA = SQRT(RIGID*TEMP*1.4406E+28)
      SIGMA = SIGMA*1.E+10
      EO = EN
```

```
      GO TO 6666
   98 READ 99,NGE
   90 READ 111,SIGMA
      READ 99,L
 6666 PUNCH 776,NGC
      PUNCH 778,SIGMA
      CL=L
      PUNCH 775,L
      FJMAX=CL+CJI
      PUNCH 7779,FJMAX
      J=CJI
      CJ=J
      I=0
      IF(CJI-CJ)133,134,133
  133 FJ1=0.5
      GO TO 155
  134 FJ1=0.
  155 FJ=FJ1
  255 I=I+1
      ARG=-(((FJ+.5)**2.)/(2.*SIGMA*SIGMA))
      RHO(I)=(2.*FJ+1.)*EXP(ARG)
      FJ=FJ+1.
      IF(FJ-FJMAX-2.*CL)255,255,256
  256 FJS=FJ1
      J=1
  372 ULL=FJS+CL
      BLL=ABSF(FJS-CL)
      CJ=BLL
      IF(FJ1)88,1813,1812
 1813 JI=CJ
      GO TO 375
 1812 JI=CJ-.5
  375 FML=CJ+CL
      FLL=ABSF(CJ-CL)
      CI=FLL
      IF(FJ1)88,1814,1815
 1814 I=CI
      GO TO 1816
 1815 I=CI-.5
 1816 SUM=0.
  370 SUM=SUM+RHO(I+1)
      I=I+1
      CI=CI+1.
      IF(FML-CI)371,370,370
  371 IF(SUM)1371,1372,1371
 1371 FJFS(J)=FJFS(J)+(FJK(JI+1)*RHO(J   )/SUM)
 1372 CJ=CJ+1.
      JI=JI+1
      IF(ULL-CJ)373,375,375
  373 J=J+1
```

```
      FJS=FJS+1.
      IF(FJMAX-FJS)374,372,372
  374 FJ=FJ1
      FSUM=0.
      AVE=0.
      DO 222 I=1,J
      AVE=FJ*FJ*FJFS(I)+AVE
  222 FJ=FJ+1.
      JJ=FJMAX+1.
      I=1
      SUM=0.
      PUNCH 780
      SUM=SUM+FJFS(I)
      FJ=FJ1
      PUNCH 781,FJ,FJK(I),FJ,FJFS(I),SUM
      IF(NFJI-1)88,1264,1263
 1263 DO 263 I=2,NFJI
      FJ=FJ+1.
      SUM=SUM+FJFS(I)
  263 PUNCH 782,FJ,FJK(I),FJ,FJFS(I),SUM
 1264 FJ=FJ+1.
      I=NFJI+1
  150 SUM=SUM+FJFS(I)
      PUNCH 783,FJ,FJFS(I),SUM
      I=I+1
      FJ=FJ+1.
      IF(FJMAX-FJ)140,150,150
  140 NGE=NGE-1
      NGC=NGC+1
      IF(NGE-1)19,18,18
   18 DO 166 I=1,100
      FJK(I)=FJFS(I)
      RHO(I)=0.
  166 FJFS(I)=0.
      NFJI=NFJI+L
      CJI=FJMAX
      GO TO (90,809),LL
   19 GO TO 1001
   88 STOP
      END
```

APPENDIX B

Description of IBM-1410 Computer Program Used to Fit Photopeak Experimental Data to Gaussian Curves.*

To evaluate the isomeric cross section ratio it was necessary to determine the gamma ray photopeak area. This program written in FORTRAN II performs an iterative calculation, using the method of least squares and Taylor's expansion, to "best fit" photopeak experimental data to Gaussian Curves.

The photopeak of a gamma ray spectrum obtained by using a NaI(Tl) crystal is normally distributed. A normal distribution, often called a Gaussian distribution, has a density function

$$n(x) = \frac{1}{\sqrt{2\pi}\,\underline{\sigma}} \exp[-(x - x_o)^2/2\underline{\sigma}^2] \tag{B-1}$$

the area under this curve is unity, that is

$$\int_{-\infty}^{\infty} n(x)\, dx = 1 \,. \tag{B-2}$$

Integrating over a finite interval will give the total peak area. Using the equations

$$S(x) = S_{max} \exp[-(x - x_o)^2/2\underline{\sigma}^2] \tag{B-3}$$

and

$$AREA = \int_{-\infty}^{\infty} S_{max} \exp[-(x - x_o)^2/2\underline{\sigma}^2]dx = S_{max}\, \underline{\sigma} \sqrt{2\pi} \tag{B-4}$$

where

x_o = channel number corresponding to the peak count

* Subprograms GAUSS and FUNCT programmed by Dr. J. O. Mingle were used with slight modifications.

x = channel number

S_{max} = peak count rate

$\underline{\sigma}^2$ = variance or spread of photopeak

The portion of the photopeak that was fit to the Gaussian curve was one channel less than 0.5 S_{max} on the low energy side and one channel greater than 0.3 S_{max} on the high energy side. This was an arbitrary choice.

The method of least squares was used where the minimum squared error is

$$E = \sum_i |S_i - S_{max} \exp[-\beta(x_i - x_o)^2]|^2. \tag{B-5}$$

In equation (B-5)

$$\beta = 1/(2\underline{\sigma}^2) \tag{B-6}$$

$$S_i = i^{th} \text{ count rate}$$

$$x_i = i^{th} \text{ channel number} .$$

Taking the partial dervatives of E gives

$$R_1 = \frac{\partial E}{\partial \beta} = 0 = 2 \sum_i \{[S_i - S_{max} \exp[-\beta(x_i - x_o)^2]] \tag{B-7}$$

$$[-S_{max} \exp[-\beta(x_i - x_o)^2]] [-(x_i - x_o)^2]\}$$

or

$$R_1 = \frac{\partial E}{\partial \beta} = 0 = \sum_i \{S_i - S_{max} \exp[-\beta(x_i - x_o)^2]\} \tag{B-8}$$

$$\exp[-\beta(x_i - x_o)^2](x_i - x_o)^2$$

and (B-9)

$$R_2 = \frac{\partial E}{\partial x_o} = 0 = \sum_i \{S_i - S_{max} \exp[-\beta(x_i - x_o)^2\} \exp[-\beta(x_i - x_o)^2](x_i - x_o)$$

To determine x_o and β, R_1 and R_2 were expanded in a Taylor's expansion,

$$R_1 = 0 = R_{10} + (x_o - x_{oo}) \frac{\partial R_1}{\partial x_o} + (\beta - \beta_o) \frac{\partial R_1}{\partial \beta} \qquad \text{(B-10)}$$

or

$$R_1 = 0 = R_{10} + \Delta x_o \frac{\partial R_1}{\partial x_o} + \Delta\beta \frac{\partial R_1}{\partial \beta} \qquad \text{(B-11)}$$

and

$$R_2 = 0 = R_{20} + \Delta x_o \frac{\partial R_2}{\partial x_o} + \Delta\beta \frac{\partial R_2}{\partial \beta} \quad . \qquad \text{(B-12)}$$

Eqs. (B-11) and (B-12) contain 2 unknowns Δx_o and $\Delta\beta$. These may be determined by forming the matrix

$$\begin{bmatrix} G_{11} = R_1(x_o,\beta) & G_{12} = R_2(x_o,\beta) \\ G_{21} = R_1(1.05x_o,\beta) & G_{22} = R_2(1.05x_o,\beta) \\ G_{31} = R_1(x_o,1.05\beta) & G_{32} = R_2(x_o,1.05\beta) \end{bmatrix}$$

and evaluating each "G" element in the matrix by using Eqs. (B-8), (B-9) and experimental data. The partials of R_1 and R_2 can then be determined using the above matrix elements. The above "G" terms are redefined as

$$G_{21} = \frac{\partial R_1}{\partial x_o} = \frac{R_1(1.05x_o,\beta) - R_1(x_o,\beta)}{0.05x_o} \qquad \text{(B-13)}$$

$$G_{22} = \frac{\partial R_2}{\partial x_o} = \frac{R_2(1.05x_o,\beta) - R_2(x_o,\beta)}{0.05x_o} \qquad \text{(B-14)}$$

$$G_{31} = \frac{\partial R_1}{\partial \beta} = \frac{R_1(x_o,1.05\beta) - R_1(x_o,\beta)}{0.05\beta} \qquad \text{(B-15)}$$

$$G_{32} = \frac{\partial R_2}{\partial \beta} = \frac{R_2(x_o,1.05\beta) - R_1(x_o,\beta)}{0.05\beta} \qquad \text{(B-16)}$$

Using the standard matrix method Eqs. (B-11) and (B-12) can be solved for Δx_o,

$$\Delta x_o = \frac{-G_{11}G_{32} + G_{12}G_{31}}{G_{21}G_{32} - G_{22}G_{31}} \tag{B-17}$$

and from Eq. (B-11)

$$\Delta\beta = \frac{-G_{11} - G_{21}\,\Delta x_o}{G_{31}} \tag{B-18}$$

This is only the first approximation to Δx_o and $\Delta\beta$. To check the approximation a new x_o and β were calculated

$$^2x_o = {}^1x_o + \Delta{}^1x_o \tag{B-19}$$

and

$$^2\beta = {}^1\beta + \Delta{}^1\beta \tag{B-20}$$

where the superscripts correspond to the number of iterations. From Eq. (B-3)

$$^2S_{max} = {}^2S_{max_o} \exp[(x_o - x_{oo})(x_o - x_{oo})/2\underline{\sigma}^2] \tag{B-21}$$

or

$$^2S_{max} = {}^2S_{max_o} \exp[\beta(x_o - x_{oo})^2] \; . \tag{B-22}$$

If at this stage $\Delta x_o \ll x_o$ and $\Delta\beta \ll \beta$ then an accurate value for x_o and β has been determined. Iteration was continued until this was true. The total peak area, following the k^{th} iteration, is given by

$$\text{AREA} = {}^kS = {}^kS_{max}\,\underline{\sigma}\,(2\pi)^{1/2} \tag{B-23}$$

where

$$\underline{\sigma} = \frac{1}{(2\beta)^{1/2}} \tag{B-24}$$

LOGIC DIAGRAM FOR APPENDIX B

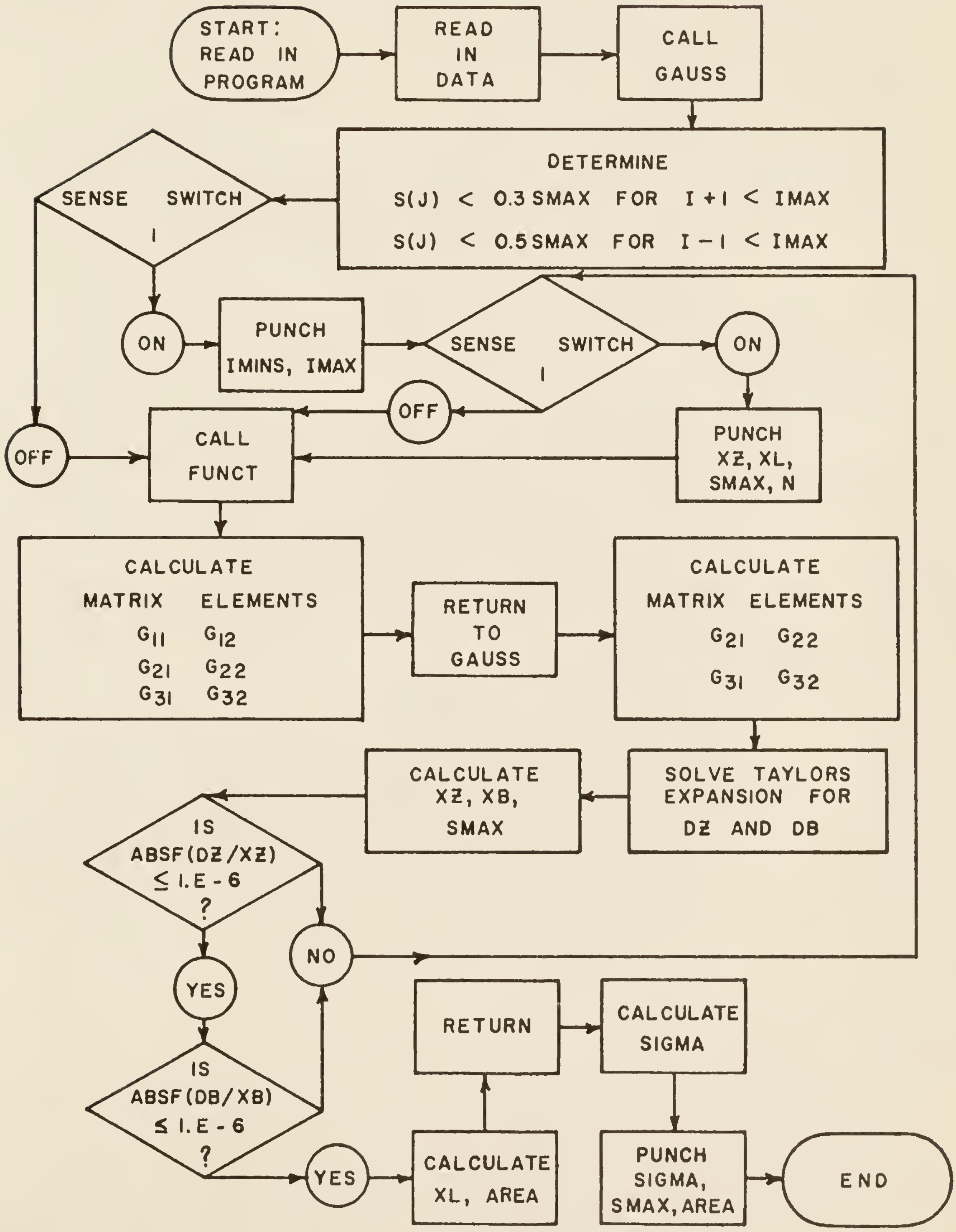

Table B. Symbols used in the fitting of data to a Gaussian curve.

Symbol	Meaning
CHMAX	Maximum channel number used as input data
CHMIN	Minimum channel number used as input data
X	Channel number
S(J)	Count rate of J^{th} data point
SMAX	Maximum count rate
AMAX, XZERO	Channel number corresponding to SMAX
IMINS	Lowest channel number used in the curve fitting
IMAX	Highest channel number used in the curve fitting
XZ	Same as IMAX
XL	Lambda = $1/\underline{\sigma}$
N	Number of iterations
XB	Beta = $1/(2\underline{\sigma}^2)$
DZ	$\Delta x_o = x_o - x_{oo}$
DB	$\Delta\beta = \beta - \beta_o$
SIGMA	Standard deviation of Gaussian curve ($\underline{\sigma}$)
LAMBDA	$\lambda = 1/\underline{\sigma}$
AREA	Area under Gaussian curve
GAUSS	Name of subprogram which fits experimental data to Gaussian curve
FUNCT	Name of subprogram which forms matrix elements from $\partial E/\partial\beta$ and $\partial E/\partial x_o$

The sense switches do not alter the program on off position. Only sense switch one is used. When it is on, the following additional statements are executed

PUNCH IMINS, IMAXS

Calculate XL, AREA after each iteration

PUNCH AREA, XZERO, LAMBDA, SMAX, N.

```
C     MAIN PROGRAM TO FIT EXPERIMENTAL PHOTOPEAK DATA TO A
C     GAUSSIAN CURVE        PROGRAMMED BY SIMONS
    1 FORMAT(4F10.0)
    2 FORMAT(2H0,4X6HX ZERO,12X5HSIGMA,12X4HSMAX,12X4HAREA)
    3 FORMAT(2X,E14.8,3(2XE14.8))
      DIMENSION CHAN(200),COUNT(200)
      COMMON COUNT,CHAN
   50 READ INPUT TAPE 5,1, CHMAX,CHMIN
      READ INPUT TAPE 5,1, AMAX,SMAX
      IMAX = AMAX
      JJ = CHMIN
      KK = CHMAX
      DO 100 I = JJ,KK
  100 READ INPUT TAPE 5,1, CHAN(I),COUNT(I)
      CALL GAUSS(IMAX,SMAX,XZ,XL,AREA)
      SIGMA = 1./XL
      AREA = SMAX*(1./XL)*SQRTF(2.*3.1415926)
      WRITE OUTPUT TAPE 6,2
      WRITE OUTPUT TAPE 6,3,XZ,SIGMA,SMAX,AREA
      GO TO 50
      CALL EXIT
      STOP
      END
=
```

```
C     LEAST SQUARES FIT TO GAUSSIAN PROGRAMMED BY MINGLE
C     MODIFIED BY SIMONS
C     SS 1 ON FOR  IMINS, IMAXS, XZ, XL ITERATION PRINTOUT
      SUBROUTINE GAUSS(IMAX,SMAX,XZ,XL,AREA)
      DIMENSION G(3,2),XX(2),X(200),S(200)
      COMMON S,X
      N=1
      XZ=IMAX
      SMAX1=SMAX
      IMAX1=IMAX+1
      DO 200 I=IMAX1,400
      IF(.3*SMAX-S(I))200,200,201
  201 IMAXS=I
      GO TO 202
  200 CONTINUE
  202 DO 210 I=IMAX1,400
      J=2*IMAX-I
      IF(.5*SMAX-S(J))210,210,211
  211 IMINS=J
      XL=SQRTF(.69314718)/FLOAT(IMAX-J)
      GO TO 212
```

```
 210 CONTINUE
 212 XB=.5*XL**2
     IF(SENSE SWITCH 1)400,411
 400 WRITE OUTPUT TAPE 6,450,IMINS,IMAXS
 450 FORMAT(2H0 ,7HIMIN = I5,4X7HIMAX = I5,/)
     WRITE OUTPUT TAPE 6,451
 451 FORMAT(2H0 ,4X6HX ZERO,12X6HLAMBDA,13X4HSMAX,9X1HN//)
4511 FORMAT(2H0,6X4HAREA)
 401 IF(SENSE SWITCH 1)499,411
 499 XL=SQRTF(2.*XB)
     AREA = SMAX*(1./XL)*SQRTF(2.*3.1415926)
     WRITE OUTPUT TAPE 6,452,XZ,XL,SMAX,N
     WRITE OUTPUT TAPE 6, 4511
 452 FORMAT(2X,E14.8,2(4XE14.8),I5)
     WRITE OUTPUT TAPE 6,452,AREA
 411 XX(1)=XZ
     XX(2)=XB
     DO 300 I=1,2
     CALL FUNCT(XX(2),XX(1),IMINS,IMAXS,G(I,1),G(I,2),SMAX)
 300 XX(1)=XX(1)*1.05
     XX(1)=XZ
     XX(2)=XX(2)*1.05
     CALL FUNCT(XX(2),XX(1),IMINS,IMAXS,G(3,1),G(3,2),SMAX)
     XX(2)=XB
     DO 301 J=2,3
     DO 301 I=1,2
 301 G(J,I)=(G(J,I)-G(1,I))/(.05*XX(J-1))
     DZ=(-G(1,1)*G(3,2)+G(1,2)*G(3,1))/(G(2,1)*G(3,2)-G(2,2)*G(3,1))
     DB=(-G(1,1)-G(2,1)*DZ)/G(3,1)
     XZ=XZ+DZ*0.5
     XB=XB+DB*0.5
     N=N+1
     SMAX=SMAX1*EXPF(XB*(FLOAT(IMAX)-XZ)**2)
     IF(ABSF(DZ/XZ)-1.E-6)305,305,401
 305 IF(ABSF(DB/XB)-1.E-6)306,306,401
 306 XL=SQRTF(2.*XB)
     AREA = SMAX*(1./XL)*SQRTF(2.*3.1415926)
     RETURN
     END


C    GAUSSIAN FUNCTION PROGRAMMED BY MINGLE
     SUBROUTINE FUNCT(XB,XZ,IMIN,IMAX,R1,R2,SMAX)
     DIMENSION S(200),X(200)
     COMMON S,X
     R1=0.
     R2=0.
     DO 100 I=IMIN,IMAX
     A=XB*(X(I)-XZ)**2
     C=EXPF(-A)
     R1=R1+(S(I)-SMAX*C)*C*A/XB
 100 R2=R2+(S(I)-SMAX*C)*C*(X(I)-XZ)
     RETURN
     END
```

APPENDIX C

Description of IBM-1620 Computer Program Used to Calculate Isomeric Cross Section Ratios from Experimental Data

Section 3.1 contained a development of the equations used to calculate isomeric cross section ratios from experimental gamma ray spectra data.

For the case where no appreciable decay occurred during counting the equation obtained was

$$\frac{\delta_2}{\delta_1} = \frac{1}{(1 - e^{-\lambda_2 t})} \left\{ \frac{(\lambda_2 N_2)_{w2} e^{\lambda_2 t_{w2}}}{(\lambda_1 N_1)_{w1} e^{\lambda_1 t_{w1}}} (1 - e^{-\lambda_1 t}) - \frac{\lambda_2}{\lambda_1 - \lambda_2} (e^{-\lambda_1 t} - e^{-\lambda_2 t}) \right\} - 1 \tag{C-1}$$

where

$$\frac{(\lambda_2 N_2)_{w2}}{(\lambda_1 N_1)_{w1}} = \frac{A_2 E_{T1}}{A_1 E_{T2}} \tag{C-2}$$

For the case where significant decay did occur during counting, the equation obtained was

$$\frac{\delta_1}{\delta_1 + \delta_2} = \frac{\lambda_1 N_{t1} (1 - e^{-\lambda_2 t}) e^{\lambda_1 t_{w1}}}{\left\{ (\lambda_2 N_2) - (\frac{\lambda_2}{\lambda_2 - \lambda_1}) [e^{-\lambda_1 t} - e^{-\lambda_2 t}] \right\} (1 - e^{-\lambda_1 t_c})} \tag{C-3}$$

where

$$\lambda_2 N_2 = \frac{A_2 e^{\lambda_2 t_{w2}}}{E_{T2}} \tag{C-4}$$

and

$$N_{t1} = \frac{A_{t1}}{E_{T1}} \tag{C-5}$$

This program, called ISOMERIC CROSS SECTION RATIOS and written in FORTRAN II, uses the half lives of the isomers, irradiation, decay and counting times, photopeak area and detector efficiencies to determine the cross section ratios from Eq. (C-1) or Eq. (C-2) above.

The area due to photoelectric gamma ray interaction with the NaI(Tl) crystal is computed by subtracting the area due to Compton scattered gamma rays (Appendix D) from the total area under the photopeak. This total area was calculated using the PHOTOPEAK program, Appendix B.

The deviation listed is the standard deviation due to counting statistics, i.e., square root of the count rate.

Table C lists and defines the input and output symbols used.

Table C. Symbols used in the experimental isomeric cross section ratio calculations

Symbol	Meaning
TRANS	1 if no decay occurs during counting and 2 if decay occurs during counting
AMETA	Total peak area of metastable state given in counts per x minutes
STAB	Total peak area of stable state given in counts per y minutes
TW1	Time after irradiation until start of count for metastable state
TE1	Irradiation time of metastable state
TC1	Counting time of metastable state (x minutes)
TW2	Time after irradiation until start of count for stable state
TE2	Irradiation time of stable state
TC2	Counting time of stable state (y minutes)
CHLO1	Minimum channel number of metastable state
CHHI1	Maximum channel number of metastable state
CRLO1	Sample count rate minus background corresponding to channel CHLO1
CRHI1	Sample count rate minus background corresponding to channel CHHI1
CHLO2	Minimum channel number of stable state
CHHI2	Maximum channel number of stable state
CRLO2	Count rate minus background corresponding to CHLO2
CRHI2	Count rate minus background corresponding to CHHI1
HALF1	Half life of metastable state in minutes
HALF2	Half life of stable state in minutes

Table C (continued)

Symbol	Meaning
EFF1	Efficiency of detector for metastable state
EFF2	Efficiency of detector for stable state
CROSS	Cross section ratio
DEV	Standard deviation
X	See Figure D
Y	See Figure D

```
C     ISOMERIC CROSS SECTION RATIOS          PROGRAMMED BY G G SIMONS
C     TRANS IS ONE IF NO DECAY OCCURS DURING COUNTING AND IS TWO IF
C     DECAY OCCURS DURING COUNTING
   10 FORMAT(50H                                                  )
   20 FORMAT(6F10.0)
   30 FORMAT(4X19HCROSS SECTION RATIO,4X9HDEVIATION)
   40 FORMAT(5XE14.8.6XE14.8)
   41 READ 10
      READ 20,AMETA,STAB,TRANS
      READ 20,TW1,TE1,TC1,TW2,TE2,TC2
      READ 20,CHLO1,CHHI1,CRLO1,CRHI1
      READ 20,CHLO2.CHHI2,CRLO2,CRHI2
      READ 20, HALF1,HALF2
      READ 20,EFF1,EFF2
      CHLO1 = CHLO1+1.
      CHHI2 = CHHI2-1.
      CHLO2 = CHLO2+1.
      CHHI1 = CHHI1-1.
      AMETA =AMETA/TC1
      STAB = STAB/TC2
      COMP1 = ((CRHI1+CRLO1)/2.)*(CHHI1-CHLO1)/TC1
      COMP2 = ((CRHI2+CRLO2)/2.)*(CHHI2-CHLO2)/TC2
      PHOT1 = AMETA-COMP1
      PHOT2 = STAB-COMP2
      ALAM1 = 0.693/HALF1
      ALAM2 = 0.693/HALF2
      IF(TRANS) 1,2
    1 BUS = 1./(1.-EXP(-ALAM2*TE2))
      CUS=(EFF1/EFF2)*(PHOT2/PHOT1)*EXP(ALAM2*TW2)/EXP(ALAM1*TW1)
      DUS = 1.-EXP(-ALAM1*TE1)
      FUS=(ALAM2/(ALAM1-ALAM2))* (EXP(-ALAM1*TE1)-EXP(-ALAM2*TE2))
      RAT = BUS*(CUS*DUS-FUS)-1.
      CROSS = 1./(1.+RAT)
      GO TO 3
    2 BUS = ALAM1*PHOT1*TC1*(1.-EXP(-ALAM2*TE2))/EFF1
      CUS=PHOT2*EXP(ALAM2*TE2)/EFF2
      DUS=(ALAM2/(ALAM2-ALAM1))*(EXP(-ALAM1*TE1)-EXP(-ALAM2*TE2))
      FUS = 1./(EXP(-ALAM1*TW1)*(1.-EXP(-ALAM1*TC1)))
      CROSS=(BUS/(CUS-DUS))*FUS
    3 DEV1 = SQRT((AMETA/TC1)+(COMP1/TC1))
      DEV2 = SQRT((STAB/TC2)+(COMP2/TC2))
      AM = (DEV1/PHOT1)
      AG = (DEV2/PHOT2)
      DEV = (AM+AG)*CROSS
      PUNCH 10
      PUNCH 30
      PUNCH 40, CROSS, DEV
      GO TO 41
      END
```

APPENDIX D

Subtraction of Compton Scattered Gamma Rays from the Photopeak Area

As mentioned in Section 3.5 experimental photopeak data were fit to a Gaussian curve, and then the counts due to Compton scattered gamma rays falling under the photopeak were subtracted. The following explains how the Compton distribution was subtracted.

As seen in Figure D the photopeak curve begins to deviate from the Gaussian curve for channel numbers with count rates less than 1/2 S_{max} on the low energy side and less than 1/3 S_{max} on the high energy side of the peak. To determine the correct area due to Compton scattered gamma rays the following steps were executed for each gamma ray photopeak investigated:

1.) Gamma ray photopeak was plotted.

2.) Gaussian curve was hand fitted to the photopeak.

3.) Line AB was drawn (Figure D) between the points of minimum count rate on each side of the peak.

4.) Point of intersection between line AB and Gaussian curve was found, this determined the number of channels X and Y (Figure D).

5.) Area of Gaussian curve below line AB was determined, this was the Compton area portion of the Gaussian curve.

Several photopeaks were plotted for each gamma ray investigated. X and Y were found invariant for each energy gamma ray. Feeding the channel numbers with the minimum count rates on each side of the peak into the computer and fixing X and Y for each energy gamma ray, the area due to Compton scattering was therefore determined. This area was subtracted from the Gaussian area.

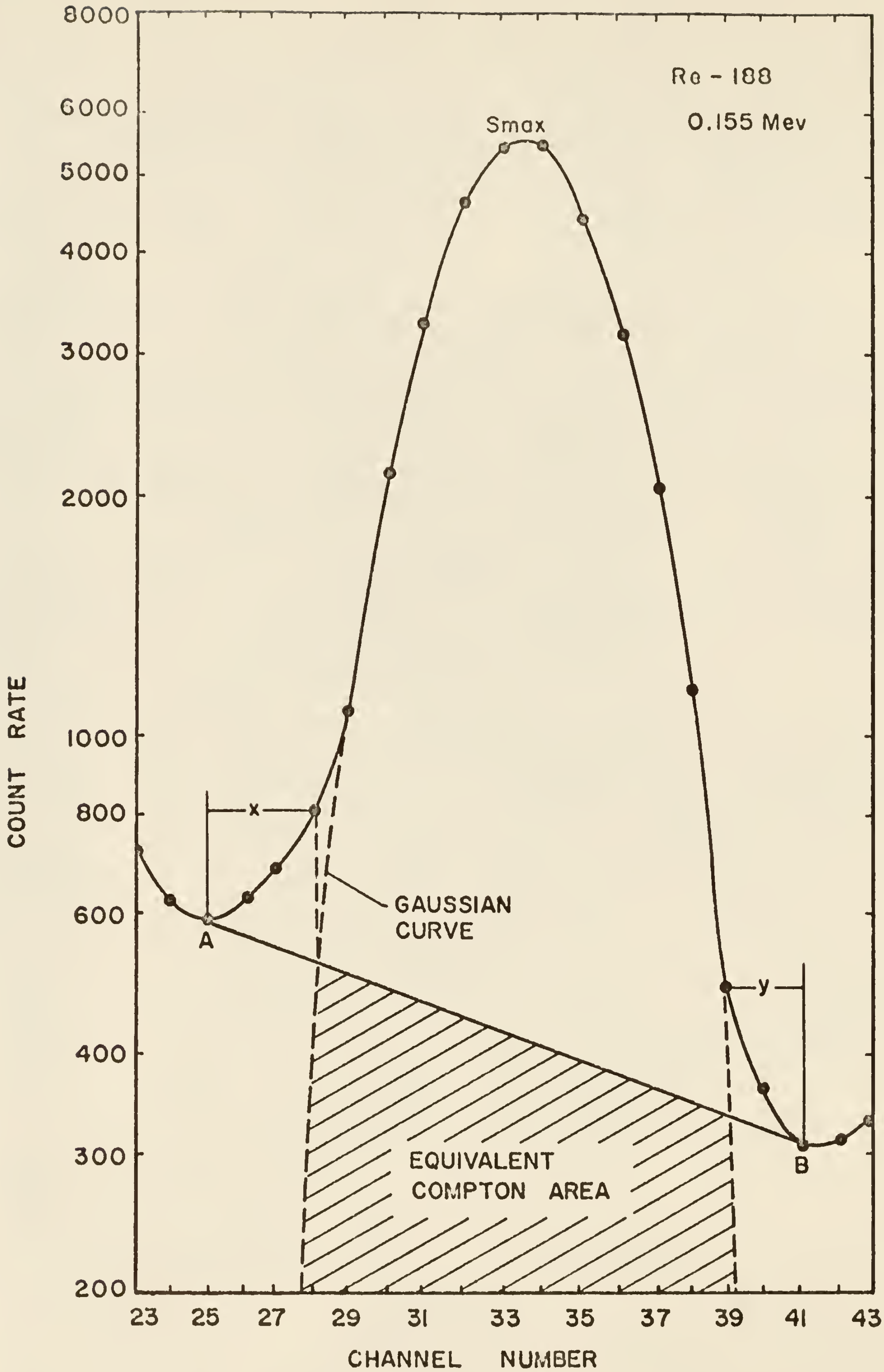

Figure D AREA DUE TO COMPTON SCATTERING

ISOMERIC CROSS SECTION RATIOS FOR
THE Sc-46, Cs-134 AND Re-188 ISOMERS

by

GALE GENE SIMONS

B. S. Kansas State University, 1962

AN ABSTRACT OF
A MASTER'S THESIS

submitted in partial fulfillment of the

requirements for the degree

MASTER OF SCIENCE

Department of Nuclear Engineering

KANSAS STATE UNIVERSITY
Manhattan, Kansas

1965

ABSTRACT

Isomeric cross section ratios using (n,γ) reactions induced by reactor neutron bombardment were determined in this work for the isomeric pairs Sc-46, 46m and Re-188,188m, which have not been investigated before, and for the isomeric pair Cs-134,134m which was previously studied (1) using a different approach from the one used in this investigation.

The TRIGA Mark II Reactor was used to irradiate samples of scandium oxide, cesium oxide, and rhenium metal in the following locations/conditions; rotary specimen rack/bare, rotary specimen rack/cadmium covered, and thermal column/bare. The corresponding neutron energies in these locations will henceforth be designated as RSR, epi-cadmium, and thermal respectively. The cross section ratios were determined by a modified absolute counting method using a 3 x 3 inch well scintillation detector and a 256 channel analyzer. The IBM-1410 computer was programmed to determine the area under the photopeaks by fitting the gamma photopeak data to a Gaussian curve using a least squares method combined with Taylor's expansion. The IBM-1620 computer was programmed to subtract the area due to Compton scattered gamma rays from the total area under the photopeak found above and then to calculate the experimental isomeric cross section ratios.

Isomers	Neutron Energy		
	RSR	Thermal	Epi-cadmium
Sc-46,46m	0.4955±0.0630	0.5645±0.0365	0.5048±0.0500
Cs-134,134m	0.0952±0.0178	0.1368±0.0165	0.1057±0.0153
Re-188,188m	0.1578±0.0145	0.1618±0.010	0.1381±0.0124

Each value given in the above table is an average of at least 9 individual results obtained from completely independent experiments.

The isomeric cross section ratios were also calculated using the statistical model for compound nucleus formation. By matching the theoretically calculated and experimentally determined cross section ratios the applicability of this model was determined for the isomeric pairs studied.

The following conclusions were drawn:

1.) In the case of Re-188,188m, theoretical and experimental values agreed very well for a σ between 3 and 4, $N_\gamma=4$ and $J=I-1/2$ where I is the angular momentum of the parent element (Re-187). Also, very good agreement was found using a calculated σ when $N_\gamma=4$ and $J=I-1/2$. It is to be noted that in both cases agreement was obtained for $J=I-1/2$ and that values obtained using $J=I+1/2$ were far from being in agreement with experimental values.

2.) In the case of Cs-134,134m, theoretical and experimental values agreed for σ between 7 and 8, $N_\gamma=6$, and $J=I+1/2$. Using a calculated σ, experimental ratios were greater than the theoretical ratios. In constrast to the case of Re-188,188m, theoretical cross section ratios obtained using $J=I+1/2$ were in much closer agreement with the experimental values than those obtained using $J=I-1/2$.

3.) For Sc-46,46m, the theoretically calculated values were always less than those experimentally determined for all values of σ provided N_γ was less than or equal to 6. The average number of gamma rays emitted from an excited nucleus, as stated by several investigators, is approximately 4. In this work $N_\gamma=6$ was chosen as an arbitrary maximum, although agreement could have been obtained between theoretical and experimental ratios by increasing N_γ above 6.

4.) The statistical model seems applicable to the Re-188,188m isomeric pair for the same range of σ (3 to 5) and $N_\gamma=4$ as found to give agreement in several other cases reported in the literature. On the other hand, agreement in the case of Cs-134,134m was only obtained by using higher values of N_γ and σ. For Sc-46,46m the statistical model does not seem to hold.

LITERATURE CITED

1. Bishop, C. T.
Isomeric Cross Section Ratios for Some (n,γ) and (α,xn) Reactions, ANL-6405, 1961.